

**GEOCHEMICAL AND PETROGRAPHIC CHARACTERIZATION OF
SERPENTINIZED PERIDOTITE IN THE INDIAN OCEAN: INSIGHTS
INTO MANTLE PROCESSES AND TECTONIC EVOLUTION**

A Dissertation Report for

GEO-651: Dissertation

Credits: 16

Submitted in partial fulfilment of

Masters in Science

In

Applied Geology

By

MRUNALI DEEPAK PILGAONKAR

Seat No: 22P0450013

ABC ID: 262832487122

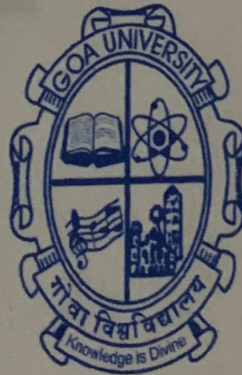
PRN: 201900884

Under the supervision of

Dr. POORNIMA ROHAN SAWANT

School of Earth Ocean and Atmospheric Sciences

Applied Geology



GOA UNIVERSITY

May 2024



Examined by:

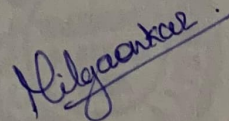
Seal of the School

DECLARATION BY STUDENT

I hereby declare that the data presented in this Dissertation report entitled, "GEOCHEMICAL AND PETROGRAPHIC CHARACTERIZATION OF SERPENTINIZED PERIDOTITE IN THE INDIAN OCEAN: INSIGHTS INTO MANTLE PROCESSES AND TECTONIC EVOLUTION" is based on the results of investigations carried out by me in the at the Masters of Science in the Discipline MSc. Applied Geology at the School of Earth Ocean and Atmospheric Sciences, Goa University.

under the Supervision of Dr. POORNIMA ROHAN SAWANT and the same has not been submitted elsewhere for the award of a degree or diploma by me. Further, I understand that Goa University or its authorities will be not be responsible for the correctness of observations or other findings given the dissertation.

I hereby authorize the University authorities to upload this dissertation on the dissertation repository or anywhere else as the UGC regulations demand and make it available to any one as needed.



Ms. Mrunali Deepak Pilgaonkar

22P0450013

MSc. Applied geology

School of Earth Ocean and Atmospheric Sciences.

Date: 02-05-2024

Place: Goa University

COMPLETION CERTIFICATE

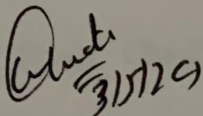
This is to certify that the dissertation report “**GEOCHEMICAL AND PETROGRAPHIC CHARACTERIZATION OF SERPENTINIZED PERIDOTITE IN THE INDIAN OCEAN: INSIGHTS INTO MANTLE PROCESSES AND TECTONIC EVOLUTION**” is a bonafide work carried out by **Ms. Mrunali Deepak Pilgaonkar** under my supervision in partial fulfilment of the requirements for the award of the degree of Masters of Science in the Discipline MSc. Applied Geology at the School of Earth Ocean and Atmospheric Sciences, Goa University.



Dr. POORNIMA ROHAN SAWANT
Assistant Professor, Applied Geology

SEOAS

Date: 02/05/2024



Senior Professor,

Sanjeev C. Ghadi.

Dean of the School of Earth, Ocean and Atmospheric Sciences.

Goa University.

Place: Goa University

**GEOCHEMICAL AND PETROGRAPHIC
CHARACTERIZATION OF SERPENTINIZED PERIDOTITE IN
THE INDIAN OCEAN: INSIGHTS INTO MANTLE PROCESSES
AND TECTONIC EVOLUTION**

A Dissertation Report for

GEO-651: Dissertation

Credits:16

Submitted in partial fulfilment of

Masters in Science

In

Applied Geology

By

MRUNALI DEEPAK PILGAONKAR

Seat No: 22P0450013

ABC ID: 262832487122

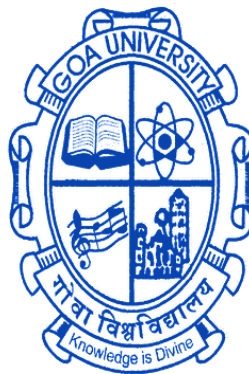
PRN: 201900884

Under the supervision of

Dr. POORNIMA ROHAN SAWANT

School of Earth Ocean and Atmospheric Sciences

Applied Geology



GOA UNIVERSITY

May 2024

Examined by:

Seal of the School

DECLARATION BY STUDENT

I hereby declare that the data presented in this Dissertation report entitled, **“GEOCHEMICAL AND PETROGRAPHIC CHARACTERIZATION OF SERPENTINIZED PERIDOTITE IN THE INDIAN OCEAN: INSIGHTS INTO MANTLE PROCESSES AND TECTONIC EVOLUTION”** is based on the results of investigations carried out by me in the at the Masters of Science in the Discipline MSc. Applied Geology at the School of Earth Ocean and Atmospheric Sciences, Goa University.

under the Supervision of Dr. POORNIMA ROHAN SAWANT and the same has not been submitted elsewhere for the award of a degree or diploma by me. Further, I understand that Goa University or its authorities will be not be responsible for the correctness of observations or other findings given the dissertation.

I hereby authorize the University authorities to upload this dissertation on the dissertation repository or anywhere else as the UGC regulations demand and make it available to any one as needed.

Ms. Mrunali Deepak Pilgaonkar

22P0450013

MSc. Applied geology

School of Earth Ocean and Atmospheric Sciences.

Date:

Place: Goa University

COMPLETION CERTIFICATE

This is to certify that the dissertation report “**GEOCHEMICAL AND PETROGRAPHIC CHARACTERIZATION OF SERPENTINIZED PERIDOTITE IN THE INDIAN OCEAN: INSIGHTS INTO MANTLE PROCESSES AND TECTONIC EVOLUTION**” is a bonafide work carried out by **Ms. Mrunali Deepak Pilgaonkar** under my supervision in partial fulfilment of the requirements for the award of the degree of Masters of Science in the Discipline MSc. Applied Geology at the School of Earth Ocean and Atmospheric Sciences, Goa University.

Dr. POORNIMA ROHAN SAWANT
Assistant Professor, Applied Geology
SEOAS

Date:

Senior Professor,
Sanjeev C. Ghadi.
Dean of the School of Earth, Ocean and Atmospheric Sciences.
Goa University.

Place: Goa University

ACKNOWLEDGEMENT

In humble acknowledgment of the divine grace that has guided and sustained me throughout this academic odyssey, I begin by expressing my deepest gratitude to God, whose boundless wisdom and benevolence have illuminated my path and bestowed upon me the fortitude to persevere in the face of challenges.

Foremost, I express my deepest gratitude to Dr. POORNIMA ROHAN SAWANT, whose mentorship transcends the traditional bounds of academic guidance. Their wisdom, patience, and unwavering belief in my capabilities have not only enriched this dissertation but have also fostered my intellectual and personal growth in immeasurable ways. I am truly fortunate to have had Dr. POORNIMA ROHAN SAWANT as a mentor and guide throughout this transformative journey.

The completion of this research endeavor has been made possible through the collective efforts and unwavering support of the academic community at Applied Geology discipline of School of Earth Ocean and Atmospheric Sciences (SEOAS), Goa University. I am deeply grateful for the intellectual camaraderie, scholarly discourse, and collaborative spirit that have enriched my academic journey. My sincere gratitude goes out to Dr. A.A.A. Viegas, Dr. Niyati Kalangutkar., Dr. Nicole Sequeira, Dr. Pooja Ghadi and Mr. Mahesh Mayekar for their constant support and encouragement. I would also like to extend my thanks to non- teaching staff of the School of Earth Ocean and Atmospheric Sciences for always being supportive and helping with all the necessary facilities.

I am indebted to National Institute of Oceanography, Dona Paula, Panjim, for their support, which has facilitated the execution of this research and underscored the importance of scholarly inquiry in addressing pressing societal challenges.

I would like to extend my sincere gratitude for NGRI (National Geophysical Research Institute, Hyderabad) for the invaluable assistance in conducting geochemical analysis. Additionally, a special thanks to Lab Crystals Kolkata for their expertise and support in preparing thin sections. Your contribution has significantly enriched the quality depth of our research.

My deepest gratitude goes to my family, whose unwavering love, encouragement, and sacrifices have been a source of strength and inspiration. Their steadfast support has sustained me through the peaks and valleys of this academic pursuit.

I am immensely grateful to my friends Aaron, Aditi, Ashita, Chandrakant, colleagues Meldrin and Sakshi, and roommate Teja for thier camaraderie, intellectual camaraderie, and unwavering encouragement, which have enriched my scholarly pursuits immeasurably.

Finally, I extend my heartfelt appreciation to the participants of this study, whose willingness to share their insights and experiences has enriched this research endeavor immeasurably. Their contributions are a testament to the collaborative spirit that underpins scholarly inquiry.

In profound reflection, I recognize that this dissertation stands as a testament to the collective efforts of the myriad individuals and institutions who have contributed to its fruition. May the lessons learned and the knowledge gained serve as a beacon of hope and inspiration for future endeavor.

CHAPTER	SR. No.:	TITLE	PAGE NO.:
CHAPTER I	1	INTRODUCTION	1
	1.1	Serpentinised peridotite	2
	1.1.1	Classification of serpentinized peridotite based on tectonic setting	7
	1.1.2.	Formation of serpentinised peridotite	10
	1.1.3.	Importance of studying serpentinized peridotite	11
	1.2.	Geochemistry	13
	1.3.	Regional geology	17
	1.4.	Study area and location	23
	1.5.	Sampling Approach	24
	1.6.	Aims and Objective	27
	1.7.	Brief structure	28
CHAPTER II	2	LITERATURE REVIEW	31
CHAPTER III	3	METHODOLOGY	79
	3.1	Analytical methods	80
	3.1.1.	Petrography and mineral assemblage	80
	3.1.2.	Mineral chemistry	81
	3.1.3.	Geochemical analysis	82
CHAPTER IV	4	RESULTS AND OBSERVATIONS	86
	4.1	Petrographic observation	87
	4.2	Mineral chemistry	99
	4.3	Trace and REE	116

CHAPTER	SR. No.:	TITLE	PAGE NO.:
CHAPTER V	5	DISCUSSION	119
	5.1	Effect of serpentinisation	120
	5.2	Degree of mantle melting	123
	5.3	Melt rock interaction and hydrothermal interaction	136
	5.4	Tectonic setting	140
CHAPTER VI	6	CONCLUSION	145
		REFERENCES	147

CHAPTER	SR. No.	LIST OF FIGURES	PAGE NO.:
CHAPTER I	1.1	Classification diagram for peridotite and pyroxenite, based on proportions of olivine and pyroxene. The pale green area encompasses the most common compositions of peridotite in the upper part of the Earth's mantle (partly adapted from Bodinier and Godard (2004)).	3
	1.2	Peridotite undergone process called serpentinization.	6
	1.3	Schematic model of formation of serpentinites in forearc regions, Abyssal serpentinites are from Hattori, K. (2019).	8
	1.4	Map of Indian Ocean showing Ridge system- Central Indian Ridge, from (Mazzullo et al., 2017)	20
	1.5	Study area and location map, on Central Indian Ridge between Vema and Vityaz Fracture Zone.	24
CHAPTER III	3.1	Mineral chemical composition analyses using wavelength dispersive spectrometry (WDS) Electron Probe Micro Analyses (EPMA) at NIO, Goa.	83
	3.2	Major element analyses of Serpentinised Peridotite by using (PANalytical, Axios mode with 4 KW power) wavelength dispersive x-rays fluorescence spectroscopy (WD-XRF) at NIO, Goa.	84
	3.3	Trace and REE analyses of Serpentinised peridotite sample using high resolution inductively coupled mass spectrometer (HR-ICP-MS) National geophysical Research Institute (NGRI), Hyderabad.	85

CHAPTER	SR. No.	LIST OF FIGURES	PAGE NO.:
CHAPTER IV	4.1.1.	(A) Plane Polarised light (B) between cross polars, Pyroxene grain surrounded by mesh texture in serpentinised peridotite.	94
	4.1.2.	(A) Plane polarized light (B) Between cross polars, Mesh texture observed in studied samples.	95
	4.1.3.	(A) Plane polarized Light (B) Between cross polars, Antigorite veins along with magnetite with deformed grains of Pyroxene.	96
	4.1.4.	(A) Highly altered and deformed olivine grain in studied sample of serpentinised peridotite. (B) Veins of antigorite, magnetite mineral and deformed olivine alteration to serpentine.	97
	4.1.5.	(A) Plane polarized light (B) Between cross polars, Bastite texture where in orthopyrosene grain is altered to serpentine but retaining the original shape.	98
	4.2.1.	Al ₂ O ₃ vs. SiO ₂ (wt%). Fields of different serpentine minerals after Schwartz et al. (2013).	111
	4.2.2.	NiO vs. Cr ₂ O ₃ (wt%). Fields for olivine and orthopyroxene after Kodolányi et al. (2012).	112
	4.2.3.	Triangular diagram showing chemical compositions of magnetite which plotted onto the Fe axis Fields of different metamorphic facies for altered spinel phases were concluded by Hamdy and Lebda (2011).	113

CHAPTER	SR. No.	LIST OF FIGURES	PAGE NO.:
CHAPTER IV	4.2.4.	A trivalent cation classification triangular diagram, in the context of spinel-group minerals from serpentinite-hosted peridotites (SSPs), is used to illustrate the compositional variations based on three trivalent cations: Cr ³⁺ , Fe ³⁺ , and Al ³⁺ .	113
	4.2.5.	Compositional variability in spinel-group minerals from SSPs in a triangular Cr ³⁺ – Fe ³⁺ – Al ³⁺ plot.	114
	4.2.6.	Spinel-group mineral compositions from SSPs plotted in (a) Cr ³⁺ /(Cr ³⁺ + Fe ³⁺) against Mg ²⁺ /(Mg ²⁺ + Fe ²⁺)	115
	4.2.7.	Spinel Fe ³⁺ # versus Cr#. Fields of forearc, backarc and abyssal peridotites are from Lian et al. (2019)	115
	4.3.1.	Chondrite normalised V/S REE plot showing U shape trend and positive Eu anomaly for serpentinitised peridotite. Normalising factors are from Sun and Mc Donough (1989).	118
	4.3.2.	Primitive Mantle normalised V/S REE plot showing U shape trend and positive Eu anomaly for serpentinitised peridotite. Normalising factors are from Sun and Mc Donough (1989).	118
	CHAPTER V	5.1.1.	In MgO/SiO ₂ , vs. Al ₂ O ₃ /SiO ₂ , space the data of the abyssal peridotite from the CIR area show a considerable variability whereas analyses of a global set of abyssal Peridotite presented by Niu (2004) define a trend parallel to the terrestrial array (Jagoutz et al., 1979).

CHAPTER	SR. No.	LIST OF FIGURES	PAGE NO.:
CHAPTER V	5.2.1.	Diagram showing the chemical composition of spinels (blue dots) which are plotted in lherzolite, Harzbergites and abyssal peridotite fields. The range of spinel from different rocks was concluded by Dick and Bullen (1984).	130
	5.2.2.	Plot Of FeO vs. MgO, Al ₂ O ₃ vs. MgO, SiO ₂ vs. MgO, CaO vs. MgO, indicative of the type of abyssal peridotite.	131
	5.2.3.	Spinel compositions of the studied serpentinite samples plotted on Mg# [Mg/ (Mg + Fe ²⁺)] vs. Cr# [Cr/(Cr + Al)] diagram. Partial melting trend (red arrow) is from Dick and Bullen (1984) and Arai (1992).	133
	5.2.4.	Cr# [Cr/(Cr + Al)] vs. Tio ₂ (wt%). The degrees of melt extractions are from Hellebrand et al. (2001) and Uysal et al. (2012).	133
	5.2.5	Plots of whole-rock MgO contents against Al ₂ O ₃ , (a), CaO (b), and Na ₂ O (c) (all in wt.%). Element concentrations have been recalculated to 100% on an LOI-free basis. The calculated melting trend for residual serpentinitised peridotites using the model of Niu (1997) is shown, which assumes anhydrous polybaric near-fractional melting of a PM source from 2.5 GPa to 0.4 GPa. Numbers along the line indicate percentage melting.	134
	5.2.6.	Serpentinites from the given study show relatively high immobile trace element concentration indicative for melt-rock interaction processes. Symbols as in Figure. 3. (A). U vs. Th (B). Zr vs.Th).	135

CHAPTER	SR. No.	LIST OF FIGURES	PAGE NO.:
CHAPTER V	5.3.1.	Deviating trends for melt-rock interaction and hydrothermal alteration are defined in LREE vs. HFSE space. This is due to the higher solubility of LREE in aqueous solutions compared to HFSE. In contrast, LEE and HFSE are equally soluble in silicic melts. (A). Nb vs. La (B). Th vs. Ce (C). Nd vs. Gd /Lu(D). Th vs. Gd /Lu	138
	5.4.1.	Al ₂ O ₃ vs. TiO ₂ binary plot (after Kamenetsky et al., 2001) of Cr-spinels in comparison to modern-day tectonic settings.	143
	5.4.2.	Triangular trivalent cation plot of Al ³⁺ – (Fe ³⁺ + 2Ti ⁴⁺) – Cr ³⁺ (after Jan and Windley, 1990) for Cr-spinels from SSP's.	144
	5.4.3.	Ternary plot of Fe-Cr-Al showing fields such as nidar peridotites mariana forearc peridotites abyssal peridotites where in the spinel samples are plotting in the field of abyssal peridotites.	144

CHAPTER	SR. No.	LIST OF TABLES	PAGE NO.:
CHAPTER IV	4.1.1.	Representative EPMA data of Magnetite	104
	4.1.2.	Representative EPMA data of Spinel	104
	4.1.3.	Representative EPMA data of Serpentine	105
	4.1.3.	Representative EPMA data of Serpentine (Contd.)	106
	4.1.3.	Representative EPMA data of Serpentine (Contd.)	106
	4.1.3.	Representative EPMA data of Serpentine (Contd.)	106

LIST OF ABBREVIATIONS:

REE- Rare Earth Elements	Dy-Dysprosium
%- Percent	Eu- Europium
Al- Aluminium	O- Oxygen
Ba- Barium	Si- Silica
Ca- Calcium	P- Phosphorus
Co- Cobalt	K- Potassium
Cr-Chromium	Ti- Titanium
Cs-Cesium	Pr- Praseodymium
Nd- Neodymium	Ho- Holmium
Sm- Samarium	Tm- Thulium
Gd- Gadolinium	Yb- Ytterbium
Tb- Terbium	Lu- Lutetium
Mn- Manganese	U- Uranium
TiO ₂ – Titanium Oxide	Na- sodium
MnO- Manganese Oxide	La – Lanthanum
CO ₂ -Carbon Dioxide	Sr- Strontium
Fe- Iron	Cs- Cesium
Mg- Magnesium	Zr- Zircon
Ni- Nickel	Hf- Hafnium

Ta- Tantalum	FZ- Fracture zone
Th- Thorium	CR- Carlsberg Ridge
U- Uranium	SEIR- South East Indian Ridge
Sc- Scandium	SWIR- South West Indian Ridge
Pd- Palladium	NCIR- Northern Central Indian Ridge
Pt- Platinum	HFSE- High Field Strength Elements
Pb- Lead	Ppm- Parts per million
Rh- Rhodium	LREE- Light Rare Earth Elements
Ir – Iridium	MREE- Middle Rare Earth Elements
Os- Osmium	HREE- Heavy Rare Earth Elements
Ru- Ruthenium	EPMA- Electron Probe Micro
CIR- Central Indian Ridge	Analyses
RTJ- Rodrigues Triple Junction	PPL- Plane Polarised Light
BXP- Between Cross Polars	HR-IC-PMS- High Resolution
V- Vanadium	Inductively Coupled Plasma Mass
Nb- Niobium	Spectroscopy
	LILE- Large Ion Lithophile Elements
	PGE- Platinum Group elements

CHAPTER I: INTRODUCTION

1.1. Serpentinised peridotite

To understand the rock type Serpentinised peridotite it is crucial to know what peridotite is so to begin with, Peridotite is an igneous rock that is dense and coarse-grained, mostly made up of the silicate minerals pyroxene and olivine. Since fewer than 45% of the rock is silica, peridotite is ultramafic. It has a high magnesium (Mg^{2+}) content because to the significant amounts of magnesium-rich olivine and iron. The Earth's mantle is the source of peridotite, which can be found there as crystals collected from magmas that originated in the mantle or as solid blocks and pieces. Peridotites from these layered igneous complexes have a wide range of compositions, which are indicative of the relative amounts of pyroxenes, chromite, plagioclase, and amphibole. The predominant rock in the upper mantle of Earth is peridotite.

Classification of Peridotites:

Ultramafic rocks are coarse-grained igneous rocks that contain more than 90% of their volume in mafic minerals, which are rich in iron and magnesium. Usually, these rocks have less than 45% silica in them. The most common families of mafic minerals found in most ultramafic rocks are olivine, orthopyroxene, clinopyroxene, and hornblende. These rocks are further categorised based on the relative amounts of these minerals. The term "peridotite" then refers to coarse-grained ultramafic rock in which at least 40% of the four mineral families present in the rock are olivine.

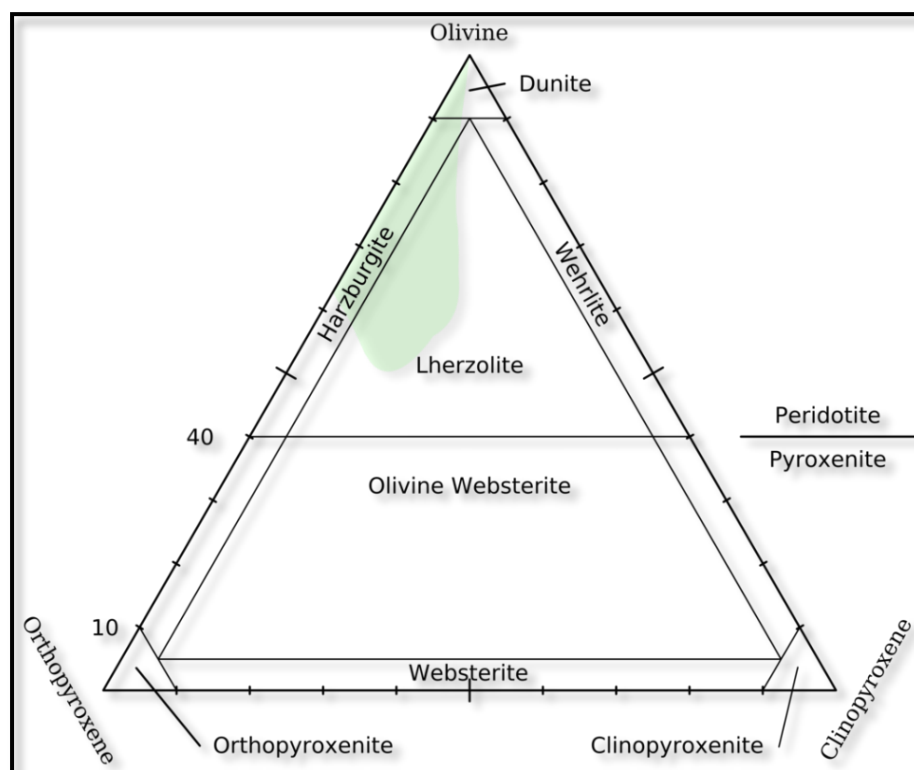


Figure.1.1 Classification diagram for peridotite and pyroxenite, based on proportions of olivine and pyroxene. The pale green area encompasses the most common compositions of peridotite in the upper part of the Earth's mantle (partly adapted from Bodinier and Godard (2004)).

Source: Peridotite Olivine-Orthopyroxene-Clinopyroxene - Common Peridotites highlighted - Peridotite - Wikipedia

Here are several further classifications for peridotites:

1.Dunite: More than ninety percent of dunite is olivine. The peridotite layer of ophiolites contains noticeable veins of dunite, which are thought to be pieces of oceanic lithosphere (upper mantle and crust) that have been driven onto continents. In layered intrusions, when olivine crystallised out of a slowly cooling magma body and collected on the magma body's floor to create the lowest layer of the intrusion, dunite can also exist as a cumulate. Accessory chromite is nearly always present in dunite.

2.Kimberlite: composed of at least 35% olivine and produced in volcanic pipes
Diamonds are known to be hosted in kimberlite, a highly brecciated type of peridotite

that forms in volcanic pipes. Kimberlite is far more uncommon than other peridotite varieties.

3. Pyroxene peridotite: From 40% to 90% olivine and less than 5% hornblende

3.1. Harzburgite: less than 5% clinopyroxene.

The majority of ophiolites' peridotite layer is composed of harzburgite. It is thought to be depleted mantle rock that has had basaltic magma removed from it. In Type I layered intrusions, it also occurs as a cumulate, creating a layer just above the dunite layer. Most of the mantle lithosphere under continental cratons is probably composed of harzburgite. (Herzberg, 2004)

3.2. Wehrlite: less than 5% orthopyroxene.

A portion of the transition zone between the peridotite layer and the ophiolites' gabbro layer that covers it is made up of wehrlite. It replaces harzburgite as the layer immediately above the dunite layer in Type II layered intrusions.

3.3. Lherzolite: clinopyroxene and orthopyroxene concentration in an intermediate state.

Most of the upper mantle is assumed to be composed of lherzolite. It is the most likely source rock for basaltic magma and is nearly identically composed of one-part tholeiitic basalt (pyrolite) and three parts harzburgite. In basalt, it can be discovered as uncommon xenoliths in locations like Kilbourne Hole in southern New Mexico, US, and Oahu, Hawaii, US. (Yang et al., 1998)

4. Hornblende peridotite:

Between 40% and 90% olivine and fewer than 5% pyroxene make up hornblende peridotite.

Rare xenoliths called hornblende peridotite can be discovered in andesites above subduction zones. They provide concrete proof that fluids produced by the subducting slab have altered the mantle rock. (Blatter & Carmichael, 1998)

5. Pyroxene hornblende peridotite:

In between pyroxene peridotite and hornblende peridotite is pyroxene hornblende peridotite.

Rare xenoliths called pyroxene hornblende peridotite, can be discovered in places like Wilcza Góra in southwest Poland. Here, it most likely developed as a result of volcanism-related carbonated hydrous silicic fluids altering the mantle rock. (Matusiak-Małek et al., 2017)

Now, it is very important to know that apart from all these various rock types belonging to the peridotite rock family there is one more type of Peridotite of geologic importance and found on the most interesting tectonic settings those are mid oceanic ridges and the rock type is Serpentinised Peridotite.

The term "Serpentined peridotite" describes a particular kind of rock that has experienced the geological phenomenon known as serpentinization. Pyroxene and olivine make up the majority of the coarse-grained igneous rock known as peridotite. Peridotite absorbs water during serpentinization, which causes it to change mineralogically.

As shown in **Figure (1.2)** when olivine in peridotite becomes hydrated, it changes into serpentine minerals like lizardite, antigorite, and chrysotile. This process is known as serpentinization. These serpentine minerals resemble waxy or fibrous materials and are usually greenish in colour. The rock type consist of the minerals spinel, magnetite,

talc, tremolite, brucite other than olivine and pyroxene. The process is frequently linked to the tectonic plate boundaries, where the interaction between oceanic lithosphere and seawater causes it to become hydrated.



Figure: 1.2. Peridotite undergone phenomenon called Serpentinisation.

There are several different geological places where serpentinized peridotite can be found, such as subduction zones, ophiolite complexes (where portions of the oceanic lithosphere are exposed on land), and oceanic habitats. Serpentinised peridotite can have significant effects on the geochemistry and dynamics of the Earth's mantle. It can even have the ability to support distinct organisms in harsh settings like deep-sea hydrothermal vents. Furthermore, the study of certain geological processes, such the movement of water and elements through the Earth's crust, has shown interest in serpentinized peridotite.

Serpentinization modifies the physical characteristics of rocks. In serpentinites, the density drops dramatically from 3300 kg/m³ in non-serpentinized peridotites to about 2600 kg/m³. Furthermore, during this phase, the speed at which seismic waves propagate diminishes. In comparison to olivine and pyroxenes, serpentine is less tolerant of deformation; even a modest amount (15–20%) of serpentine in peridotites can lessen the rock's resistance to deformation and promote fault migration.

1.1.1. Classification of serpentinized peridotite based on tectonic setting:

Depending on the tectonic environments in which they occur, serpentinized peridotites may display differences. Diverse tectonic settings impact the serpentinization process, resulting in the formation of distinct varieties of serpentinized peridotite. According to tectonic settings, the following categories exist:

The term "abyssal serpentinized peridotite" refers to peridotite that has been hydrated along mid-ocean ridges. This kind of peridotite is found in marine settings. The process of seafloor spreading in these conditions involves the contact of mantle rocks with saltwater. When fresh oceanic crust is formed, peridotite frequently undergoes serpentinization.

Ophiolitic Serpentinites: Projections of oceanic lithosphere onto continental edges are known as ophiolites. Different forms of serpentinized peridotites can be found inside ophiolites, depending on the degree of serpentinization and the particular mineral assemblages that are present. These rocks shed light on the processes taking place at mid-ocean ridges and the makeup of the Earth's mantle.

Serpentines in the Forearc:

Forearc serpentinites as shown in **Figure (1.3)** are formed when the descending oceanic plate experiences hydration and serpentinization in subduction zones, which are regions where two tectonic plates fall beneath one other. Antigorite is frequently the main component of these serpentinites, which are linked to high pressure and low temperatures.

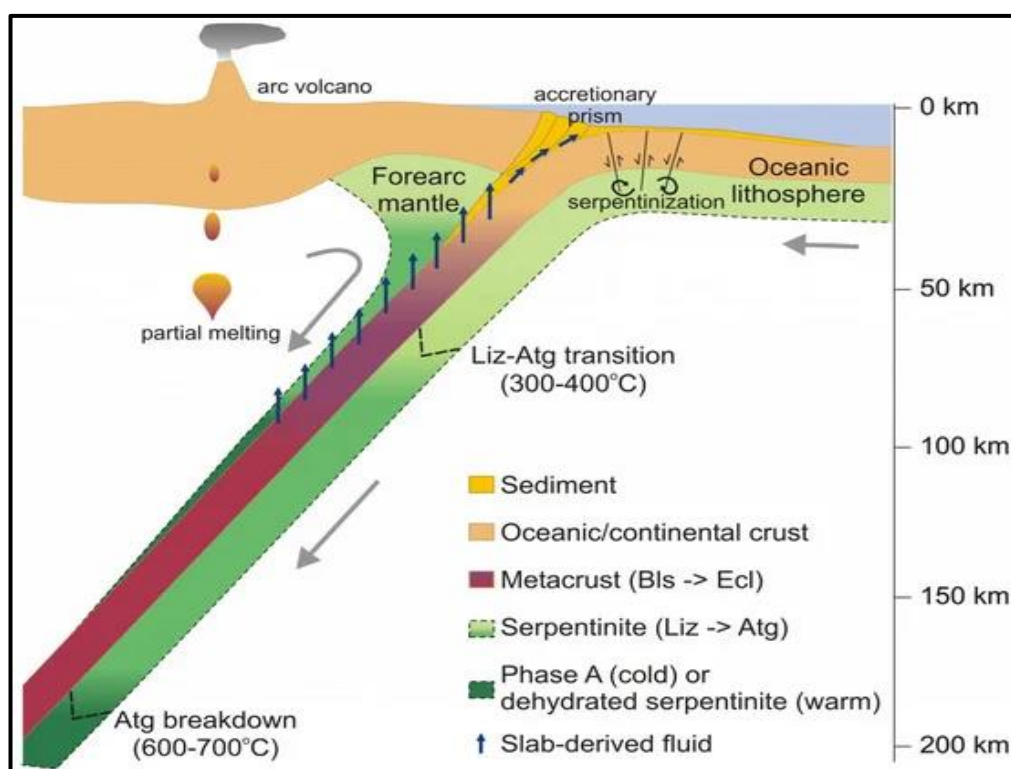


Figure: 1.3. Schematic model of formation of serpentinites in forearc regions, Abyssal serpentinites are from Hattori, K. (2019).

Source: minerals-09-00061-g002.png (2465×2123) (mdpi.com)

Spinel Serpentinites:

Subduction zones in the overriding plate are the source of back arc serpentinites. In reaction to extensional tectonic stresses, they are the outcome of mantle material upwelling and subsequent serpentinization. The mantle dynamics may be understood

by examining the different serpentine minerals that may be present in these serpentinites.

Mantle Wedge Serpentinites:

The wedge-shaped area above the subducting slab is where mantle wedge serpentinites originate in specific subduction conditions. In this area, the hydration of mantle rocks may lead to the formation of serpentinites with particular mineralogical traits.

Continental Serpentinites:

Serpentinized peridotites may also be found in continental environments, and they are frequently linked to prehistoric orogenic events. Mountain ranges and continental rift zones may contain these serpentinites.

Transform Fault Serpentinites:

Serpentineites may be found on transform faults, which are places where tectonic plates move past one another horizontally. Transform faults can cause shearing and fracture, which can lead to the serpentinization of peridotites.

Serpentinite connected to the Rift:

Serpentineized peridotite may also be found in rift settings, which are created when tectonic plates collide. This kind of serpentinite is linked to extensional tectonic processes and may contain a mixture of serpentine minerals.

In some geological contexts, these varieties of serpentinized peridotite can overlap and are not mutually exclusive. In a particular tectonic environment, the fluid composition,

the history of tectonic deformation and metamorphism, and the current pressure-temperature circumstances all affect the unique properties of serpentinized peridotite.

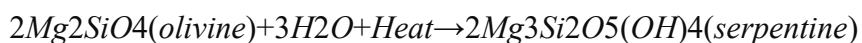
1.1.2. Formation of serpentinised peridotite:

In the oceanic lithosphere, serpentinized peridotite is frequently encountered, particularly along mid-ocean ridges. It is an important part of the Earth's mantle and is connected to tectonic plate boundaries.

Serpentinized peridotite is a rock formed via the serpentinization process. Ultramafic rocks, including peridotite, when undergo alteration in this geological process when they come into contact with water and/or carbon dioxide. The primary constituents of peridotite are olivine, pyroxenes (often enstatite and/or diopside), and trace quantities of other minerals.

As a result, they form a mineral assemblage with serpentine minerals.

The primary reaction involved in serpentinization is the hydration of olivine, the dominant mineral in peridotite. Olivine reacts with water to form serpentine minerals, typically antigorite, lizardite, or chrysotile, depending on pressure, temperature, and fluid composition. The chemical reaction for the serpentinization of olivine can be simplified as follows:



This process releases heat and consumes water, which can lead to the generation of hydrothermal fluids and alteration of the surrounding rock.

Hydrogen gas is also the result of this process. Serpentinization frequently results in increased volume, which causes the rock to enlarge. General structure of the rock may

change causing fractures. Also, certain elements, such as magnesium release and the absorption of water and other ions, might become mobile.

When tectonic plates converge, serpentinized peridotite can be carried into subduction zones. Deep-sea trenches and volcanic arcs may occur as a result of subduction zone dynamics influenced by water released during serpentinization.

1.1.3. Importance of studying serpentinized peridotite:

There are a number of reasons why studying serpentinized peridotite is important, including geological, environmental, and economic ones. The following are some main reasons to research serpentinized peridotite:

Firstly, Peridotite that has been serpentinized offers a glimpse into the mantle's processes. Comprehending the serpentinization process of ultramafic rocks advances our understanding of the geochemistry of deep Earth processes, water-rock interactions, and mantle dynamics.

Serpentinized peridotite is frequently found along tectonic plate boundaries, such as subduction zones and mid-ocean ridges. By examining these rocks, we may better comprehend plate tectonics and the underlying dynamics of the Earth by gaining insight into the processes taking place at these significant geological sites.

Water is taken up by serpentinization and discharged into the mantle, where it changes the fluid chemistry. Studying serpentinized peridotite offers insights on the transfer of water and other elements between the Earth's surface and interior. This process is essential to the planet's water cycle.

The dynamics of subduction zones can be affected by the subduction of serpentinized peridotite. Volcanic arcs, deep-sea trenches, and other geological features connected

to subduction zones can be explained by an understanding of these rocks' function in subduction processes.

Secondly, Minerals that are commercially useful, such nickel and asbestos, can be found in serpentinized peridotite. Economic geology will be impacted by the exploration of these rocks because it will reveal possible mineral deposits and resources that can be taken out for a range of industrial uses.

Stable carbonate minerals can be formed when carbon dioxide reacts with serpentinized peridotite. This procedure has been investigated as a possible carbon capture and sequestration technique, providing a means of lessening the atmospheric effects of carbon dioxide emissions.

Another reason for studying this rock type is deep under the Earth's crust, serpentinization can generate conditions that are favourable for microbial life. Researching the microbial communities linked to serpentinized peridotite advances our knowledge of the deep biosphere and the possibility of life under harsh circumstances.

Understanding the serpentinization of peridotite on Earth can help us understand comparable processes occurring on other planets and celestial bodies. Studying the geological mechanisms associated with ultramafic rocks bears significance for both planetary science and our more extensive comprehension of the solar system.

From a geochemical standpoint, the main goal of researching serpentinized peridotite is to decipher the complex chemical changes that take place throughout the serpentinization process. These geological phenomena are the creation of serpentine

crystals as a result of the hydration of peridotite, an ultramafic rock that is rich in olivine and pyroxene minerals. Close examination of the fluid composition during serpentinization, highlighting the significance of water in changing the rock's mineralogical composition. Serpentinized peridotite geochemical investigations give important insights into the mobilisation and sequestration of elements in the Earth's mantle, providing a window into the geochemical cycle of the mantle.

Furthermore, as serpentinized peridotite deposits are frequently linked to commercially significant metals like nickel and chromite, these studies aid in understanding the effects of serpentinization on the distribution of these elements. Our knowledge of Earth's tectonic processes, mantle dynamics, and the wider implications for global elements cycling are greatly enhanced by an understanding of the geochemistry of serpentinized peridotite.

1.2. Geochemistry:

The study of chemical composition of the Earth and other planets, chemical processes and reactions that govern the composition of rocks and soils it also includes the cycles of matter and energy that transport the Earth's chemical components in time and space and their interaction with the hydrosphere and the atmosphere.

Geochemistry studies the origin, evolution and distribution of chemical elements on Earth which are contained in the rock forming minerals and the products derived from it, as well as in living beings, water and atmosphere. One of the goals of geochemistry is to determine the abundance of elements in nature, as this information is essential to hypothesis development about the origin and structure of our planet and the universe.

Major elements:

Determines the proportions of rock-forming minerals such as feldspar, quartz, micas, olivine, pyroxenes and amphiboles. They are abundant and typically make up more than 1% of a rock's composition. They are in order of increasing atomic number O, Na, Mg, Al, Si, P, K, Ca, Ti, Mn and Fe. The bulk Earth, including the crust, mantle, and metallic core, primarily consists of these major elements.

Minor Elements:

Falling between major and trace elements, minor elements make up **0.1–1 wt%** of a system. They are not essential to a phase's structure and do not directly impact its properties. Instead, minor elements occur passively as dissolved constituents or in small amounts within accessory phases. Example includes TiO_2 , MnO , P_2O_5 , CO_2 .

Trace Elements:

These elements are present in even smaller quantities, constituting less than **0.1 wt.%**. They do not significantly influence a phase's properties but occur as dissolved constituents or minor accessory phases.

Electronic structure of lithophile Trace elements is such that they can be modelled as approximately as hard spheres; bonding is primarily ionic. Geochemical behaviour of lithophile trace elements is governed by how easily they substitute for other ions in crystal lattice.

This substitution depends primarily by two factors 1) the ionic charge and 2) ionic radius.

The greater the difference in charge or radius between the ion normally in the site and the ion being substituted the more difficult the situation.

Classification based on the radii and charge of the elements and are divided into

1. Rare Earth Elements (REE),
2. Large Ion Lithophile Elements (LILE),
3. High Field Strength Elements (HFSE),
4. Transition elements and
5. Platinum Group elements (PGE)

1. Rare Earth Elements (REE):

A group of elements with atomic numbers between 57 (La) and 72 (Lu) having large ionic radii and valences of either +2 or +3. Occur together in nature forming the lanthanide series and are difficult to separate. LREE: La, Ce, Pr, Nd.; MREE: Sm, Eu, Gd.; HREE: Tb, Dy, Ho, Er, Tm, Yb, Lu.

The lanthanides have similar outer electron orbit configuration and an ionic charge of +3 (except Ce and Eu under certain conditions which can be +2 and +4 respectively).

Ionic radius shrinks steadily from La to Lu filling f orbitals and this is called lanthanoid contraction. As a consequence, geochemical behaviour varies smoothly from highly incompatible (La) to slightly incompatible (Lu).

2. Large Ion Lithophile Elements (LILE):

Elements having large ionic radius and low ionic charge with Ionic radius/ionic charge ratio is large. Ionic radii greater than Ca^{2+} and Na^{1+} , the largest cations common to rock forming minerals. Elements include K, Rb, Sr, Ba, Cs.

3. High Field Strength Elements (HFSE):

Elements having high ionic charge and with ionic charge to ionic radius ratio ($Z/r > 2$).

Elements include Zr, Hf, Nb, Ta, Ti, Th and U

4. Transition elements:

Elements having small ionic radii and strongly partitioned into the solid phases that crystallize during the early stages of magmatic evolution. Elements include Ni, Co, Cr, Sc.

5. Platinum Group Elements:

Platinum Group Elements (PGE) includes Pd, Pt, Rh (PPGE) and Ir, Os, Ru (IPGE) and are Siderophile and chalcophile in nature. This group of elements is abundant in ultramafic rocks.

Serpentinised peridotite rock having geochemical implications, it is very important to understand and study the geochemistry of this rock. Firstly, Major, minor, and trace elements provide valuable information about the origin, evolution, and transformation of geological materials. They can be used to unravel processes such as magma generation, crustal recycling, and ore formation. To locate possible mineral resources and assess their economic feasibility, geochemical examination of major, minor, and trace elements is necessary.

Fundamental ideas in geochemistry, the distribution and categorization of major, minor, and trace elements have a big impact on how we understand Earth processes, resource development, environmental management, and the interpretation of the geological record.

1.3. Regional geology:

With an area of around 20% of the water on Earth's surface, or 70,560,000 km² (27,240,000 sq mi), the Indian Ocean is the third biggest of the world's five oceanic divisions. (Eakins & Sharman 2010) Australia is to the east, Africa is to the west, and Asia is to the north. Depending on the definition being used, it is bordered to the south by Antarctica or the Southern Ocean. The Arabian Sea, Laccadive Sea, Bay of Bengal, and Andaman Sea are only a few of the major marginal or regional seas that encircle the Indian Ocean. The Latitude of Indian Ocean is -20° 00' 0.00" S and Longitude is 80° 00' 0.00" E.

The Indian Ocean plays a key role in the global climate system, enabling upwelling of the lower cell of the meridional overturning circulation from abyssal to upper-deep and intermediate waters through diffusive mixing (Schmitz, 1995; Lumpkin and Speer, 2007; McDonagh et al., 2008; Talley, 2013; Hernández-Guerra and Talley, 2016) and exporting the largest poleward heat flux of all Southern Hemisphere basins (Roxy et al., 2014). In recent decades, the upper 700 m of the entire Indian Ocean has warmed rapidly (Desbruyères et al., 2017). In the southern Indian Ocean, the warming was directly linked primarily to heat advection from a strengthened Indonesian Throughflow (ITF) and secondly to a decrease in mean air–sea flux cooling (Li et al., 2017b; L. Zhang et al., 2018). This coupling between the ocean and atmosphere in the Indian Ocean and Pacific Ocean shifted the balance of global warming, accelerating ocean warming and causing a hiatus in the warming of Earth's surface atmosphere. Marine heatwaves have emerged as an increasing threat to marine ecosystems as ocean temperatures warm (e.g. Oliver et al., 2018). Increasingly vulnerable populations need more reliable monsoon predictions, a task complicated by variability across timescales

from intra-seasonal to interannual, decadal, and beyond in a tightly coupled ocean–atmosphere system (Hazra et al., 2017).

While we discuss about the air sea interaction as it is important to know that from the locally intense heat and moisture fluxes that fuel tropical cyclones to large-scale convection in the ascending branch of the Hadley circulation and basin-scale ocean heat transport carried by overturning cells that contribute to decadal variability and trends, the tropical Indian Ocean is highly variable across multiple scales, all of which involve atmosphere–ocean interaction. Strong air-sea interaction is involved in the intra-seasonal oscillations at intermediate timeframes (e.g. DeMott et al., 2015). One instance of an intrinsically connected mode of variability is the Indian Ocean Dipole (IOD) (Saji et al., 1999; Webster et al., 1999; Murtugudde et al., 2000). The significant sea-to-air moisture fluxes and warm sea surface temperatures in the Indian Ocean region are the main drivers of the monsoonal rains. Monsoon reconstructions from the northern Indian Ocean suggest that the SW monsoon weakened and NE monsoon intensified during glacial periods (Prell et al., 1980; Cullen, 1981; Duplessy, 1982; Fontugne and Duplessy, 1986)

Water circulation at the southern tip of the Indian peninsula experiences seasonal changes, a low saline-water current from the BoB in winter monsoon whereas in summer monsoon the current reverses and brings in high salinity water from the Arabian Sea at depths of 0–100 m. This region experiences upwelling during the summer monsoon, leading to high productivity in this region (Levy et al., 2007). However, upwelling ceases towards the South and productivity then is not related to upwelling but to deepening of the mixed layer depth (Schulte et al., 1999). In the central equatorial Indian Ocean (CEIO), winds are weak nearer the equator during SW and NE monsoons, while high winds occur in this region during monsoon transition

periods (Shaji and Ruma, 2020) and surface productivity conditions are circulation induced (Strutton et al., 2015).

One of the main characteristics of the Indian Ocean is mid-ocean ridges. Divergent plate borders, where tectonic plates are pulling apart and enabling magma to fill up and form new oceanic crust, are marked by these underwater mountain ranges. This Indian Ocean is consisting of the ridge system of four Mid oceanic Ridges those are Central Indian Ridge, Carlsberg Ridge, South east Indian Ridge, South West Indian Ridge.

The (CIR) located in the middle of the Indian Ocean, is a significant underwater mountain range, where tectonic plates are diverging at this plate boundary, magma is able to emerge from the Earth's mantle and form new oceanic crust. Coordinate includes Latitude $34^{\circ} 39' 19.8''$ S, and Longitude $54^{\circ} 28' 58.08''$ E as shown in **Figure (1.4)**. The axial valley is 500–1000 m deep; 50–100 km-long ridge segments are separated by 30 km-long transform faults and 10 km-long non-transform discontinuities. Melt supply comes from axial volcanic ridges that are 15 km-long, 1–2 km wide, and reaches 100–200 m above the axial floor (Murton et al. 2005).

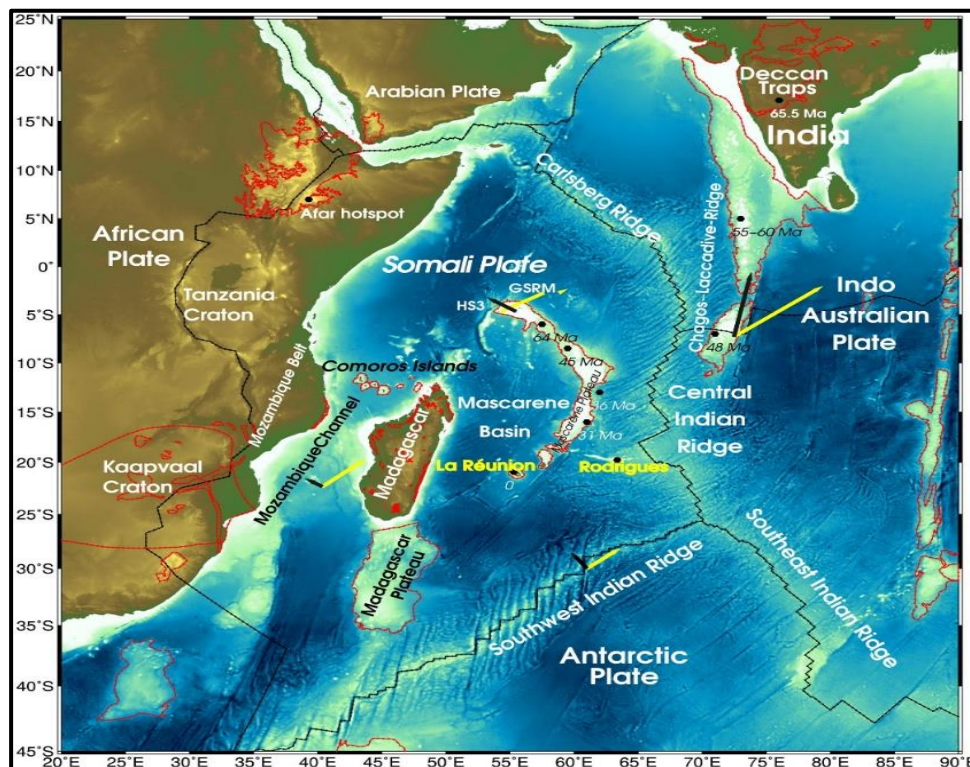


Figure:1.4. Map of Indian Ocean showing Ridge system- Central Indian Ridge, from (Mazzullo et al., 2017)

Source: Bathymetry-and-topography-map-of-the-study-area-ETOPO1-Amante-Eakins-2009.png (850×905) (researchgate.net)

With a spreading rate of 30 mm/yr near the Equator and 49 mm/yr near the Rodrigues Triple Junction (RTJ) at its southern end, the CIR is an intermediately fast spreading ridge characterised by moderate obliquity and few large offsets, the obvious exception being the almost 300 km-long Mary Celeste Fracture Zone at 18°S. (Hellebrand et al. 2002)

Between 21°S and the Mary Celeste Fracture Zone (18°S) the CIR deviates westward. Along this section the larger offsets switch from right-lateral to left-lateral but return to right-lateral north of 18°S. (Murton et al. 2005).

Otherwise, the southern section (RTJ-Argo Fracture Zone, 25°S-13°S) of the CIR is near-orthogonal relative to the spreading direction. North of the Argo FZ it is highly oblique and dominated by numerous small ridge segments. The northern section of the CIR, including the Carlsberg Ridge, trends NNW and lacks fracture zones. The axial depth of the CIR increases from 3200 m at 20°S to 4000 m at the RTJ. (Hellebrand et al. 2002)

The Antarctic Plate to the east and the Indo-Australian Plate to the west are the two tectonic plates that separate at the Central Indian Ridge. Magma rises to fill the space left by these plates' separation, forming new oceanic crust.

There is a lot of volcanic activity on the Central Indian Ridge. Seamounts, hydrothermal vent systems, and underwater volcanoes can occur as magma rises to the surface. The region's ecological and geological richness is enhanced by these characteristics. The minerals that are released from these vents also influence the ocean floor's geology. Along the Central Indian Ridge, basalt is the most common form of rock. It occurs when quickly cooling, mantle-derived lava rises to the surface and turns into finely grained, dark-colored volcanic rock. Oceanic crust frequently consists of basalt, which is also found in the volcanic formations connected to mid-ocean ridges.

Related to basalt, gabbro is a coarse-grained, intrusive igneous rock. It originates from the solidification of mantle magma under the Earth's surface. Within the CIR gabbro is frequently located at a deeper level of the crust as a component of the intrusive complexes linked to the creation of oceanic crust.

Similar to basalt chemically, dolerite is an intrusive, medium-grained igneous rock. It frequently manifests as oceanic crust dikes, or vertical intrusions. The solidification and cooling of magma beneath the seabed is linked to dolerite dikes.

When lava explodes underwater, a unique kind of basalt known as pillow basalt forms. Structures in the form of pillows are created when lava cools and becomes quenched quickly. The Central Indian Ridge locations where volcanic activity is actively forming new oceanic crust are where these formations are most frequently seen.

Tectonic forces have exposed pre-existing rocks to high pressure and temperature, leading them to undergo metamorphism. These locations are home to metamorphic rocks including gneiss and schist.

Peridotite is essential to the geological processes along mid-ocean ridges, such as the Central Indian Ridge (CIR), even though it is not commonly exposed at the Earth's surface.

Peridotite makes up the majority of the Earth's mantle. Magma emerges from the mantle to form new oceanic crust as tectonic plates divide along mid-ocean ridges. The partial melting of peridotite in the mantle is the source of this rising magma. Also, rocks such as serpentinites are found in the CIR and the fracture zones making the geology most interesting and significant for scientific exploration.

As well as there are occasional peridotite xenoliths/fragments of mantle rock that have been exposed by volcanic eruptions in volcanic rocks connected to mid-ocean ridges.

1.4. Study area and location:

The study area includes understanding of the Indian Ocean in broader aspects so basically Indian Ocean is the third largest ocean in the world's five oceanic divisions, covering more than 70,000,000 km² water on the surface of earth.

The coordinates include Latitude -20° 00' 0.00" S and Longitude is 80° 00' 0.00" E and maximum length of 9,600 km from Antarctica to Bay of Bengal. This Indian Ocean is consisting of the ridge system Central Indian Ridge, Carlsberg Ridge, South east Indian Ridge, South West Indian Ridge are the four Mid oceanic Ridge systems in the Indian Ocean. The central Indian ridge is a North-South trending mid oceanic ridge in the western side of the Indian Ocean, it is a slow to intermediate spreading ridge and is traditionally said to separate the African plate from the Indo-Australian Plate. Furthermore, the study area is located between Vema fracture zone and vityaz fracture zone on Central Indian ridge (Latitude 6°38.506 (°S), longitude 68 °19.340 (°E)) as shown in **Figure (1.5)**. Approximately 1200 Kg of dredge sample which includes serpentinite, serpentinite basalt, Gabbro and calcareous sediments was retrieved. Chain bag dredge was used for successful recovery of Serpentinites from depth of 2700m. Rocks are of varying sizes between 2.5 to 50cm. Certain samples exhibit distinct striations and slickenside structure, Fe-Mn oxides in a brownish black coating are present. The green tints in the rocks might be olivine, serpentine, or chlorite, and there are white or pink feldspar mineral streaks throughout. Fe-Mn oxides in a brownish-black coating are seen in a few samples. There is a flaky, rectangular micaceous mineral present in several samples, which suggests metamorphic processes. Biological creatures such as shell pieces and tubes of benthic foraminifera were gathered in addition to the samples of rock and mud.

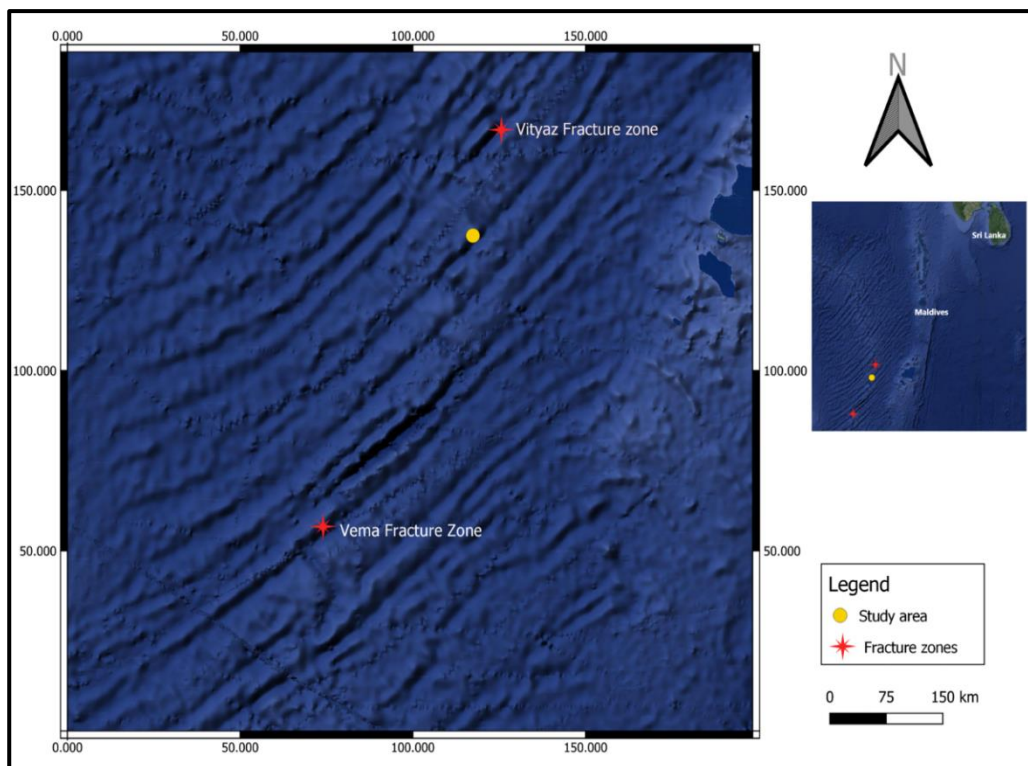


Figure: 1.5. Study area and location map, on Central Indian Ridge between Vema and Vityaz Fracture Zone.

1.5.Sampling Approach:

Carlsberg Ridge (CR), Central Indian Ridge (CIR), South West Indian Ridge (SWIR), and South East Indian Ridge (SEIR) are the four mid-ocean ridge systems in the Indian Ocean. The CR, CIR, and Andaman backarc systems are less investigated than the SWIR and a portion of the SEIR among these ridge systems. The CIR spreading axis is traced from north of the Vema fracture zone.

Now, expedition by voyages has been done in the year 2003 to explore and to do scientific study of the CIR, where in the second of four voyages slated for the joint CSIR-DOD Network Programme themed "Tectonic and Oceanic processes along the Indian ridge system and the backarc basins" is the SK-195 cruise aboard ORV Sagar

Kanya. Obtaining Multibeam Swath Bathymetry (Hydrosweep) bathymetry, Geophysical data, and conducting CTD observations were the primary goals of the voyage. Additionally, water, sediment, and rock samples were to be collected at specific places for geological, biological, physical, and chemical oceanographic investigations. With the use of geological, chemical, and biological signs, these research hope to define the hydrothermal mineralization zones and characterise the ridge axis in terms of tectonic segmentation.

There were 39 sample activities conducted in all, comprising 2 spade core operations, 14 dredge operations using chain bag dredge, and 23 deep CTD casts. On the off-axis highs and within the rift valley zone, the CTD casts are chosen. The swath bathymetric map showed that the whole rift valley was measured at intervals of around 10 to 15 miles. The purpose of these activities was to investigate the chemical fingerprints near the bottom. An altimeter was used to lower and suspend the CTD to a height of approximately 5 metres over the seafloor. There were nine successful dredging operations out of a total of fourteen; the recovered weight ranged from 5 kg to 900 kg, and the rocks collected were diverse.

While 14 dredging operations were completed, DR # 01—the first chain bag dredge—was lost. A pipe dredge was employed in the second, third, and fourth operations, but no recovery was obtained. A chain bag dredge was utilised for dredging tasks ranging from 5 to 14". DR#06, DR#09, and DR#14 surgeries resulted in several successful recoveries. Few biological samples, such as prawns and brittle stars, were gathered by DR#5 and DR#7, however DR #8 did not gather any samples.

Rocks were found in a number of topographic areas, including the Kurchatov Seamount, the rift valley, and the rift flanks. The samples that were gathered included gabbros, pumice, serpentinites, fresh and aged columnar and pillow basalts, and the surrounding calcareous silt. A thin layer of ferromanganese coating was seen on a few samples.

Individual chain bag dredge sampling was carried out and the serpentinites were found in the DR#9, where in Approximately 1200 kg of various rocks, including conglomerate/breccia, pumice, gabbros, and serpentinites, were retrieved by the dredge. This Chain bag dredge sample was retrieved from depth of 2700 meters with latitude $06^{\circ} 38.506$ (S $^{\circ}$) and longitude $68^{\circ}19.340$ (E $^{\circ}$). Calcareous sediment was discovered to accompany the rocks, as demonstrated by a reaction with diluted HCl. The size of the rock ranges from 2.5 cm to 50 cm. The green tints in the rocks might be olivine, serpentine, or chlorite, and there are white or pink feldspar mineral streaks throughout. Fe-Mg oxides in a brownish-black coating are seen in a few samples. Certain samples exhibit distinct striations that signify both shearing characteristics and slickenside structure. There is a flaky, rectangular micaceous mineral present in several samples, which suggests metamorphic processes. Biological creatures such as shell pieces and tubes of benthic foraminifera were gathered in addition to the samples of rock and mud.

1.6. Aims and Objective:

The objective of this geochemical investigation is to thoroughly examine serpentinised peridotite samples that were obtained from the Indian ocean. The study will specifically concentrate on clarifying elemental compositions in order to improve our comprehension of geological processes within the distinct marine habitat.

Objective of the study includes:

1. Conduct petrographic analyses of serpentinized peridotite to assess mineralogy, inclusions, veins, texture, structural features, and the degree of serpentinization.
2. Perform EPMA and geochemical studies to investigate fluid influence during serpentinization, mineral replacement and element mobility.
3. Determine the tectonic setting of serpentinized peridotite to understand its geological context.
4. Investigate the mantle source characteristics to elucidate the origin, evolution, melt-rock interactions, and degree of melting in the serpentinised peridotite.

1.7. Brief structure:

The chemical makeup of rocks containing serpentine minerals that result from peridotite alteration is examined in a geochemical study of serpentine peridotite. Research of this kind sheds light on tectonic settings, Earth's lithosphere development, and geological processes. Peridotite is the parent rock from which basaltic lava is partially melted. Because the peridotite melt is less thick than the leftover solid, it rises to the Earth's surface and fuels volcanic activity and the creation of oceanic crust. Peridotite has a direct impact on plate tectonics, affecting how tectonic plates behave at mid-ocean ridges and subduction zones. It is essential to the lithosphere's formation, recycling, and differentiation on Earth. Our knowledge of the Earth's interior structure, heat distribution, and the mechanics behind geological processes is aided by the study of peridotite. It facilitates the deciphering of the intricate relationships that exist between the Earth's surface and the mantle, including the genesis and development of oceanic and continental crust. Evaluating the concentrations of major and trace elements in the serpentine peridotite samples is one of the objectives of the geochemical research of serpentine peridotite is to determine changes in elemental abundances to study the rock's geochemical properties. Examine any associations or irregularities that can shed light on the petrogenesis and modification history. Evaluating the concentrations of major and trace elements in the serpentine peridotite samples is one of the objectives of the geochemical research of serpentine peridotite.

The study area is situated in Indian Ocean between Vityaz and Vema Fracture zone. This Chain bag dredge sample was retrieved from depth of 2700 meters with latitude $06^{\circ} 38.506$ (S $^{\circ}$) and longitude $68^{\circ} 19.340$ (E $^{\circ}$). Carlsberg Ridge, Central Indian Ridge, South West Indian Ridge, and South East Indian Ridge are four mid-ocean ridge

systems in the Indian Ocean. These systems, including the Andaman Sea region's backarc spreading system, offer opportunities to study global ridge systematics. However, they are less studied than SWIR and SEIR. The CSIR-DOD Network Programme is embarking on a SK-195 cruise aboard ORV Sagar Kanya, aiming to collect hydrothermal bathymetry, geophysical data, and CTD observations, as well as collect water, sediment, and rock samples for geological, biological, physical, and chemical oceanographic investigations. During 14 dredging operations, the first chain bag dredge was lost, and several successful recoveries were made. Rocks were found in topographic areas like the Kurchatov Seamount, rift valley, and rift flanks. Samples included gabbros, pumice, serpentinites, fresh and aged basalts, and calcareous silt. A thin layer of ferromanganese coating was observed on some samples. The DR#9 sample retrieved approximately 1200 kg of rocks, including serpentinites, from depths of 2700 meters. Calcareous sediment was found, and some samples exhibited distinct striations and metamorphic processes. The Core is retrieved from NIO repository and further was sent to Lab Crystal Kolkata, to prepare thin sections which was made in order to assess the degree of serpentinization and identify the mineral assemblages by studying the thin sections under a polarising microscope Nikon LV E200, considering the quantity of serpentine minerals and any related phases. Further the rock samples were prepared to identify and measure the mineral phases included in the serpentine peridotite, use mineralogical techniques such as High Resolution Inductively Coupled Plasma Mass Spectrometry (HR-ICPMS) or Electron Micro Probe Analysis (EPMA). By virtue of which the samples have undergone crushing under pulveriser, and then the powdered sample was analysed by decomposing the samples using acid mixtures and using standard procedures and by doing so the desired data for EPMA and HR-ICPMS was obtained. With help of the data obtained from the mentioned analytical

techniques various geochemical plots for EPMA data was plotted and observations were made, and along with EPMA, Major and Whole Rock Geochemistry with special emphasis on the certain Trace element is made in order to understand the origin, the genesis and the setting in which the rock must have originally formed. Data Interpretation will include presenting the data in geochemical plots, various graphs and diagrams highlighting the major and trace elements, this will be carried out in order to determine any patterns or irregularities in the data and connect them to other geological characteristics and the extent of serpentinization. By doing so will get the expected outcome will be to talk about the results' significance in relation to tectonic settings and mantle dynamics. Examination of the effects of subduction zones, mid-ocean ridge environments, and plate tectonic models on the detected geochemical fingerprints. The key findings will include observed changes in elemental abundances, which shed light on the rocks' geochemical properties. Identifying the mineral assemblages, including the quantity of serpentine minerals and related phases, and characterised the degree of serpentinization. Recognition of the geochemical ramifications of serpentinization, such as the, hydrogen release, and possible impacts on the Earth's water cycle along with combined field observations, such as the degree of serpentinization, mineralogical changes, and structural characteristics, with geochemical data. Linking certain geological characteristics to geochemical patterns might improve the understanding of the genesis and development of serpentine peridotite. The findings will also include filling up knowledge gaps and establish the groundwork for more research on the function of serpentine peridotite in Earth's processes.

CHAPTER II: LITERATURE REVIEW

The literature review consisting of the important studies which are carried out across the world in order to understand the studies done on Serpentinised peridotite a unique rock type. This previous work is consisting of various paper which tell us about the important findings in each study and also the research gaps which can be addressed and worked upon. This literature work also speaks about origin of the rock type, occurrence in different tectonic setting, worldwide occurrences of serpentinised peridotite.

2.1. Petrology and geochemistry of serpentinized peridotites from Hahajima Seamount in Izu-Bonin forearc region.

The study provides a comprehensive analysis of the petrology and geochemistry of serpentinized peridotites from Hahajima Seamount in the Izu-Bonin forearc region. The geological setting describes the location of Hahajima Seamount and the various proposed models for its origin. The samples collected from the seamount were heavily serpentinized and displayed a submarine weathering appearance. Analytical methods involved thin section preparation and geochemical analyses using X-ray fluorescence and Inductively Coupled Plasma-Mass Spectrometer.

The results and discussion highlighted that the ultramafic samples were extensively serpentinized, exhibiting a light greenish to yellowish color based on the degree of weathering. Whole rock geochemistry analyses revealed that the samples were MgO-rich (~42 wt%) with low Al_2O_3 , CaO, and TiO_2 contents. Additionally, the rare earth element abundances were found to be very low and variable. These findings contribute valuable insights into the composition and characteristics of the serpentinized peridotites in the region, enhancing our understanding of chemical recycling in subduction zones. Furthermore, the MgO-rich nature of the Hahajima serpentinized

peridotite samples suggests a potential link to the collision and subduction of the Ogasawara Plateau at 5 Ma, indicating a fault-bounded massif of forearc ophiolite uplift.

The article by Catherine Mével provides a comprehensive review of the mineralogical associations and conditions under which serpentinization occurs in abyssal peridotites at mid-ocean ridges. The research highlights the importance of serpentinites in the oceanic crust and their formation through serpentinization. The article discusses the typical mineralogical association found in serpentinites sampled in ridge environments, the fluid responsible for serpentinization, and how it interacts with the crust. The research also explores how serpentinization affects the trace element composition of peridotites and its implications for the formation of the oceanic crust. Overall, the article provides valuable insights into the processes that shape the oceanic lithosphere and the role of serpentinites in this context.

The paper acknowledges the lack of comprehensive knowledge about the geochemical compositions of serpentinites, the localities of serpentinization, and the potential sources of serpentinizing fluids. Further research could focus on filling these knowledge gaps to gain a more thorough understanding of serpentinite geochemistry in subduction zones. The present study suggests the need for more research on the potential sources of serpentinizing fluids and the geochemical effects of deep serpentinite dehydration. Investigating the origins and compositions of these fluids, as well as their impact on the surrounding geological environment, have provide valuable insights into subduction zone processes

The observed variability in rare earth element abundances in the Hahajima serpentinites raises questions about the factors influencing this variability and its

implications for the overall geochemical processes in the region. Further studies could aim to elucidate the underlying causes and significance of this variability.

The distinct geochemical signature of the Hahajima Seamount compared to typical IBM forearc serpentinite seamounts suggests a potential tectonic formation as a forearc ophiolite. Investigating the tectonic processes responsible for this unique signature and its implications for the broader understanding of seamount formation could be a valuable area for future research.

Addressing these research gaps could contribute to a more comprehensive understanding of serpentinite geochemistry, subduction zone processes, and the tectonic formation of seamounts in the Izu-Bonin forearc region.

The ultramafic samples collected from Hahajima Seamount were heavily serpentinitized, with olivine grains replaced by serpentine minerals, indicating significant hydration processes. The serpentinitized peridotite samples were found to be MgO-rich (~42 wt%) but had low contents of Al_2O_3 , CaO, and rare earth elements, consistent with the overall depleted character of their mantle protoliths. The study revealed strong enrichment in fluid-mobile and lithophile elements (Li, Sr, Pb, and U) in serpentinites from the Hahajima Seamount, with notable differences in enrichment patterns compared to other forearc seamounts in the region. The geochemical signature of the Hahajima serpentinites suggests a potential tectonic formation as a fault-bounded massif of forearc ophiolite, distinct from typical IBM forearc serpentinite seamounts. This finding has implications for understanding the tectonic processes and geological history of the region. It also contribute to our understanding the composition, formation, and geochemical characteristics of serpentinitized peridotites

in the Izu-Bonin forearc region, shedding light on the processes of hydration, element cycling, and tectonic formation in subduction zones.

2.2. Serpentinization of abyssal peridotites at mid-ocean ridges

The article by Catherine Mevel provides a comprehensive review of the mineralogical associations and conditions under which serpentinization occurs in abyssal peridotites at mid-ocean ridges. The research highlights the importance of serpentinites in the oceanic crust and their formation through serpentinization. The article discusses the typical mineralogical association found in serpentinites sampled in ridge environments, the fluid responsible for serpentinization, and how it interacts with the crust. The research also explores how serpentinization affects the trace element composition of peridotites and its implications for the formation of the oceanic crust. Overall, the article provides valuable insights into the processes that shape the oceanic lithosphere and the role of serpentinites in this context.

Detailed study of the specific mechanisms and processes involved in the interaction between the fluid phase and the peridotites during serpentinization, particularly in different tectonic settings. Further exploration of the conditions of serpentinization, including the pressure, temperature, and composition of the fluid phase, to gain a more comprehensive understanding of the serpentinization process. Investigation into the long-term implications of serpentinization on the physical and chemical properties of the oceanic lithosphere, including its role in elemental fluxes and the overall evolution of the oceanic crust.

Addressing these research gaps could contribute to a deeper understanding of the processes and implications of serpentinization in abyssal peridotites at mid-ocean ridges.

Serpentinites are mainly found in slow to ultraslow spreading ridges, where the lithosphere is thicker and tectonic activity is possible. They occur along the axial valley walls and even at the axial valley floor. Serpentinization of abyssal peridotites results from their interaction with large volumes of a hydrous fluid, at temperatures below 500°C, although seawater penetration in the peridotites may start at a higher temperature. Serpentinization is accompanied by a decrease in density and an increase in volume. The mineralogical association found in serpentinites sampled in ridge environments is dominated by lizardite and minor chrysotile, associated with magnetite. Other phases are much less abundant and are associated with particular mineral domains. Serpentinites are enriched in water, chlorine, fluorine, boron, sulfur, $\delta^{34}\text{S}$, ^{87}Sr compared with fresh peridotites. The subduction of heterogeneous oceanic lithosphere drives water and other elements, in particular halogens, into the mantle. Serpentinites must therefore be considered as one of the components of the subduction factory. Due to massive hydration and crystallization of secondary phases, the physical properties of abyssal peridotites are strongly modified by serpentinization. Serpentinization results in a strong decrease in density and an increase in volume, which is likely accommodated by tectonic activity.

These findings provide valuable insights into the processes and implications of serpentinization in abyssal peridotites at mid-ocean ridges, and contribute to a deeper understanding of the formation and evolution of the oceanic crust.

2. 3. Major and Trace Elements Exchanges During Fluid-Rock Interaction at Ultra-Slow Spreading Oceanic Lithosphere: Example of The South West Indian Ridge (o)

The study found that fluid-rock interaction at ultra-slow spreading oceanic lithosphere, specifically at the South West Indian Ridge, results in significant exchanges of major and trace elements. The research also revealed that the composition of the oceanic lithosphere entering subduction and the fluids released to the mantle wedge are influenced by these exchanges. The study provides valuable insights into the geological processes occurring in this unique environment.

The article does not explicitly mention any research gap with respect to geochemical study. However, it does highlight the challenges of studying element transfers related to serpentinization of abyssal peridotites, such as the non-uniqueness of peridotite protolith, the common lack of primary mineral relics due to the advanced stages of serpentinization of oceanic peridotites, and the multiple stages of serpentinization affecting the peridotites. The article also notes that low-temperature alteration processes can occur secondary to serpentinization, transforming the serpentine minerals to clays and iron (oxyhydro)oxides, and causing gains and losses in several chemical elements. These challenges suggest that there may be gaps in our understanding of the geochemical processes occurring in this environment.

Significant exchanges of major and trace elements occur during fluid-rock interaction at ultra-slow spreading oceanic lithosphere, particularly at the South West Indian Ridge. The composition of the oceanic lithosphere entering subduction and the fluids released to the mantle wedge are influenced by these exchanges. The study sheds light on the consequences of fluid-rock interactions during long-lived exhumation and hydration history in an ultra-slow spreading context. These findings contribute to our understanding of the geological processes occurring in ultra-slow spreading oceanic lithosphere and have implications for the field of geology and our understanding of oceanic lithosphere processes.

The research on the South West Indian Ridge contributes to our understanding of fluid-rock interaction in ultra-slow spreading oceanic lithosphere in several ways. It provides insights into the exchanges of major and trace elements during fluid-rock interaction at ultra-slow spreading oceanic lithosphere, specifically at the South West Indian Ridge.

The study sheds light on the consequences of fluid-rock interactions during long-lived exhumation and hydration history in an ultra-slow spreading context, enhancing our understanding of the geological processes occurring in this unique environment.

By investigating the influence of serpentinization with increasing distance from the ridge and the role of detachment faulting, the research helps to elucidate the impact of these factors on fluid-rock interactions and the chemical budget of the oceanic lithosphere

Overall, the research on the South West Indian Ridge provides valuable insights into the geochemical processes and fluid-rock interactions specific to ultra-slow spreading oceanic lithosphere, contributing to our understanding of this type of environment.

The study on major and trace elements exchanges during fluid-rock interaction at ultra-slow spreading oceanic lithosphere, specifically at the South West Indian Ridge, has several implications for the field of geology and our understanding of oceanic lithosphere processes

The study provides new insights into the geochemical processes occurring in ultra-slow spreading oceanic lithosphere, which can help to refine our understanding of the formation and evolution of oceanic lithosphere.

The research highlights the importance of fluid-rock interactions in the biogeochemical cycles of the oceanic lithosphere, which can have implications for the deep and shallow biosphere.

The study sheds light on the composition of the oceanic lithosphere entering subduction and the fluids released to the mantle wedge, which can have implications for the formation of magmas and the evolution of subduction zones.

The research also highlights the challenges of studying element transfers related to serpentinization of abyssal peridotites, which can inform future research in this area. Overall, the study has important implications for our understanding of the processes occurring in ultra-slow spreading oceanic lithosphere and can inform future research in this area.

2. 4. Hydrothermal signatures in sediments from eastern Southwest Indian ridge 63°E to 68°E.

The sediments were analyzed using acid digestion for major, trace, and REE analysis. The samples were also subjected to a leaching experiment to separate the authigenic and lithogenic phases. For the authigenic phase, a 1.0-g sample was leached with 6N HCl (shaken for 30 min), and the resultant solution was analyzed.

Previous studies have shown that hydrothermal activity in the slow to ultra-slow spreading ridges is restricted owing to less tectonic activity and a lower melt supply. However, recent studies have demonstrated the presence of more frequent hydrothermal activity in the ultra-slow spreading Southwest Indian Ridge (SWIR). The main objective of the present study is to assess the evidence of hydrothermal activity in the sediments from eastern SWIR between 63°E/28°50'S to 68°E/26°50'S.

The research provides evidence for the presence of hydrothermal inputs in the sediments of the easternmost section of the ultra-slow spreading Southwest Indian Ridge (SWIR). The findings suggest the presence of hydrothermally derived components in the sediments, which can contribute to a better understanding of the geological processes occurring in this region. Additionally, the study introduces a new geochemical tool (Zn/Fe vs Co/Zn proxy) for assessing the contribution of hydrothermal components in the sediments, which can further enhance our understanding of the geological processes in the region.

The study found that sediments influenced by hydrothermal input strongly indicate the incorporation of sulfate phases in these sediments derived from hydrothermal processes, which can be derived from serpentinized peridotite. The presence of serpentinized peridotite was also indicated by the high Mg content and a higher amount of kaolinite-serpentine mineral (chrysotile) in the sediments. The incorporation of sulfate phases in these sediments derived from hydrothermal processes can provide useful insights into the exploration of hydrothermal vents.

The research gaps in the geochemical study of serpentinized peridotite may include the need for further investigation into the specific mechanisms and processes governing the incorporation of sulfate phases derived from serpentinized peridotite in sediments influenced by hydrothermal input. Additionally, there may be a need for more comprehensive studies to understand the geochemical signatures and distribution of specific elements associated with serpentinized peridotite in different geological settings. Furthermore, the interactions between hydrothermal fluids and serpentinized peridotite, and their implications for the geochemistry of sediments, could be an area for future research.

2. 5. Strength of slightly serpentinized peridotites and its implications for tectonics.

The strength of slightly serpentinized peridotites has significant implications for tectonics, particularly in the context of the oceanic lithosphere. Deformation experiments on slightly serpentinized peridotites indicate that the presence of only 10% serpentine dramatically reduces the strength of the altered peridotite to that of pure serpentinite. This suggests that deformation is primarily accommodated by serpentine, while olivine remains nominally undeformed.

Furthermore, the transition from a "strong," dilatant dunite rheology to a "weak," nondilatant serpentinite rheology is not a linear function of the degree of serpentinization. Instead, an abrupt transition in strength is observed at low degrees of serpentinization. The pressure of the transition from localized to distributed deformation also decreases abruptly, from over 1000 MPa to 150–350 MPa. This change in rheological behavior occurs at a serpentine content of 10%–15% or less, which corresponds to published compressional seismic velocity of over 7.8–7.5 km/s at a pressure of 200 MPa. Therefore, the seismic velocity of the oceanic lithosphere, particularly that formed at slow spreading ridges, can provide constraints on its mechanical properties at depth.

In summary, the strength of slightly serpentinized peridotites has implications for understanding the mechanical behavior of the oceanic lithosphere, particularly in relation to deformation and tectonic processes.

The provided study primarily focuses on the mechanical properties and rheology of slightly serpentinized peridotites. However, it does mention some important findings related to the geochemical study of serpentinized peridotite.

Seismic velocity profiles combined with mechanical measurements provide limits on the rheology of the oceanic lithosphere from seismic velocity data. The presence of serpentine, even in small amounts (less than 25%), has profound consequences for the strength and deformation of the oceanic lithosphere ...Refraction experiments at some Mid-Atlantic Ridge offsets show crustal velocities intermediate between those of gabbro and unaltered peridotite, suggesting the presence of partially serpentinized peridotite in the oceanic lithosphere.

While the study does not extensively cover the geochemical study of serpentinized peridotite, it does highlight the importance of considering geochemical aspects in understanding the mechanical and rheological behaviour of the oceanic lithosphere.

The provided study primarily focuses on the mechanical properties and rheology of slightly serpentinized peridotites, and it does not extensively cover the geochemical study of serpentinized peridotite. As a result, it does not explicitly outline research gaps in the geochemical study of serpentinized peridotite.

Understanding the specific geochemical processes involved in the serpentinization of peridotite and their implications for the overall composition and stability of the oceanic lithosphere. Investigating the geochemical signatures of different serpentine phases (e.g., lizardite, chrysotile, antigorite) and their variations in different oceanic lithospheric settings. Exploring the geochemical controls on the mechanical and rheological properties of serpentinized peridotite, and how these properties evolve with varying degrees of serpentinization.

These potential research gaps highlight the need for further investigation into the geochemical aspects of serpentinized peridotite and its implications for the behavior of the oceanic lithosphere.

2.6. Petrology of peridotites and related gabbroic rocks around the Kairei hydrothermal field in the Central Indian Ridge.

The Kairei hydrothermal field holds significant importance in relation to the peridotites and gabbroic rocks in the Central Indian Ridge due to its association with the highly depleted peridotites and diverse gabbros recovered from the area. The field is located on the eastern axial valley wall of the Central Indian Ridge (CIR) and is linked to the Yokoniwa Rise. The gabbros recovered from this region exhibit a wide range of variations in terms of mineral chemistry and mineral assemblages, including olivine-gabbro, gabbronorite, and highly evolved oxide gabbro. These gabbros are similar to those found in other ultraslow-spreading ocean ridges, such as the Atlantis Bank of the Southwest Indian Ridge. Additionally, the peridotites recovered from the Kairei hydrothermal field and the Yokoniwa Rise are characterized by moderately to highly depleted melt components, indicating a complex history of partial melting and chemical modification.

Furthermore, the Kairei hydrothermal field provides insights into the geochemical characteristics of the hydrothermal fluids and associated hydrothermal plumes in this region. The study of this hydrothermal field contributes to our understanding of the magmatism, petrology, and mineralogy of the rocks in the Central Indian Ridge, shedding light on the processes and dynamics occurring in this geologically significant area.

The moderately to highly depleted melt components found in the peridotites studied in this field can be attributed to several factors related to their formation and evolution. The peridotites are believed to be residues left after moderate to high degrees of partial melting, ranging from 13% to 15% in the majority of samples and up to 17% in some

cases. This partial melting process contributes to the depletion of certain melt components in the peridotites. The peridotites have undergone chemical modification through interaction with a wide range of melts, from relatively less evolved to highly evolved characteristics. This interaction with different melts has further contributed to the depletion of certain components in the peridotites. It is expected that peridotites associated with leucocratic veins were petrologically and geochemically modified during the formation of the leucocratic veins. Leucocratic veins are observed as networks in several peridotites from the 25S OCC and Yokoniwa Rise, indicating infiltration of multiple melts that could have contributed to the depletion of certain components in the peridotites. The depleted peridotites may be residues after a relatively high-melt productivity period in intermediate-spreading ridges, indicating a link between magmatic activity and the depletion of melt components in the peridotites.

The geochemical study of serpentinized peridotite has revealed the presence of hydrogen-based microbial ecosystems in the subsurface lithoautotrophic microbial ecosystem (HyperSLiME) beneath the Kairei hydrothermal field. These microbial ecosystems are supported by the serpentinization process, which produces hydrogen gas as a by product

The study of serpentinized peridotite has provided insights into the formation of serpentinite, which is a common rock type found in ophiolites and oceanic lithosphere. Serpentinite is formed through the hydration of peridotite, which occurs when seawater infiltrates the uppermost section of the oceanic plate along the ocean ridge and reacts with peridotites. The geochemical study of serpentinized peridotite has revealed that the process of serpentinization can lead to the depletion of certain elements, such as calcium, magnesium, and potassium, in the peridotite. This depletion is due to the

preferential removal of these elements during the serpentinization process. The study of serpentinized peridotite has also revealed that the process of serpentinization can lead to the formation of ore deposits, such as nickel and platinum group element deposits. These deposits are formed through the mobilization and concentration of these elements during the serpentinization process.

Further research is needed to better understand the diversity, distribution, and metabolic activities of microbial communities associated with serpentinized peridotite. This includes investigating the specific microbial species present, their interactions with the rock, and their potential biogeochemical roles in the serpentinization process. There is a need for detailed studies on the geochemical and mineralogical changes that occur during fluid-rock interactions in serpentinized peridotite. Understanding the mechanisms of element mobilization, transport, and precipitation within the serpentinized rock matrix is crucial for elucidating the geochemical processes associated with serpentinization.

Research gaps exist in the understanding of trace element behaviour during serpentinization. Investigating the partitioning of trace elements between the fluid phase and the serpentinized rock, as well as the factors controlling their mobility and fractionation, would contribute to a more comprehensive understanding of the geochemical dynamics of serpentinized peridotite.

Further research is needed to investigate the kinetics of serpentinization processes, including the rates of mineral dissolution, hydration, and secondary mineral precipitation. Understanding the timescales of these processes is essential for constraining the geochemical evolution of serpentinized peridotite. Studies focusing on the composition and origin of fluids involved in serpentinization processes are

essential for understanding the sources of energy and nutrients that support microbial life in these environments. Investigating the geochemical characteristics of the fluids and their interactions with the host peridotite would provide valuable insights into the geochemical conditions within serpentinized systems.

2.7. Mineral chemistry and alteration characteristics of spinel in serpentinised peridotites from the Northern Central Indian Ridge.

The article discusses two types of spinel found in the serpentinised peridotites from the Northern Central Indian Ridge (NCIR): non-residual spinel (Group I) and residual spinel (Group II).

Non-residual spinel (Group I) is characterized by higher TiO₂ content (up to 0.5 wt%) and displays evidence of peridotite-gabbro interaction. This type of spinel suggests a more magma-rich phase of extension and is likely affected by the intrusion of gabbroic dykes.

Residual spinel (Group II) has lower TiO₂ content (<0.1 wt%) and a Cr# of approximately 24. This type of spinel suggests an intermediate degree of partial melting (~10%) of mantle peridotite, falling between the most depleted and most fertile peridotite. It retains its original composition despite the high degree of serpentinisation of NCIR peridotite.

The presence of gabbroic dikelets affects the mineralogy of the serpentinites in the NCIR region. The non-residual spinel (Group I) found in these rocks displays evidence of peridotite-gabbro interaction, which has resulted in an increase in TiO₂ content.

The intrusion of the gabbroic dykes has also affected the TiO₂ content of the adjacent spinel grains. The TiO₂ content of Group I spinel has increased adjacent to the gabbroic dykes, while the TiO₂ content of Group II spinel remains low.

Therefore, the variability in TiO₂ content in spinel of NCIR serpentinites is primarily due to the effect of intrusion of the gabbroic dykes. These findings suggest that the presence of gabbroic dikelets can have a significant impact on the mineralogy and composition of the surrounding rocks.

The alteration of spinel porphyroclasts provides valuable insights into the process of serpentinisation. The article discusses the alteration of spinel porphyroclasts, which is conceded by the presence of relict fresh interior, intermediate ferritchromite zone, and secondary magnetite at the margins.

During alteration, Mg and Al leach out, while Fe content increases, resulting in the formation of secondary magnetite at the marginal areas of the spinel porphyroclasts. The alteration of spinel and the behavior of elements during serpentinisation account for their variability in Mg, Al, Cr, and Fe contents.

The presence of these alteration products and the changes in elemental composition provide evidence of the processes involved in serpentinisation and the transformation of the original mineral assemblage. Therefore, studying the alteration of spinel porphyroclasts can help in understanding the mechanisms and geochemical changes associated with the serpentinisation of mantle peridotites.

The study identified two types of spinel in the serpentinised peridotites: non-residual spinel (Group I) and residual spinel (Group II). These findings provide insights into the geological processes and history of the mantle peridotites in the NCIR region. The presence of gabbroic dikelets has been found to affect the mineralogy and composition of the serpentinites, particularly leading to an increase in TiO₂ content in the adjacent spinel grains. This highlights the impact of intrusive processes on the surrounding rocks. The alteration of spinel porphyroclasts has provided valuable insights into the

process of serpentinisation, revealing the leaching of Mg and Al, and the addition of Fe, resulting in the formation of secondary magnetite at the marginal areas of the spinel porphyroclasts. These findings contribute to our understanding of the geochemical changes associated with serpentinisation.

These findings collectively contribute to a better understanding of the geochemical processes and alteration characteristics of serpentinised peridotites, shedding light on the geological history and evolution of the NCIR region.

Based on the information provided in the study, some potential research gaps in the geochemical study of serpentinised peridotite from the Northern Central Indian Ridge (NCIR) may include:

While the study acknowledges the influence of gabbroic dikelets on the mineralogy and composition of the serpentinites, further investigation into the extent and specific mechanisms of melt-rock interaction, and its implications for the geochemistry of the peridotites, could be valuable.

Understanding the temporal evolution of serpentinisation and its geochemical effects on the peridotites could be a potential research gap. Investigating the changes in mineralogy and elemental compositions over time, especially in relation to the serpentinisation process, could provide insights into the long-term geochemical dynamics of the NCIR peridotites.

Exploring the potential influence of hydrothermal processes on the geochemistry of serpentinised peridotites in the NCIR region could be an area for further research. This could involve investigating the role of hydrothermal fluids in altering the geochemical signatures of the peridotites and associated minerals.

Comparative studies with serpentinised peridotites from other regions or similar geological settings could help in identifying region-specific geochemical signatures and understanding the broader implications of the findings from the NCIR.

Addressing these research gaps could contribute to a more comprehensive understanding of the geochemical processes and evolution of serpentinised peridotites in the NCIR region.

2.8. Serpentinization and Fluid Pathways in Tectonically Exhumed Peridotites from the Southwest Indian Ridge.

Studying peridotites exhumed in the footwall of axial detachment faults at slow-spreading ridges is significant because it provides insights into the hydrous alteration of exhumed peridotites without magmatic influences. This helps to understand the sequence of serpentinization in variably serpentinized peridotites and to study the circulation of serpentinizing fluids in and near the exhumation faults. Additionally, this type of study can provide information on the temperature and chemistry of serpentinizing fluids and their relations with hydrothermal convection cells that produce vents at the seafloor.

The nearly amagmatic working area along the Southwest Indian Ridge (62°-65° E) provides an end-member to study hydrous alteration of exhumed peridotites because it represents a setting without magmatic influences. Most mid-ocean ridge detachment settings are magmatically active, and hydrous fluid circulation in and near the fault has been shown to be influenced by the presence of melt or magmatic lithologies. Therefore, studying the hydrous alteration of exhumed peridotites in a nearly amagmatic setting allows for a better understanding of the processes involved in serpentinization without the complicating effects of magmatic influences.

The integrated petrological approach used in this study combines microstructural, mineralogical, and chemical observations to unravel the sequence of serpentinization in variably serpentinized peridotites. This approach involves the analysis of 272 dredged samples of variably serpentinized peridotites. The study includes mineralogical observations, chemistry, and oxygen isotope compositions to propose a sequence of serpentinization that occurred at relatively high temperatures and under increasing fluid-rock ratios. By integrating these different types of observations, the study provides a comprehensive understanding of the processes and conditions involved in the serpentinization of peridotites in the specific geological setting of the Southwest Indian Ridge.

One of the gaps is related to the origin of the fluids involved in serpentinization. While it is generally accepted that the fluids are derived from seawater, the exact composition and sources of these fluids are still not well understood.

Another gap is related to the extent of chemical exchange between the peridotite and the serpentinizing fluids. While it is known that some elements are preferentially incorporated into serpentine minerals, the extent of this exchange and the factors controlling it are not well understood.

Additionally, there is a need for more studies that investigate the role of microorganisms in serpentinization processes. Microorganisms have been shown to play a significant role in the alteration of rocks in hydrothermal systems, and their potential role in serpentinization processes is an area that requires further investigation.

Finally, there is a need for more studies that investigate the long-term stability of serpentinized peridotites and their potential role in the global carbon cycle. While serpentinization has been proposed as a mechanism for the long-term storage of carbon

dioxide, the stability of serpentinized peridotites over geological timescales is still not well understood.

Studies have provided evidence that the fluids involved in serpentinization are derived from seawater, and the composition of these fluids is influenced by the peridotite protolith. This understanding is crucial for unraveling the geochemical processes involved in serpentinization. Research has shown that serpentine minerals incorporate fluid-mobile trace elements derived from seawater and from prior mineral leaching by the serpentinizing fluids. This exchange of elements provides insights into the geochemical evolution of the system and the potential recycling of elements into the mantle at subduction zones. There is growing evidence suggesting that microorganisms may play a role in serpentinization processes. The release of significant amounts of H₂ into the water column during serpentinization may potentially support microbial ecosystems on the seafloor, highlighting the potential link between geochemistry and microbiology in these environments.

2.9. Petrology and P-T-t evolution of the South West Indian Ridge peridotites.

This paper presents a case study on the Petrology and P-T-t evolution of the South West Indian Ridge peridotites. The study was conducted east of the Melville Fracture zone at 62°E and provides valuable insights into the mineral and bulk rock chemistry of serpentinites recovered from the Southwest Indian Ridge. The study also sheds light on the origin and evolution of the peridotites, offering a comprehensive understanding of their formation and characteristics. The key findings of the study include the regular decrease in enrichment factors of transition metals, the negative anomaly in Ti and enrichment in Ni, and the positive anomaly of V consistent with increasing rates of hydrothermal alteration. The study also found that the lack of

equilibrium in the plagioclase-peridotite stability field impacts the ascent and evolution of the harzburgites. The study's findings have implications for our understanding of the origin and characteristics of peridotites in the upper mantle within the spinel-lherzolite stability field.

The study observed a regular decrease in enrichment factors of transition metals, indicating a consistent pattern in the distribution of these elements within the serpentinites. The serpentinites exhibited a negative anomaly in Ti and enrichment in Ni, suggesting specific geochemical processes and conditions during their formation and alteration. The presence of a positive anomaly of V in the serpentinites was consistent with increasing rates of hydrothermal alteration, providing insights into the environmental conditions and processes influencing the geochemistry of the recovered samples. These findings contribute to a better understanding of the mineral and bulk rock chemistry of the serpentinites from the Southwest Indian Ridge, offering valuable information about their formation and alteration history.

The lack of equilibrium in the plagioclase-peridotite stability field has significant implications for the ascent and evolution of the harzburgites recovered from the Southwest Indian Ridge. Specifically, this lack of equilibrium suggests a relatively slow ascent without the introduction of exotic melts or mixing between residue and melt fractions. The harzburgites ascended after the extraction of basaltic melts, and their evolution is characterized by several stages, including decompression, rising and emplacement of the residue in the upper mantle-lower crust, syn-tectonic deformation, and post-tectonic recrystallization.

This information indicates that the ascent and evolution of the harzburgites were influenced by specific geological and tectonic processes, and the lack of equilibrium

in the plagioclase-peridotite stability field provides insights into the nature of their ascent and the conditions under which they evolved.

The mineral and bulk rock chemistry, as well as the lack of equilibrium in the plagioclase-peridotite stability field, provide insights into the formation conditions of peridotites in the upper mantle. This contributes to our understanding of the processes and environments that lead to the development of these rock types.

The study's findings shed light on the ascent and evolution of peridotites, particularly harzburgites, within the upper mantle-lower crust zone. The information about their slow ascent and specific stages of evolution enhances our understanding of the geological and tectonic processes that shape these rocks. The geochemical signatures observed in the peridotites offer valuable clues about the history of these rocks, including their interaction with basaltic melts, hydrothermal alteration, and the influence of specific mantle sources. By comparing the characteristics of peridotites from different fracture zones, the study highlights regional variability and mixing between mantle sources, providing insights into the diverse nature of peridotites within the Southwest Indian Ridge.

Overall, the study's findings contribute to a more comprehensive understanding of the origin, evolution, and characteristics of peridotites in the upper mantle within the spinel-lherzolite stability field, enriching our knowledge of these important geological components.

The study observed a regular decrease in enrichment factors of transition metals, indicating a consistent pattern in the distribution of these elements within the serpentinites. The serpentinites exhibited a negative anomaly in Ti and enrichment in Ni, suggesting specific geochemical processes and conditions during their formation

and alteration. The presence of a positive anomaly of V in the serpentinites was consistent with increasing rates of hydrothermal alteration, providing insights into the environmental conditions and processes influencing the geochemistry of the recovered samples. The bulk rock chemistry of the serpentinites was consistent with that of oceanic Iherzolites, but with variations in SiO₂, TiO₂, CaO, Cr, and Ni, indicating varying degrees of partial melting of a homogeneous source represented by the more fertile Iherzolite of the peridotite sequence. These findings contribute to a better understanding of the geochemical characteristics of serpentinized peridotite, providing insights into their formation and alteration history, as well as their relationship to other mantle rocks.

Limited Sample Size: The study analyzed a relatively small number of samples, which may not be representative of the entire population of serpentinized peridotites. Further studies with larger sample sizes are needed to confirm the observed geochemical patterns and variations. **Lack of Spatial Resolution:** The study did not provide information on the spatial distribution of the observed geochemical patterns within the serpentinites. Further studies with higher spatial resolution are needed to understand the micro-scale processes and variations that contribute to the observed geochemical signatures. **Limited understanding of Alteration Processes:** While the study identified specific geochemical signatures associated with hydrothermal alteration, the exact processes and mechanisms that lead to these signatures are not well understood. Further studies are needed to investigate the specific environmental conditions and processes that influence the geochemistry of serpentinized peridotite. **Limited Comparison with Other Mantle Rocks:** The study focused primarily on the geochemical characteristics of serpentinized peridotite, without comparing them to other mantle rocks. Further studies that compare the geochemical characteristics of

serpentinized peridotite with other mantle rocks, such as dunites and lherzolites, are needed to understand their relationship and evolution within the mantle.

2.10. Serpentinized peridotites and gabbros in the Mid-Atlantic Ridge axial valley at 15°37'N and 16°52'N.

The paper "Serpentinized Peridotites and Gabbros in the Maraxial Valley" provides a comprehensive analysis of mantle-derived harzburgites and their deformation in the Mid-Atlantic Ridge axial valley at 15°37'N and 16°52'N. The study offers several key findings:

The study presents evidence of ductile and brittle deformation in the low stress/high-temperature conditions of the asthenospheric mantle. It discusses the succession of events in the deformation history, including ductile flow, recrystallization of olivine, brittle shearing, and opening of veins filled with specific minerals.

The mineral compositions of the samples from the 15°37'N dredge are analyzed, highlighting variations in the degree of depletion and studying their deformational and metamorphic history. The study also discusses the implications of these findings for understanding the emplacement of these rocks in the Mid-Atlantic Ridge

The paper discusses the implications of the findings for tectonic uplift and mantle partial melting in the axial region of the Mid-Atlantic Ridge. It also addresses the variations in the degree of depletion and the deformational history of the samples, shedding light on the geological processes in the region. Overall, the study provides valuable insights into the metamorphic stratigraphy, lithospheric stretching, and hydrothermal processes in the Mid-Atlantic Ridge axial valley, contributing to our understanding of the geological and tectonic processes in this region.

The findings of this study have significant implications for our understanding of tectonic uplift and mantle partial melting in the axial region of the Mid-Atlantic Ridge. The study suggests that the emplacement of mantle-derived and gabbroic rocks in the ridge axis seafloor is characteristic of magma-starved portions of a ridge axis, along which the diverging motion of the plates is largely accommodated by stretching of the axial lithosphere along ductile and brittle normal shear zones. The study also proposes that the motor of the first stages of tectonic uplift was not serpentinite diapirism but stretching of the axial lithosphere along normal shear zones. The deformational history of the samples is characterized by a gap between the end of the ductile event and the formation of sheared chrysotile veins, suggesting that efficient strain localization mechanisms are active in this temperature range, allowing the deformation to concentrate in discrete shear zones, and leaving the better part of the axial lithospheric mantle undeformed. These findings provide valuable insights into the geological and tectonic processes in the axial region of the Mid-Atlantic Ridge and contribute to our understanding of the emplacement of mantle-derived and gabbroic rocks in the ridge axis seafloor.

The samples show evidence of ductile deformation in low stress/high-temperature conditions in the asthenospheric mantle, followed by ductile and brittle deformation in higher stress and progressively lower temperature conditions. The deformation history of the samples is characterized by ductile flow under relatively high deviatoric stresses, recrystallization of olivine, brittle shearing along veins filled with fibrous chrysotile, and brittle shearing and opening of veins filled with aragonite and clays ..The deformation events are proposed to correspond to the tectonic uplift of the peridotites and gabbros in the lithosphere of the axial region, with the motor of the first stages of tectonic uplift being stretching of the axial lithosphere along normal shear zones.

These findings contribute to our understanding of the deformational and metamorphic history of serpentinized peridotites in the Mid-Atlantic Ridge axial valley, shedding light on the geological processes in this region, axial valley metamorphic history of serpentinized peridotites in the Mid-Atlantic Ridge axial valley, shedding light on the geological processes in this region.

The mineral compositions of the samples from the 15°37'N dredge are significantly more depleted than those of other mantle-derived Mid-Atlantic Ridge harzburgites. The pyroxene modal content of the samples is lower, their spinels and pyroxenes have lower aluminum contents and higher Mg# values, and their olivines have higher Fo values. Mineral composition differences between the samples suggest a lower degree of depletion for the dredge 13 samples than for dredge 8 samples. Dredge 8 samples have mineral compositions similar to those of the peridotites dredged from the Oceanographer Fracture Zone, whose highly refractory character has been attributed to enhanced partial melting in the mantle near the Azores hotspot. The study suggests that the depleted nature of the dredge 8 ultramafics is consistent with the high degree of partial melting predicted for anomalously hot mantle regions, indicating that emplacement of mantle-derived rocks in the seafloor at mid-ocean ridges may not systematically correlate with low degrees of partial melting in the underlying mantle.

The mineral compositions of the samples from the 15°37'N dredge are analyzed, highlighting variations in the degree of depletion and studying their deformational and metamorphic history. The study also discusses the implications of these findings for understanding the emplacement of these rocks in the Mid-Atlantic Ridge.

The study provides evidence of early, high-temperature interactions with hydrothermal fluids in the gabbros and gabbroic dykelets, which were emplaced prior to extensive

serpentinization. The hydrothermal alteration of these gabbroic intrusions appears to have begun prior to, and probably at higher temperatures than, the extensive serpentinization of their host peridotite, suggesting that hydrothermal fluids may have been preferentially channeled along the gabbroic intrusions. The study suggests that the depleted nature of the dredge 8 ultramafics is consistent with the high degree of partial melting predicted for anomalously hot mantle regions, indicating that emplacement of mantle-derived rocks in the seafloor at mid-ocean ridges may not systematically correlate with low degrees of partial melting in the underlying mantle.

Overall, the study provides valuable insights into the geochemical processes involved in the serpentinization and deformation of peridotites in the Mid-Atlantic Ridge axial valley, contributing to our understanding of the geological and tectonic processes in this region.

The study acknowledges the possibility of significant chemical variations at the scale of the outcrop for ophiolitic peridotites. Further research could focus on understanding the spatial variability of geochemical characteristics within the Mid-Atlantic Ridge axial valley, which could provide insights into the local variations in serpentinization and deformation processes.

While the study provides evidence of early, high-temperature interactions with hydrothermal fluids in the gabbros and gabbroic dykelets, there may be a research gap in understanding the detailed geochemical interactions between serpentinized peridotites and hydrothermal fluids, particularly in relation to the alteration of primary minerals and the formation of secondary mineral assemblages.

The study suggests that the emplacement of mantle-derived rocks in the seafloor at mid-ocean ridges may not systematically correlate with low degrees of partial melting

in the underlying mantle. Further research could aim to better understand the geochemical processes and conditions leading to mantle partial melting and the subsequent emplacement of these rocks in the Mid-Atlantic Ridge axial valley.

Addressing these research gaps could contribute to a more comprehensive understanding of the geochemical processes associated with serpentinized peridotites in the Mid-Atlantic Ridge axial valley and provide valuable insights into the geological and tectonic dynamics of this region.

2.11. Fluid and Element Cycling in Subducted Serpentinite.

The geochemical study of serpentinized peridotite presented in the study "Fluid and Element Cycling in Subducted Serpentinite" provides several important findings:

The study indicates that oceanic serpentinization results in the immobility of REE. This finding is significant as it contributes to our understanding of the behaviour of REE during serpentinization processes.

The research demonstrates significant Sr enrichment in serpentinized peridotites compared to unaltered peridotites, suggesting the influence of oceanic sources and high water/rock ratios on Sr uptake. The study highlights a considerable increase in water content associated with serpentinization, indicating the influx of surface waters into the mantle. The presence of appreciable Sr contents in vein-forming diopside indicates cycling of oceanic Sr in the high-pressure fluid, with the REE compositions of various clinopyroxenes indicating rock control on the vein fluids. These findings contribute to our understanding of the geochemical processes associated with serpentinized peridotites and their role in element cycling during subduction.

While the study provides valuable insights into the geochemical behaviour of elements during serpentinization, there is a potential research gap in the development of

quantitative models to predict the behaviour of specific elements (e.g., REE, Sr) under varying serpentinization conditions.

Further research could focus on detailed investigations of the mechanisms and kinetics of fluid-rock interactions during serpentinization, particularly in the context of element uptake and release.

Understanding the fate of serpentinized peridotite during subduction and the subsequent release of fluids and elements into the mantle wedge represents a potential research gap. This could involve experimental and field-based studies to elucidate the geochemical transformations and element mobility during subduction.

Investigating the influence of different tectonic settings (e.g., mid-ocean ridges, forearc regions) on the geochemical signatures of serpentinized peridotites could provide valuable insights into the variability of element cycling processes.

The paper "Fluid and Element Cycling in Subducted Serpentinite" investigates the influence of oceanic serpentinization on element cycling during subduction dewatering. The study focuses on a mantle slice (Erro-Tobbio peridotite) that was first exposed to oceanic serpentinization and later involved in alpine subduction, partial dewatering, and formation of a high-pressure olivine + titanian-clinohumite + diopside + antigorite assemblage. The study finds that diopside and Ti-clinohumite act as repositories for REE and Sr, respectively. The aqueous fluid equilibrated with such an assemblage is enriched in Cl and alkaline elements but strongly depleted in REE and HFSE (less than chondrite abundances). Sr is low, although selectively enriched relative to light REE. The study also highlights the importance of rock control on vein fluids and the cycling of oceanic Sr in the high-pressure fluid. The findings contribute

to our understanding of the geochemical processes associated with serpentinized peridotites and their role in element cycling during subduction.

Previous work on high-pressure veins in the peridotites and in veins has been conducted to understand the geochemical and mineralogical characteristics of these features. The study in the provided research discusses the analysis of samples in profiles from serpentinized oceanic peridotites to high-pressure serpentinites, and from high-pressure ultramafites to veins. This research has focused on the major- and trace-element composition of Ti-clinohumite from veins and host peridotites, indicating that most trace elements preferentially enter the clinopyroxene. The coexisting aqueous fluid has extremely low REE and HFSE contents but is strongly enriched in Cl and alkaline elements. Additionally, the study presents evidence of Sr enrichment in high-pressure fluids and the presence of pre-subduction Cl and alkalis in the vein fluid, indicating closed-system behaviour during eclogitization and internal alteration. These findings contribute to our understanding of the fluid and element cycling in subducted serpentinite and the geochemical processes associated with high-pressure veins in peridotites.

2.12. Process of Serpentinisation in Ophiolite.

The scanning electron microscope (SEM) allows for the detailed examination of the morphology of serpentine polymorphs when viewed in situ on a broken surface of the rock. This enables the recognition and characterization of different serpentine polymorphs such as lizardite and chrysotile, providing insights into their shapes, growth habits, and distribution within the samples.

The SEM provides three-dimensional clarity to the textures observed in thin sections, allowing for a finer detail study of the arrangements of the polymorphs. This aids in

understanding the spatial distribution and relationships between different serpentine polymorphs within the samples.

The optical and scanning electron microscope observations reveal morphological variations in the serpentine polymorphs, such as the formation of plates, veins, and fibrous structures. These variations provide valuable information about the stages of serpentinisation and the transformation of primary minerals into serpentine polymorphs. The combination of optical and scanning electron microscope techniques allows for the comparison of different proportions of serpentine polymorphs present in samples. This comparative analysis aids in understanding the relative abundance of different polymorphs and their distribution within the serpentinised samples. Overall, the observations of textural relationships made by optical and scanning electron microscope techniques provide detailed insights into the morphological characteristics, spatial distribution, and transformation processes of serpentine polymorphs during the serpentinisation of ophiolites, contributing to a comprehensive understanding of this geological process.

The study "Process of Serpentinisation in Ophiolites" by H.M. Prichard primarily focuses on the petrographic and mineralogical aspects of serpentinisation. While it provides detailed insights into the textural relationships and morphological characteristics of serpentine polymorphs, it does not extensively cover the geochemical study of serpentinised peridotite. Therefore, specific findings related to the geochemical study of serpentinised peridotite are not extensively discussed in this study. For comprehensive information on the geochemical study of serpentinised peridotite, it would be beneficial to refer to additional sources that specifically address the geochemical aspects of serpentinisation in ophiolites and the ocean crust.

Detailed analysis of the major and trace element compositions of serpentinised peridotite, including variations in elemental concentrations and their implications for the serpentinisation process.

Investigation of isotopic signatures (e.g., oxygen, hydrogen, and carbon isotopes) in serpentinised peridotite to understand the sources of fluids involved in serpentinisation and the interaction between peridotite and infiltrating fluids.

Examination of the geochemical changes in the peridotite and the composition of the interacting fluids during the serpentinisation process, including the role of seawater, hydrothermal fluids, and other potential sources of water.

Study of redox reactions and the evolution of redox-sensitive elements during serpentinisation, providing insights into the oxidation state of the system and its implications for associated mineral assemblages. Understanding the geochemical controls on the formation of specific serpentine polymorphs and their relationship to the geochemical environment during serpentinisation. The study reveals that lizardite forms during early stages of serpentinisation and displays a characteristically platy morphology, while chrysotile begins to crystallise as fine fibres characteristically filling veins and actually replacing lizardite throughout the rock. Antigorite is confined to sheared surfaces and is rare in the ocean floor forming the latest polymorph. The paper also discusses the morphological variations in the serpentine polymorphs, such as the formation of plates, veins, and fibrous structures, providing valuable information about the stages of serpentinisation and the transformation of primary minerals into serpentine polymorphs. Overall, the paper contributes to a comprehensive understanding of the geological process of serpentinisation in ophiolites and the ocean crust. The study indicates that serpentines from ophiolites show two morphological

types of lizardite which may have formed at different temperatures. Additionally, the paper mentions the presence of different habits of lizardite on Table Mountain, suggesting two stages of lizardite formation. These findings suggest that there are indeed differences in the morphological types of lizardite between ocean floor and ophiolite samples, potentially indicating variations in the serpentinisation process or environmental conditions between these two settings.

The process of serpentinisation involves the transformation of primary minerals in ultramafic rocks into serpentine polymorphs due to the infiltration of water into the rock. The three main serpentine polymorphs involved in this process are lizardite, chrysotile, and antigorite. Lizardite forms during the early stages of serpentinisation and displays a characteristically platy morphology. It replaces primary minerals such as olivine and orthopyroxene, forming plates and veins between grains. Lizardite is typically the first alteration product and forms veins between grains of olivine. It is characterized by its platy structure and can form larger plates than the surrounding plates replacing olivine. As the serpentinisation process progresses, chrysotile begins to crystallize as fine fibres, characteristically filling veins and replacing lizardite throughout the rock. It is distinctly fibrous, with fibers of 0.1 μm diameter and between 10 μm and 1 mm in length. Chrysotile can form in veins, on lizardite plates, and may eventually make up the entire rock. Antigorite is thought to be a high-temperature and pressure form of serpentine. It is confined to sheared surfaces and is rare in ocean floor samples, forming the latest polymorph in the serpentinisation process. Antigorite appears to be converted from lizardite and is typically found in shears. The formation of these serpentine polymorphs occurs as a result of the hydration of primary minerals in ultramafic rocks, with lizardite being the initial product, followed by the crystallization of chrysotile and, in some cases, the formation of antigorite in specific

geological settings. These polymorphs exhibit distinct morphologies and textures, providing valuable insights into the stages and conditions of the serpentinisation process.

2.13. Serpentinization of oceanic peridotites, kinetics and processes of San Carlos olivine hydrothermal alteration.

The study found that serpentinization kinetics are inversely proportional to the geometrical surface area of the starting olivine grains. Specifically, the serpentinization kinetics were one or two orders of magnitude slower than commonly used kinetics for modeling serpentinization-related processes. The study also mentions that the nature of the serpentine mineral product depended on the initial olivine grain size, with lizardite forming for grain sizes in the 5–150 mm range and chrysotile crystallizing instead of lizardite for grain sizes below 5 mm. Additionally, the linear relationship between serpentinization kinetics and initial surface area was no longer observed for initial grain sizes below 5 mm, indicating that dissolution is no longer the rate-limiting process for smaller grain sizes. The study also suggests that serpentinization is associated with the creation of new reactive surface area through etch pits formation associated with dissolution and grain fracturing for grain sizes above 20 mm.

According to the study (Malvoisin et.al., 2012) the nature of the serpentine mineral product varies based on the initial olivine grain size. Specifically, for olivine grain sizes in the 5–150 mm range, lizardite formed as the main polymorph produced during serpentinization. On the other hand, for initial grain sizes below 5 mm, chrysotile crystallized instead of lizardite, and the relationship between olivine surface area and reaction kinetics no longer held. The study suggests that this difference in the

serpentine mineral product is due to the fact that chrysotile crystallization requires a higher degree of supersaturation than lizardite crystallization at 300°C.

This finding has implications for the geochemical study of serpentinized peridotite, as the mineralogy of the serpentine product can affect the geochemical signature of the peridotite.

The study suggests that serpentinization is associated with the creation of new reactive surface area through etch pits formation associated with dissolution and grain fracturing for grain sizes above 20 μm . This finding has implications for the geochemical study of serpentinized peridotite, as the creation of new reactive surface area can affect the rate and extent of mineral alteration and the geochemical signature of the peridotite.

The study provides a new kinetic data set that encompasses a range of olivine grain sizes and reaction temperatures, which is relevant to the serpentinization of olivine in the oceanic crust insofar as water is available. This new data set can be used to improve models of serpentinization-related processes and to better understand the geochemical signature of serpentinized peridotite. Overall, the findings in the study provide important insights into the kinetics and processes of serpentinization and have implications for the geochemical study of serpentinized peridotite.

Based on the information provided in the (Malvoisin et.al.,2012) some research gaps with respect to the geochemical study of serpentinized peridotite include: The study highlights the influence of initial olivine grain size on the nature of the serpentine mineral product and the kinetics of serpentinization. Further research is needed to comprehensively understand how variations in olivine grain size impact the geochemical evolution of serpentinized peridotite.

The study indicates that the mineralogy of the serpentine product varies with olivine grain size, with lizardite and chrysotile being the main polymorphs produced. Investigating the distinct geochemical signatures associated with these different serpentine polymorphs would be valuable for understanding the geochemical study of serpentinized peridotite. The study suggests that serpentinization is associated with the creation of new reactive surface area through dissolution and grain fracturing. Further research is needed to explore how this process influences the geochemical evolution of serpentinized peridotite and its potential implications for fluid-rock interactions.

The study acknowledges the effects of temperature and grain size on serpentinization kinetics. However, further research is needed to understand the influence of thermochemical variability during natural serpentinization and its implications for the geochemical evolution of serpentinized peridotite.

Addressing these research gaps would contribute to a more comprehensive understanding of the geochemical study of serpentinized peridotite and its implications for various geological processes.

2.14. Mineralogical evidence for H₂ degassing during serpentinization at 300 °C/300 bar.

The paper by (Marcaillou et.al.,2011) investigates hydrogen degassing during the serpentinization of lherzolite at 300 °C/300 bar using X-ray diffraction, Raman spectroscopy, and X-ray absorption spectroscopy. The study reveals mineralogical changes, including the degradation of initial minerals and the appearance of lizardite and magnetite. It establishes a linear correlation between ferric iron in serpentine and hydrogen production, emphasizing the importance of accurate mineralogical characterization. The findings contribute to understanding natural ultramafic

hydrothermal systems, highlighting the need for experimental studies under varying conditions.

Key Points:

1. Linear correlation found between ferric iron content in serpentine and hydrogen production during serpentinization.
2. Hydrogen production occurs in three stages linked to magnetite crystallization and ferric iron incorporation into serpentine.
3. Serpentine and magnetite identified as significant contributors to hydrogen production during serpentinization.
4. Accurate mineralogical characterization crucial for assessing hydrogen degassing, emphasizing the importance of experimental studies in varied conditions.

Significance of Experimental Alteration:

1. Quantification of hydrogen production during serpentinization under high-temperature/pressure conditions.
2. Identification of mineral assemblages formed during serpentinization, revealing insights into mineralogical changes.
3. Characterization of iron speciation in serpentine, highlighting its role in hydrogen degassing.
4. Assessment of alteration conditions' impact on hydrogen production, offering insights into natural hydrothermal systems.

Implications of Ferric Iron Determination:

1. Linear correlation between ferric iron content and hydrogen production aids in quantifying hydrogen release during serpentinization.
2. Variations in ferric iron content in natural oceanic peridotites can indicate the hydrogen potential of ultramafic hydrothermal fields.
3. Determination of ferric iron in serpentine provides insights into mechanisms and rates of hydrogen degassing during serpentinization.
4. Broad implications for understanding geochemical processes, energy sources, and potential in ultramafic hydrothermal systems.

Overall, the study contributes valuable insights into the mineralogical evidence for hydrogen degassing during serpentinization, enhancing our understanding of this geologically significant process.

2.15. Elemental Mobilizations during Hydrothermal Alteration of Oceanic Lithosphere

This paper discusses the elemental mobilizations during hydrothermal alteration of oceanic lithosphere. It covers the factors controlling seawater chemistry, compositions of subducted materials returned to the mantle, and microbial activity in the oceanic lithosphere. The paper summarizes the results of hydrothermally altered rocks taken directly from the ocean floor, providing insights into major and trace elements combined with petrographic descriptions. The paper also discusses the importance of ophiolites in understanding the three-dimensional structure of the oceanic lithosphere. Overall, the paper provides a comprehensive overview of the processes and factors involved in hydrothermal alteration of oceanic lithosphere.

Understanding the specific mechanisms and pathways of elemental mobilization and exchange during the process of serpentinization. Investigating the long-term geochemical evolution of serpentinized peridotite and its implications for global elemental cycling. Exploring the influence of microbial activity on the geochemistry of serpentinized peridotite and associated hydrothermal systems. Examining the variations in geochemical signatures of serpentinized peridotite in different oceanic settings and tectonic environments.

Insights into the major and trace element compositions of serpentinized peridotite, shedding light on the elemental mobilization and exchange processes during serpentinization. Understanding the geochemical evolution of serpentinized peridotite and its role in global elemental cycling, particularly in the context of seawater chemistry and compositions of subducted materials returned to the mantle. Recognition of the significance of serpentinized peridotite in microbial activity and its potential implications for biogeochemical processes in hydrothermal systems associated with serpentinization.

These findings contribute to a deeper understanding of the geochemical characteristics and processes associated with serpentinized peridotite, highlighting its importance in the context of oceanic lithosphere and global elemental fluxes.

According to the paper, the key factors controlling seawater chemistry in the oceanic lithosphere are related to hydrothermal circulation. Hydrothermal circulation starts at the spreading axis where magmatic heat from a basaltic crustal formation is available (high temperature of $> 350^{\circ}\text{C}$). Low-temperature alteration ($< 150^{\circ}\text{C}$) may persist for $>$ a million of years through the ridge flanks. Due to ridge flanks occupying large regions of the seafloor, changes in chemistry, mineralogy, and physical properties of

the oceanic lithosphere are accompanied by geochemical fluxes that may be even larger than those at the ridge axis. The chemical behaviour of deep-seated rocks, such as gabbros and peridotites, during hydrothermal circulation also has a large impact on global mass budgets for many elements. Therefore, hydrothermal circulation is a key factor controlling seawater chemistry in the oceanic lithosphere.

According to the paper, hydrothermal circulation starts at the spreading axis where magmatic heat from a basaltic crustal formation is available. The high temperature of the magmatic heat is $> 350^{\circ}\text{C}$. This high temperature drives the circulation of seawater through the oceanic lithosphere. The seawater is heated by the underlying magma and becomes buoyant, rising back to the seafloor. As the seawater circulates through the oceanic lithosphere, it undergoes chemical reactions with the surrounding rocks, leading to hydrothermal alteration and the mobilization of elements.

The paper also notes that low-temperature alteration ($< 150^{\circ}\text{C}$) may persist for $>$ a million years through the ridge flanks. This alteration is driven by the circulation of cooler seawater through the oceanic lithosphere.

The paper discusses the significant findings from recent direct sampling of gabbros and peridotites on the ocean floor, particularly in the context of the Indian Ocean. The findings include:

Petrological and geochemical features of the sampled gabbros and peridotites, which are comparable to those of the basaltic rocks in DSDP/ODP Hole 504B, suggesting generalities in alteration processes and chemical exchange fluxes during hydrothermal activity across all world oceans.

Recognition of the chemical behaviour of these originally deep-seated rocks during hydrothermal circulation, which has a large impact on global mass budgets for many elements.

These findings contribute to a better understanding of the geochemical behaviour of gabbro and peridotites during hydrothermal circulation and their significance in global elemental cycling.

2.16. Petrology of abyssal peridotites and related fault rocks from an oceanic core complex along the Central Indian Ridge.

The paper investigates abyssal peridotites and fault rocks from an oceanic core complex on the Central Indian Ridge, utilizing petrography, mineral chemistry, and isotopic analysis. The results reveal multiple stages of melt extraction, refertilization, serpentinization, and deformation during exhumation. The study emphasizes the significance of abyssal peridotites in understanding mantle processes, tectonic evolution, and hydrothermal systems.

Key Findings:

1. **Peridotite Evolution:** The rocks underwent melt extraction, refertilization, serpentinization, and deformation during exhumation.
2. **Fault Rocks:** Products of brittle deformation and hydrothermal alteration, indicating fluid-rock interactions in the oceanic lithosphere.
3. **Geochemical Insights:** Serpentinization processes and hydrothermal interactions influenced fluid-mobile elements in serpentines.

4. **Research Gaps:** The study identifies gaps in understanding the mechanisms of element mobilization during serpentinization and calls for further research on serpentinite-seawater interactions.

Analytical Techniques:

- SHINKAI 6500 submersible collected samples equipped with a manipulator arm.
- Petrographic microscope identified mineral assemblages and textures.
- EMPA analyzed mineral compositions (olivine, pyroxene, spinel).
- SIMS measured oxygen, hydrogen, and strontium isotopic compositions.
- XRF and ICP-MS determined major and trace element compositions.
- SEM and TEM investigated microstructures and textures at high resolution.

Insights from Petrological Studies:

1. **Serpentinization Processes:** Pervasive and vein-controlled serpentinization, involving lizardite, chrysotile, and antigorite.
2. **Mineralogical Variations:** Significant variations in olivine, pyroxene, and spinel attributed to partial melting and melt extraction.
3. **Hydrothermal Alteration:** Formation of talc, chlorite, and carbonate minerals due to circulation of hydrothermal fluids.
4. **Fault Rocks:** Identification of cataclasites, mylonites, and ultramylonites associated with detachment fault during OCC exhumation.

Overall, the petrological studies enhance understanding of abyssal peridotites, fault rocks, and processes shaping the oceanic lithosphere, with implications for mantle dynamics, tectonic evolution, and elemental cycling.

2.17. Seawater-derived rare earth element addition to abyssal peridotites during serpentinization.

The paper "Experimental evidence for Nd–Sr decoupling during low-temperature (20–170 °C) hydrothermal alteration of olivine and clinopyroxene" by (Frisby et al.,2016) investigates the addition of rare earth elements (REEs) to abyssal peridotites during serpentinization. The study focuses on the interaction between seawater and the upper mantle, examining in situ trace and major element concentrations, bulk rock and sequential leaching experiment trace element concentrations, and Nd, Sr isotope data.

The authors discuss the significance of Nd isotopes in clinopyroxenes from serpentinized abyssal peridotites retaining their primary magmatic signature. They also highlight the elevated LREE concentrations in the secondary serpentine matrix and magnetite veins of the peridotites, comparing them to seawater trace element enrichments. The paper provides insights into the implications of these findings for our understanding of the communication between the Earth's hydrosphere and upper mantle.

The study highlights the importance of examining in situ trace and major element concentrations, bulk rock and sequential leaching experiment trace element concentrations, and Nd, Sr isotope data to understand the interaction between seawater and the upper mantle during serpentinization. The authors provide evidence for the addition of rare earth elements (REEs) to abyssal peridotites during serpentinization,

with elevated LREE concentrations in the secondary serpentine matrix and magnetite veins of the peridotites.

The paper also discusses the significance of Nd isotopes in clinopyroxenes from serpentinized abyssal peridotites retaining their primary magmatic signature, and the implications of these findings for our understanding of the communication between the Earth's hydrosphere and upper mantle.

Understanding the mechanisms and pathways of rare earth element (REE) addition to abyssal peridotites during serpentinization, including the specific processes involved in the uptake of REEs from seawater into the peridotite.

Investigating the extent of isotopic disequilibrium between bulk rock peridotite and clinopyroxene isotope ratios, and the implications of this disequilibrium for our understanding of the alteration processes and mass exchange between seawater and the Earth's upper mantle.

Exploring the behaviour of other trace elements and isotopic systems during serpentinization, beyond the focus on Nd and Sr isotopes, to gain a more comprehensive understanding of the geochemical processes and element cycling in serpentinized peridotites. Assessing the potential impact of serpentinization on the redistribution and retention of major and trace elements in the peridotite, and its implications for the refertilization of the peridotite and the cycling of these elements through the subduction system and into the upper mantle.

The paper suggests that the addition of LREE during serpentinization could have implications for the trace element budget and possibly Nd and Hf isotope systematics of recycled lithosphere, as well as the mobility of these elements during dehydration of the serpentinized lithosphere within the subduction factory. The excess LREE in

serpentinized peridotites, coupled with their preferential mobility, could result in a high LREE/HREE and possibly high REE/HFSE ratio flux from the serpentinized peridotite to the mantle wedge during dehydration melting, along with the fluid mobile elements.

The analyzed abyssal peridotites are from two on-ridge locations along the Southwest Indian Ridge (SWIR) on opposite sides of the 16°E discontinuity. The selected samples have preserved primary clinopyroxene and occasionally orthopyroxene while most of olivine has been altered to serpentine. The relic clinopyroxenes preserve the original mantle signature and have been previously characterized for their magmatic elemental and Sr, Nd, Hf compositions.

The paper does not provide a detailed description of the petrography of the serpentinized peridotites beyond this, but it does discuss the alteration processes and the implications of the findings for our understanding of the interaction between seawater and the upper mantle during serpentinization.

2.18. The geochemical character of serpentinites associated with high- to ultrahigh-pressure metamorphic rocks in the Alps, Cuba, and the Himalayas.

Ultrahigh-pressure metamorphic rocks in the Alps, Cuba, and the Himalayas. Three distinct serpentinite groups are identified: Group 1 from the Alps, Group 2 from Cuba, and Group 3 from the Himalayas, suggesting different formation processes and protolith sources. The study sheds light on the recycling of elements in subduction zones and the role of serpentinites in high-pressure metamorphic processes.

Key Findings are as follows:

1. Serpentinite Groups: Two primary groups are identified - forearc mantle serpentinites (Himalayas, Cuba's major deformation zone) and hydrated

abyssal peridotites (Alps, most of Cuba). They exhibit distinct geochemical characteristics and are associated with different tectonic settings.

2. **Source and Formation:** Forearc serpentinites form in the forearc mantle wedge through peridotite hydration, linked to exhumation of ultrahigh pressure (UHP) and high-pressure (HP) metamorphic rocks. Hydrated abyssal peridotites result from abyssal peridotite hydration in the mantle, not directly linked to UHP or HP rocks.
3. **Role in Subduction Zones:** Serpentinites act as vital water reservoirs, facilitating element transport from shallow crust to mantle. They contribute to arc magmas' production and the transfer of elements from subducted slabs to mantle wedges, influencing overall elemental recycling in subduction zones.
4. **Implications for High-Pressure Metamorphism:** Buoyant serpentinites play a significant role in exhuming UHP and HP metamorphic rocks. Dehydration-induced volume changes may contribute to deep seismic activity in subduction zones.

Research Gaps and Suggestions:

- More comprehensive geochemical mapping of serpentinites in various subduction zones is needed.
- Further exploration of fluid-rock interactions during the serpentinization process, especially in different tectonic settings.
- Investigation of specific processes facilitating element transfer from subducted slabs to mantle wedges and arc magmas.

- Additional research on serpentinites' role in high-pressure metamorphic processes and their contribution to deep seismic activity in subduction zones.
- A comprehensive understanding of petrographic characteristics may require consultation with sources specifically addressing mineralogical and textural features of serpentinitized peridotites.

Overall, the study enhances our understanding of serpentinites' geochemical characteristics, sources, and roles in subduction zones, contributing valuable insights into high-pressure metamorphic processes

CHAPTER III: METHODOLOGY

3.1 Analytical Methods

Fresh rock samples devoid of surface alteration or weathering were selected and used for various analyses. A part of the sample was used to prepare thin-section to study petrography and mineral assemblage and mineral chemistry. Another part of the selected sample was powdered using agate mortar and used for geochemical analysis.

The following analyses were made- (a) Petrography and Mineral assemblage by studying thin-sections under microscope, (b) Mineral Chemistry using EPMA, (c) geochemical studies using XRF for major elements and (d) ICP-MS for trace and rare earth element analyses,

3.1.1. PETROGRAPHY AND MINERAL ASSEMBLAGE: For detailed petrography studies, thin sections of the sampled rocks were prepared following the procedure mentioned below.

- The rock specimen was cut to a thickness of 2-4 mm and the slab is roughly flat with parallel sides of 1 sq. inch area.
- The rough sides were made approximately parallel by rubbing the sample against a circular sanding pad of about 40-60 grit.
- The rock slab was placed on the coarsest grinding disk and water is continuously poured on the disk.
- Only one finger was used on the back of the piece and is ground with medium to light pressure in a circular or elliptical motion.
- Polishing continued till all the roughness on the surface removed.
- Then the rock piece was grounded on grade #100, #200, #500 and then #1200. The grades fine upwards.
- Even while using finer grades, the pressure applied on the rock piece was low to moderate.

- The thinner the rock gets the easier it was to break. So thus pressure was applied uniformly on the rock sample.
- For polishing, a diamond polishing powder was used so as to get the best finish.
- A flat piece of glass was used over which the polishing powder was placed and then a back and forth motion was used to polish the rock surface.
- For mounting the rock piece on the slide, a slow set epoxy was used to obtain a better bond with the glass.
- Then the rock piece was further thinned by polishing it, until it looks almost transparent.

3.1.2. MINERAL CHEMISTRY: After the detailed petrographic studies, well-polished thin sections of selected samples having representative mineral assemblages were used for estimating the mineral compositions by Electron Probe Micro Analyses (EPMA). The selected thin sections were coated with a thin film of carbon, using pure graphite rods at 10^{-3} Torr vacuum condition for the purpose of obtaining uniform electrical conductivity over the sample surface in order to avoid negative charge build up at the point of electrical heating and also to measure the sample current with respect to mineral standards used during micro probe analysis. Quantitative chemical analyses of constituent mineral phases have been undertaken at National Institute of Oceanography (NIO) in Goa.

Major element compositions of constituent minerals were analyzed by wavelength dispersive spectrometry (WDS) on a CAMECA X5 electron probe micro analyzer (WDS) with computer control **Figure (3.1)**. A fully focused beam operating with beam energy of 15 keV and probe current of 12 nA were used. Typical counting times were

20-40 seconds and 1σ standard deviations of the counts were 0.5-1%. Synthetic as well as natural standards were used during the analyses. Output electron probe data were used to classify respective minerals as per existing nomenclatorial rules.

3.1.3. GEOCHEMICAL ANALYSES:

Major Element: Twelve samples of serpentinized peridotite were analysed for major element at NIO (Goa) using X-ray fluorescence spectrometry (XRF). Major element concentrations were determined by using X-ray fluorescence spectrometry (XRF) (PANalytical, Axios mode with 4 KW power; **Figure (3.2)** specifically, wavelength dispersive x-rays fluorescence spectroscopy (WD-XRF) method was used. Spectrometer is operating in sequence mode, on the basis of wavelength dispersion (WD-XRF). It is fitted with flow-through, or scintillation detector, and X-ray tube with 4 kW power rating, manufactured according to SST-mAX technology, which ensures stability of parameters over long period of time.

For WD-XRF analysis, the samples were prepared in the form of beads of 32 mm size. The mixture of 5 gm of Merck's [®]spectromelt A12 (66% Di-Lithium tetra borate + 34% Lithium Metaborate) and 1gm of powdered sample was preheated at 800°C for 3 minutes. The resulting melt was heated again with agitation at 1200°C for 7 minutes in a Platinum crucible using PANalytical Minefuse 2 furnace (high frequency electromagnetic induction heating and fusing machine). The melt was cooled with the drier, and then each glass bead was wrapped in paper and kept in desiccators. The quantitative standard analysis was performed on the basis of standards BHVO-2 and BCR-2 using PANalytical, Axios mode with 4 KW power.

Trace & REE Analyses: The trace and REE compositions of selected samples were analysed at CSIR-National Geophysical Research Institute (NGRI), Hyderabad by employing closed digestion method. The powdered samples were digested by adding double distilled acids HF: HNO₃ at a ratio of 7:3 to 0.05 g of rock powder in a Savillex[®] vessel. This mixture was kept on hot plate at 150°C for 48 hours. After 48 hours of sample digestion, the solutions were mixed with 1 ml of HClO₄ and kept for evaporation. When the mixture is completely dried, 20 ml of 1:1 HNO₃ was added and kept on hot plate at 70°C for 10-15 minutes till the clear solution is obtained. Then 5 ml of Rhodium (1 ppm concentration) was added as an internal standard and kept for cooling. After cooling the solution was made into 250 ml. 10 ml aliquot of the prepared solution was further diluted to 100 ml to achieve total dissolved solids < 200 ng/g for analytical requirements.



Figure:3.1. Mineral chemical composition analyses using wavelength dispersive spectrometry (WDS) Electron Probe Micro Analyses (EPMA) at NIO, Goa.

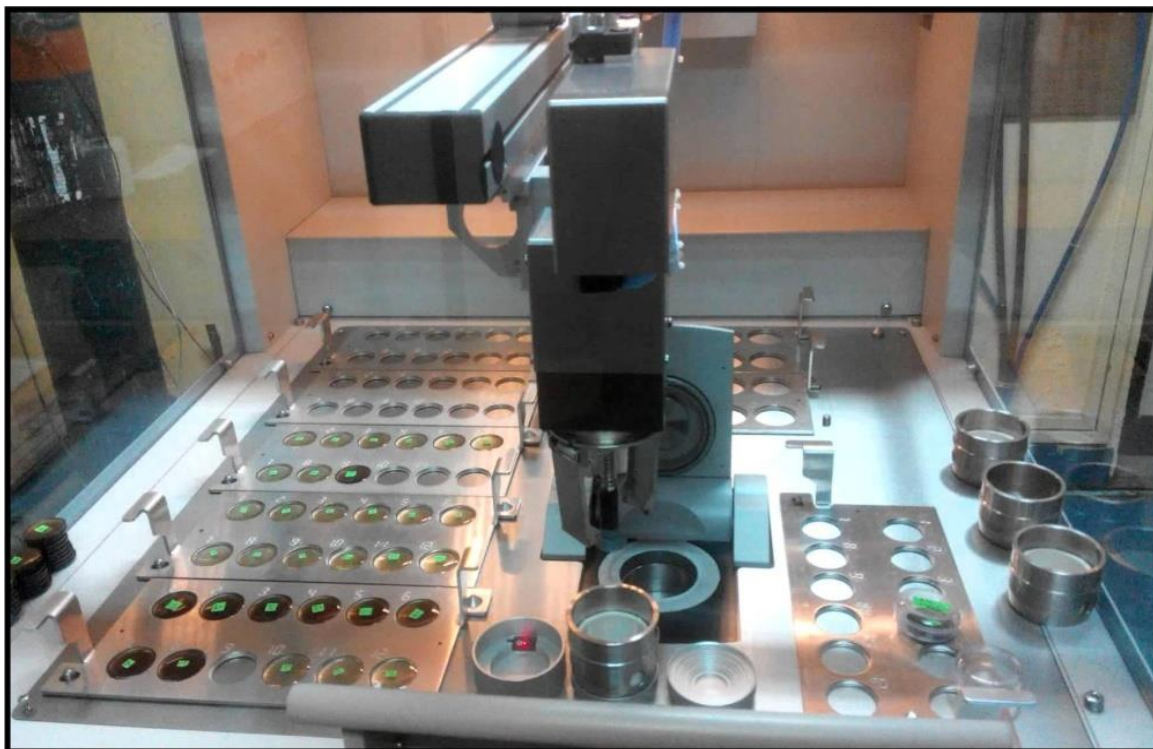


Figure:3.2. Major element analyses of Serpentinised Peridotite by using (PANalytical, Axios mode with 4 KW power) wavelength dispersive x-rays fluorescence spectroscopy (WD-XRF) at NIO, Goa.

Certified reference materials UBN were used for bulk rock analyses of serpentinized peridotite respectively and were also treated in the same way as the samples to minimize errors from reagents. All sample and standard solutions were analyzed at CSIR-NGRI, Hyderabad, using high resolution inductively coupled mass spectrometer (HR-ICP-MS) (Nu Instruments Attom, UK) in jump-wiggle mode which permits the analytes of interest to be measured accurately. Solutions were introduced through standard Meinhard[®] nebulizer with a cyclonic spray chamber housed in Peltier cooling system. All quantitative measurements were performed using the instrument software (Attolab v.1), while the data processing was done using Nu Quant[®]. This uses knowledge-driven routines in combination with numerical calculations (quantitative analysis) to perform an automated/manual interpretation of the spectrum of interest.

^{103}Rh was used as an internal standard and external drift was corrected by repeated analyses of UBN, which were also used as calibration standards accordingly. Instrument response was corroborated relative to independent digestions of UBN.



Figure:3.3. Trace element and REE analyses of Serpentinised Peridotite sample using high resolution inductively coupled mass spectrometer (HR-ICP-MS) at CSIR-National Geophysical Research Institute (NGRI), Hyderabad.

CHAPTER IV: RESULTS AND OBSERVATIONS

4.1 Petrographic observations

A petrographic study of serpentized peridotite offers a fascinating journey into the intricate world of minerals and textures.

This research delves into the petrographic intricacies of serpentized peridotite, unveiling a comprehensive examination of minerals and textures. Serpentinization, a transformative process in Earth's lithosphere, has profound implications for geodynamic and geochemical processes. Through a meticulous petrographic study, under NIKON ECLIPSE E200 polarising microscope all 12 thin sections were observed, this research aims to contribute to our understanding of the evolution of serpentized peridotite and its significance in various geological contexts. Serpentinization, a metamorphic process involving the hydration of olivine and pyroxene in peridotite, plays a pivotal role in geological dynamics. This study employs petrographic methodologies to scrutinize the mineralogical evolution and textural nuances within serpentized peridotite, contributing to a comprehensive understanding of Earth's subsurface processes.

Peridotite consisting of olivine and clinopyroxene and can be classified as a Iherzolite (as sufficient orthopyroxene is also present in areas of the rock). All the minerals show relatively high relief and little colour so it can be difficult to distinguish the pyroxenes. The olivine grains have higher relief in plane polarized light and also have brighter interference colours in crossed polars. They show the fractures which are characteristic of olivine.

The grain boundaries are very distinct due to minor alteration, probably to serpentine. The olivine grains here are small and form a texturally equilibrated granoblastic texture. The orthopyroxene shows cleavage and first order grey interference colours and is elongate (in right hand part of view), probably as a result of high temperature

deformation. An opaque mineral is also present which is likely to be a Cr spinel. As observed from the thin section there are various shapes and sizes of opaque. Are observed in the rock type, most of which are supposedly the magnetite which is irregular in shape and completely isotropic.

While olivine and pyroxene ultramafic rocks are stable under high temperature metamorphic conditions, below $\sim 400^{\circ}\text{C}$ olivine breaks down to serpentine. As seen in the thin section it consists almost entirely of the mineral serpentine, hydrated magnesium silicate $[\text{Mg}_3(\text{Si}_2\text{O}_5)(\text{OH})_4]$. The characteristics of serpentine are its low birefringence and the mesh-like texture which can be seen in the view taken with crossed polars. This form of serpentine shows a pseudomorph texture cut by veins and is formed by hydration and metamorphism of an originally coarse-grained olivine-rich peridotite. It is characteristic of the serpentine polymorph lizardite.

Serpentinites frequently have relicts of olivine and pyroxene as observed crystals from the original igneous rock from which they are formed. They are recognized by their high relief and low birefringence compared to the low relief of the serpentine. The section also contains an opaque mineral, probably iron oxide and, in the centre side dark brown crystals of spinel (an oxide of magnesium, iron and chromium) which are isotropic.

Subsequent prograde metamorphism of a serpentinite produces the serpentine polymorph antigorite, which characteristically forms a more uniform fine-grained decussate texture as seen in the thin section. Most thin section is composed of serpentinite which here forms fine grained laths with low relief and low interference colours, an opaque mineral and a higher relief mineral with higher interference colours which is probably olivine. In the fine-grained decussate serpentinite (antigorite)

(**Figure 4.1.3.**) is intergrown with euhedral olivine (high interference colours in crossed polars). In this case the olivine is not relict from the original periodotite, but is forming by neomineralization of new olivine grains as a result of reaction during prograde contact metamorphism of the serpentinite.

Chemically the commonest clinopyroxenes differ from orthopyroxenes in that the former contain essential calcium. The compositions of clinopyroxenes in basic and intermediate igneous rock are such that they usually lie in the composition range of the mineral known as augite.

Augite which is type of pyroxene is observed where in PPL it is shown that the grain is more than 3mm and it is brown in colour with moderate to high relief and consisting of lot of fractures. In cross polars it is observed that the augite grain shows Second order interference colours in the shade of pink and the surrounding ground mass is consisting of serpentine mineral showing traces of mesh texture so basically the augite grain is situated between the mesh texture also at the left side left corner of the thin section two small grains of olivine are observed which showed green color in ppl with fractures and shows again the second order interference color also to note the relief of the olivine in comparison to the other minerals which makes the mineral prominent and it stands out amongst them. In these photographs the characteristic augite cleavages is seen. The birefringence of augite is such that the maximum interference colour is at the top of the second-order, in some orientations, extinction is oblique.

The chemistry of this mineral series can be compared with the olivines in that it represents a magnesium-iron silicate series with complete solid solution between the pure magnesium end-member (MgSiO_2) and the iron end-member (FeSiO_2): the orthopyroxenes however contain more SiO_2 , than the olivines.

Some of the orthopyroxene crystals have a pink colour whereas others they have a greenish colour. As observed in the thin section a large grain more than 4mm is observed (**Figure 4.1.1.**) in the slide where in it appears to have one cleavage set and numerous fractures onto it and has high relief and is appeared in shades of brown throughout the thin section at various places in single slide, when observed under cross polars it appears to have This pleochroism from pink to green is useful as an indicator of the presence of orthopyroxene, but unfortunately it is not always seen. Some of the crystals show cleavages but irregular cracks are also visible. In thin section taken with crossed polars, The interference colours are first-order only and this illustrates the low birefringence of this mineral. Crystals of orthopyroxene show straight extinction in all sections showing only one cleavage.

Talc is observed in the thin section where in PPL it is showing the randomly oriented aggregates of irregular flakes or fibers resembling the micas. Individual broken grains are also observed it appears colorless in nature and has random cracks or fractures with no distinct cleavage. The relief shown is low to moderate. When observed under cross polars it showed anisotropic nature with third order colours of yellow blue and pink shades, and extinction varies from $0 - 3^\circ$. The tremolite in thin section is observed to be form from a point a single point and then it is protruded in different direction with habit/form which is accicular in nature and are parallel. Tremolite is a relatively common mineral in some metamorphic rocks. It occurs from the conversion of dolomite, silica and water into tremolite, calcite and carbon dioxide. Tremolite occurs as a result of contact metamorphism of calcium and magnesium rich siliceous rocks and in greenschist facies metamorphic rocks derived from ultramafic or magnesium carbonate bearing rocks. They usually have cleavage but not distinct in the given section and pleochroism is absent and very weak in the section. In cross polars the

second order interference colors are shown, Medium-high and decreases with increasing Fe^{2+} content. It shows extinction which is Oblique. Tremolite has a greater presence of magnesium over iron.

The relief for spinel mineral is High positive, and crystals are usually octahedrons yielding triangular, square, or diamond-shaped cross sections in thin section. Subsequent anhedral grains also are common in the thin section.

Cleavage is Absent or can be said undistinguishable. It is one of the few isometric minerals that is invariably isotropic. Color in thin section corresponds with hand sample color, some can be opaque. Generally distinguished by high relief in thin section, strong color, and isotropic character. Different crystal shape and lighter color distinguishes garnet from spinel. In grain mounts it may be difficult to differentiate between the spinel and garnet groups, and X-ray or other techniques may be required.

The serpentinization of olivine-rich rocks, such dunites and peridotites, may or may not be complete. If the transition is not complete, we see a lattice work of longitudinally split cross-fibre veins encircling olivine cores, like a serpentine mesh structure. A single olivine grain can be split into many cores (**Figure 4.1.4.**) that stay in their original orientation. Usually, a black band of tiny magnetite aggregates divides two parallel lines of fibrous material that make up the serpentine veins. If the transformation is successful, serpentine micro aggregates fill the inside spaces of the mesh structure. Serpentine minerals are always secondary, they occur together as alteration products of Al-poor, magnesian minerals, especially olivine, Mg-Pyroxenes. The most characteristic occurrence of serpentine is that derived from dunites, peridotites and other ultramafic-mafic rocks. When we discuss about the serpentine mineral it is evident to speak about the polymorph as well now those are antigorite

chrysotile and lizardite which are observed in the thin section in mesh texture along with serpentine mineral this varies based on the Mg and Fe content present. The most observed form is Asbestiform, as parallel fibers ore aggregate with cross fibers. The mineral is Colourless to pale green, and shows low relief, there are fractures and irregularity observed throughout and between cross polars it becomes anisotropic with Interference colors: Low, grey, yellow, which are basically the first order colors.

Within the peridotite rock, bastite crystals tend to connect with other serpentine minerals and with one another, forming a coherent network. Depending on impurities, bastite usually has a tint of brown. The initial olivine crystals in the peridotite are replaced by bastite, which may lead to pseudomorphic textures in which the olivine's form is retained but its mineralogy has changed to bastite. The overall structure and content of the serpentinized peridotite are influenced by the presence of bastite(**Figure 4.1.5.**) in conjunction with other secondary minerals including brucite, magnetite, and chromite, which are generated during the process of serpentinization.

Brucite is a mineral primarily composed of magnesium hydroxide. It is a low-temperature hydrothermal vein mineral that forms during the serpentinization of dunites and is a frequent alteration result of periclase in marble and chlorite schists. As shown in the thin section, brucite is frequently found in conjunction with chrysotile, aragonite, serpentine, and talc. Colorless in thin section and displays anomalous second-order red or blue interference colors.

A feature which is common to many minerals is alteration and most prominent in serpentinised peridotite. Many of the common rock-forming minerals crystallize at relatively high temperatures but when they cool they may be partly replaced by other minerals which are stable at lower temperatures. This is usually associated with to the introduction of water and many alteration minerals are hydrous. Alteration of the

primary minerals may take place at any time. The alteration products are commonly too fine grained to be identified optically. However, the observation that some grains are altered and others are not may be of diagnostic importance. Alteration products like serpentine or amphibole minerals (like tremolite) may be seen in veins rich in pyroxene. Secondary minerals like talc or serpentine can be found in olivine-rich veins as a result of the initial olivine crystals being hydrated and changing. In cross-polarized light, these secondary minerals frequently exhibit distinctive hues and textures; for example, serpentine appears green, whereas talc appears white to pale green. Alternate veins of olivine and pyroxene, as observed in thin sections of serpentinized peridotite, usually appear as discontinuous, irregular structures cutting through the serpentine matrix. The original peridotite minerals in these veins have changed; this alteration is frequently the result of reactive fluids, such as hydrothermal fluids, seeping into the rock's cracks and fissures.

The preservation of original mineral shapes within serpentine minerals, known as pseudomorphic replacement, offers clues about the kinetics and pathways of alteration.

This petrographic study unveils the rich tapestry of minerals and textures within serpentinized peridotite, providing a deeper understanding of the transformative processes occurring in Earth's lithosphere. The identification and characterization of distinct mineralogical phases and textures contribute valuable insights into the geological evolution of peridotite in diverse geological settings.

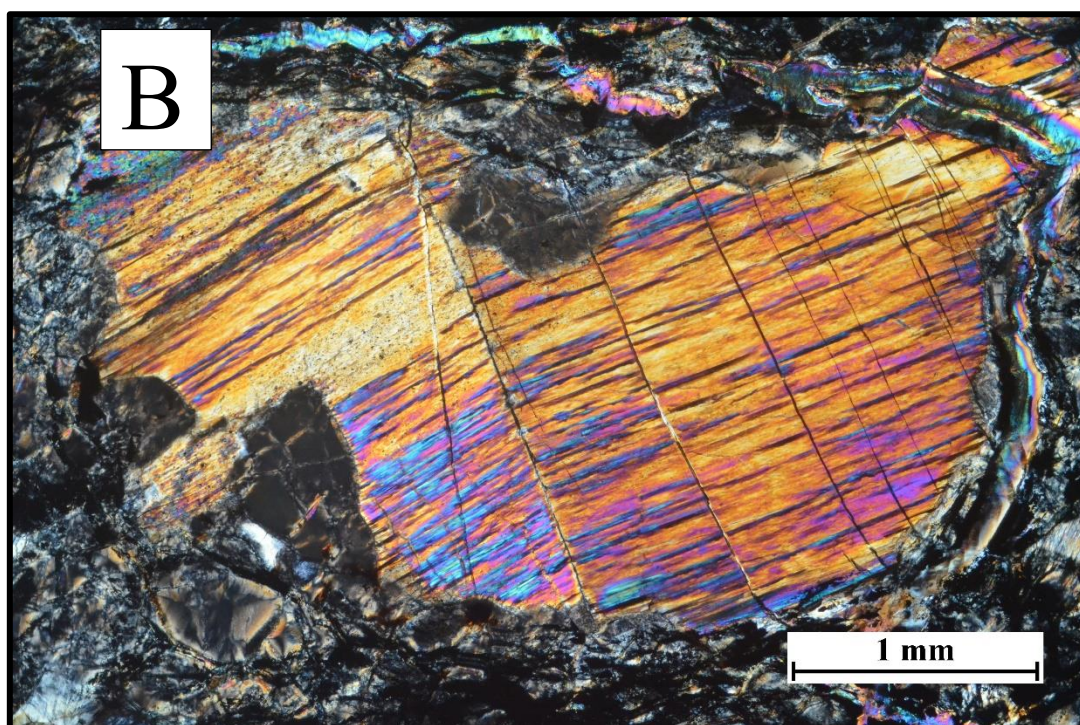
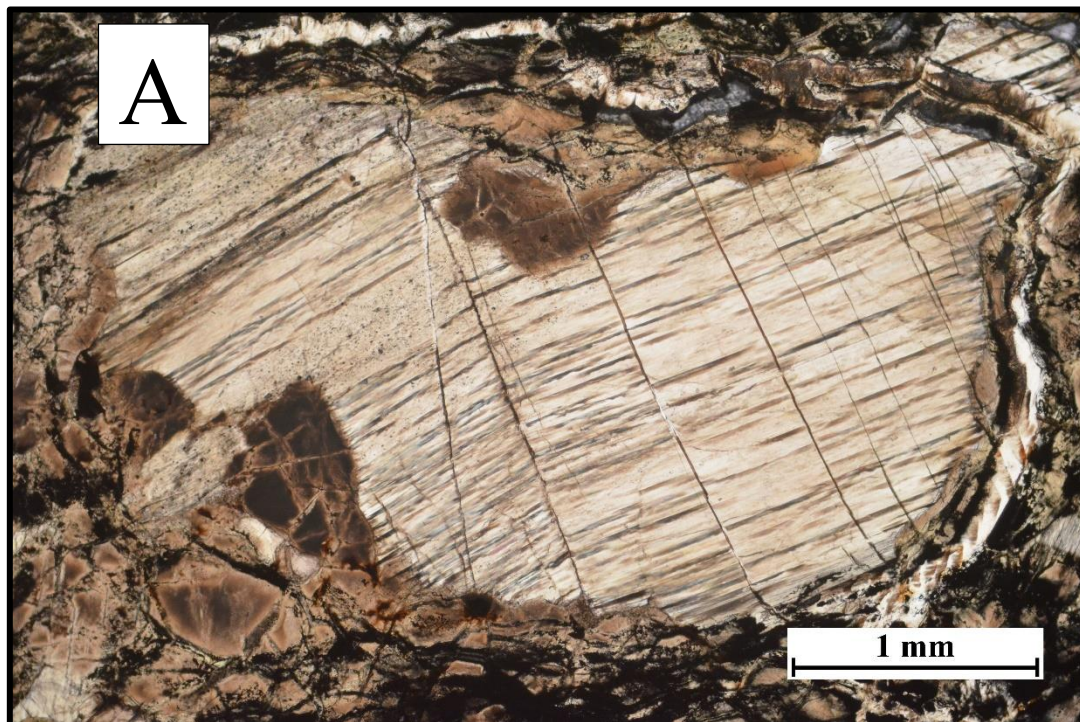


Figure:4.1.1. (A) Plane Polarised light (B) between cross polars, Pyroxene grain surrounded by mesh texture in serpentinised peridotite.

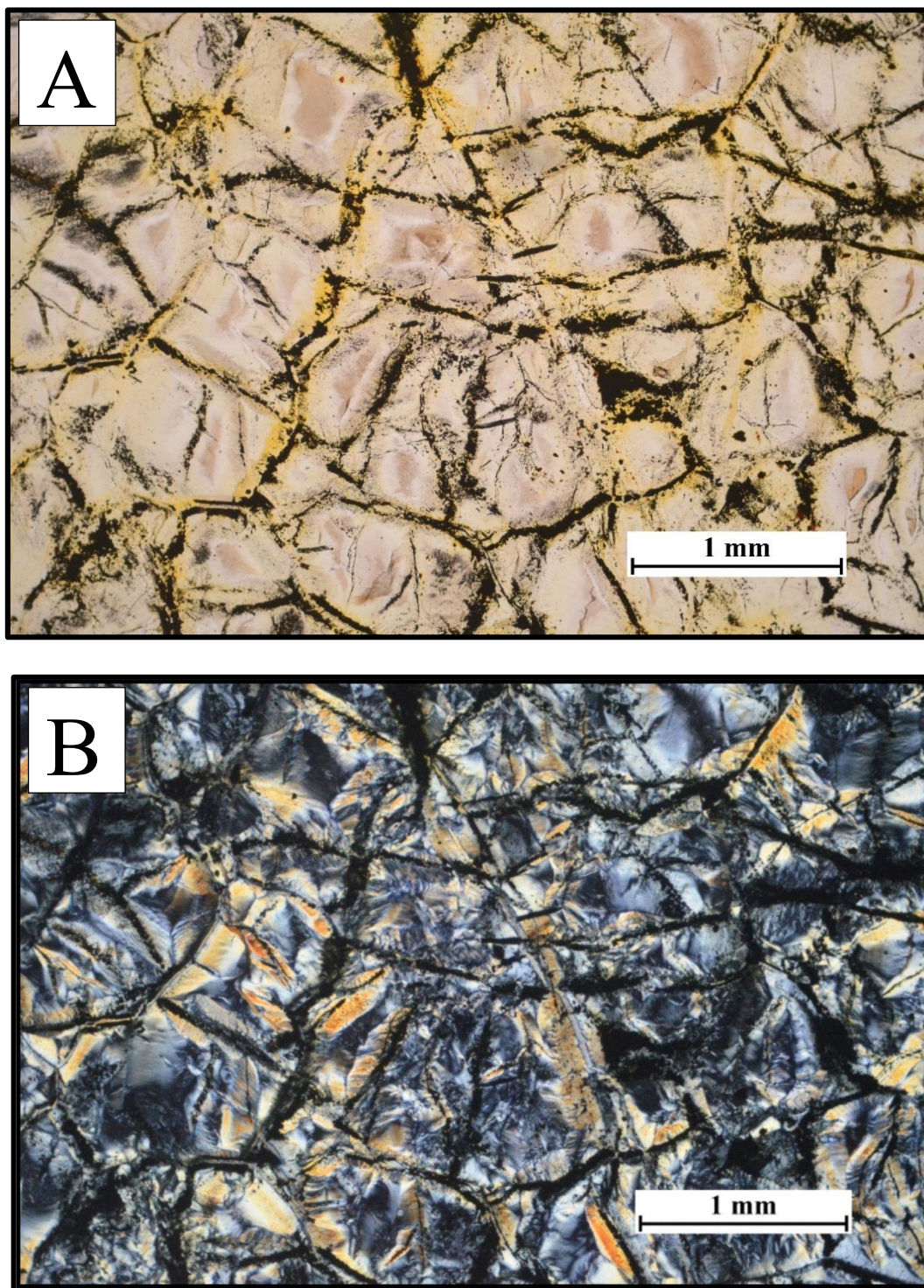


Figure:4.1.2. (A) Plane polarized light (B) Between cross polars, Mesh texture observed in studied samples.

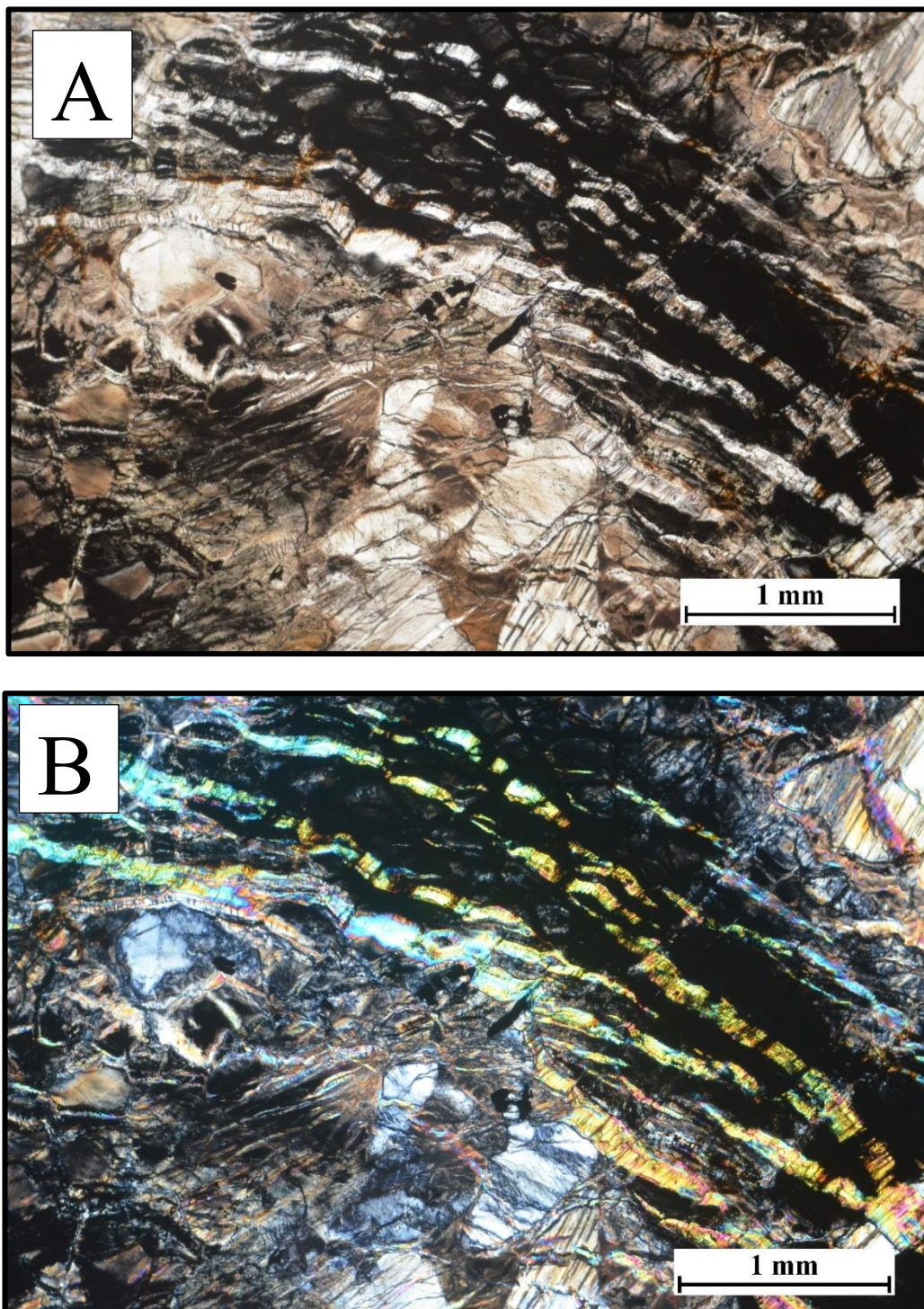


Figure: 4.1.3. (A) Plane polarized Light (B) Between cross polars, Antigorite veins along with magnetite with deformed grains of Pyroxene.

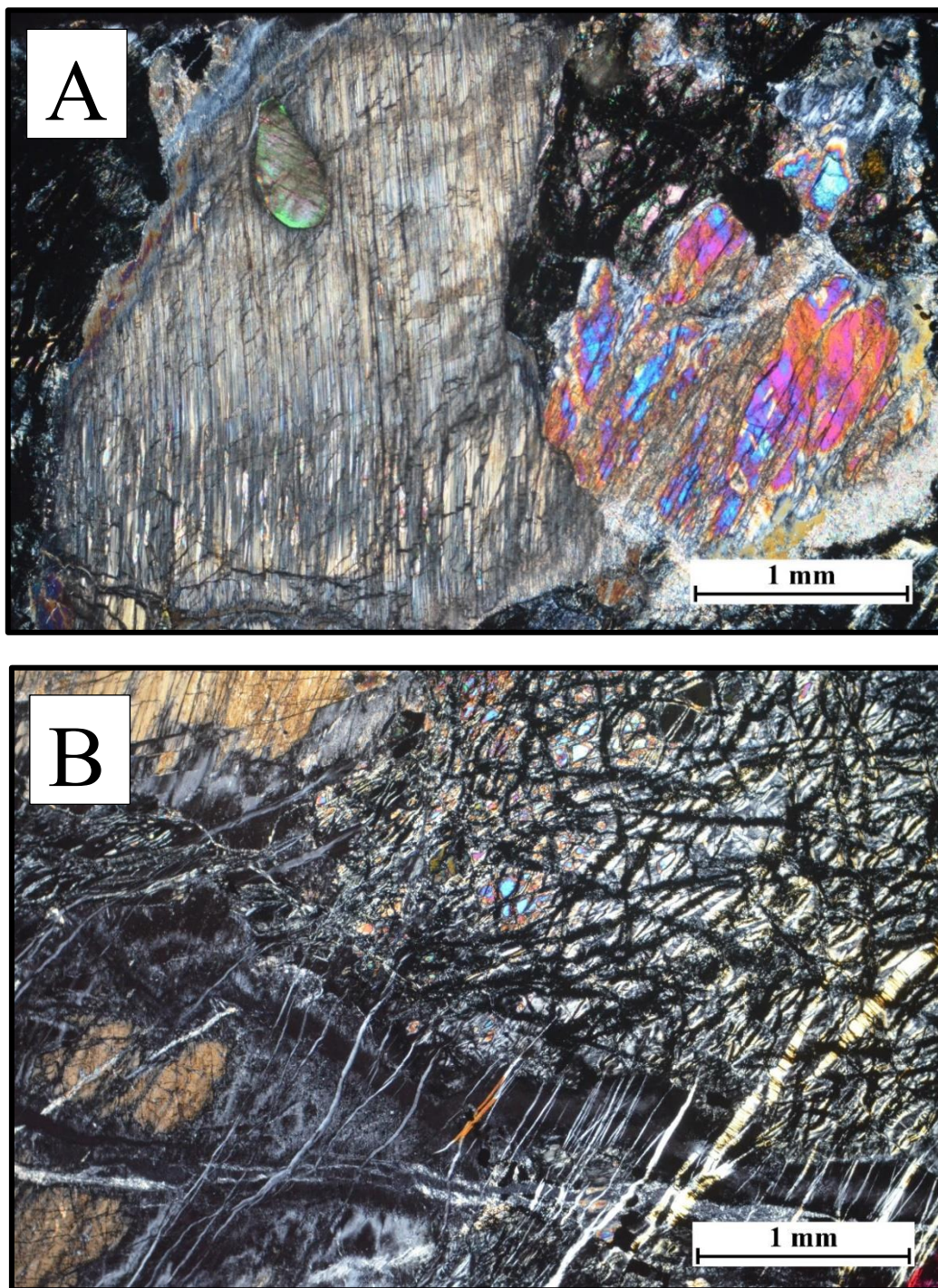


Figure:4.1.4. (A) Highly altered and deformed olivine grain in studied sample of serpentinised peridotite. (B) Veins of antigorite, magnetite mineral and deformed olivine alteration to serpentine.

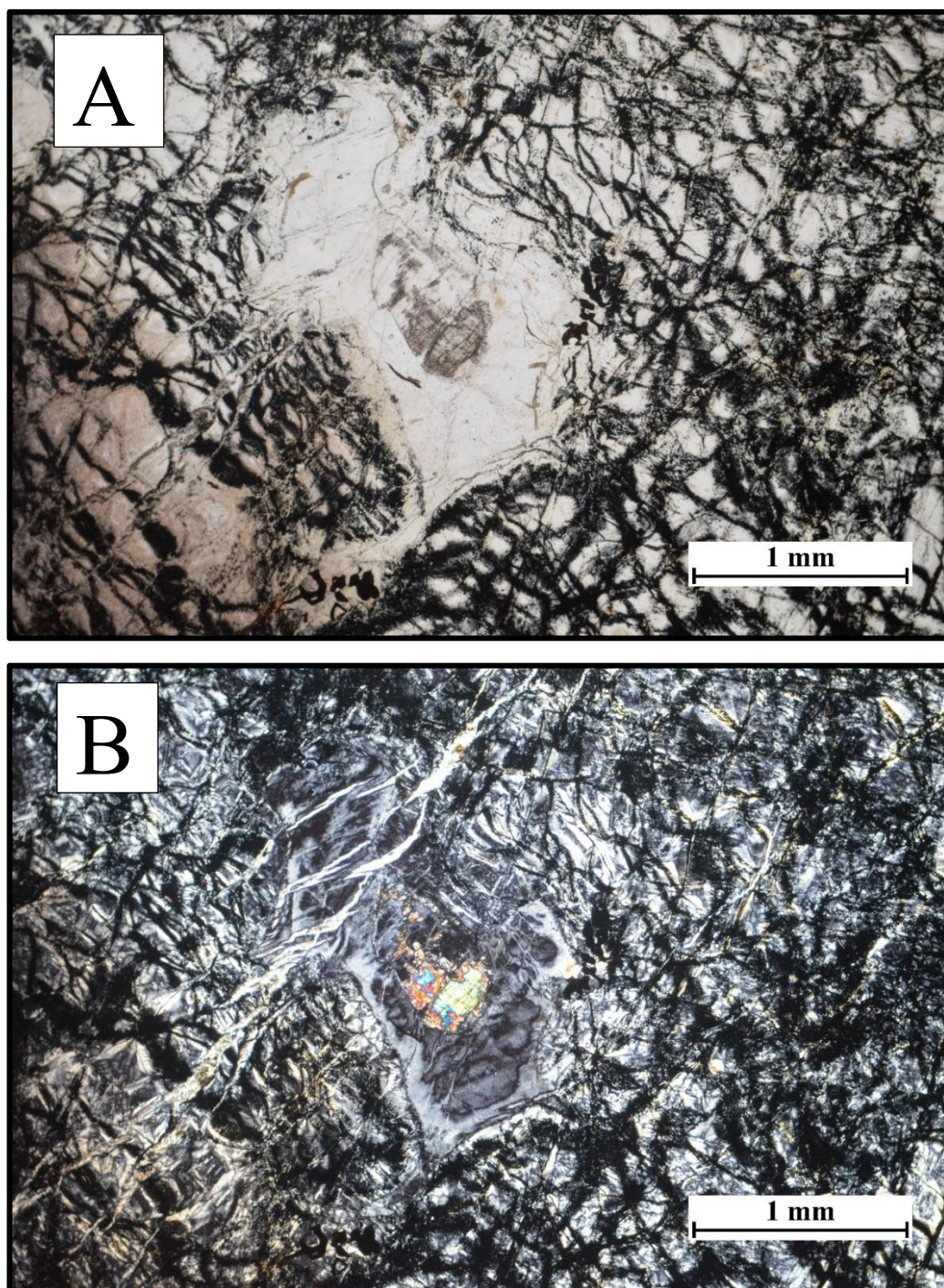


Figure:4.1.5. (A) Plane polarized light (B) Between cross polars, Bastite texture where in orthopyrosene grain is altered to serpentine but retaining the original shape.

4.2 Mineral Chemistry

Representative EPMA of Serpentine, Spinel and Magnetite are listed in Tables 4.1. Electron microprobe analyses of constituent mineral phases of investigated serpentinitized peridotites were performed at the CSIR-NIO, Dona Paula Goa, using wavelength dispersive spectrometry (WDS) on a CAMECA X5. Microprobe counts were obtained simultaneously using a 15 KeV accelerating voltage, a 1-2 μm beam diameter, and a beam current of 15 nA. Synthetic as well as natural standards were used during the analyses.

Stoichiometry has been calculated for each crystal that was probed, and normalized to the number of oxygens in the chemical formula of that mineral. End member compositions of each probed mineral were also calculated, and are presented as a molar percentage in tables. The weight percentage of each oxide was divided by the formula weight of that oxide. Secondly, the resulting "mole number" of each oxide was multiplied by the number of oxygens in the oxide formula. Then the resulting oxygen number of each oxide was multiplied by a normalization constant (equal to the number of oxygens in the desired formula divided by the sum of the oxygen numbers). Finally, the normalized oxygen numbers of each oxide were multiplied by the number of cations per oxygen in the oxide formula. Only then could the percentages of each end member, present in each probed crystal, be calculated according to their elemental makeup.

The BSE images are employed to distinguish different zones of minerals by using the contrast function, which essentially depends upon differences in average atomic number. Backscattered Electron (BSE) images are a valuable tool in distinguishing different mineral zones within a sample under study. This imaging technique relies on

the principle that atoms with higher atomic numbers exhibit brighter contrast in the resulting images. Essentially, areas with minerals containing elements of higher atomic numbers appear brighter in the BSE images.

Researchers often use these BSE images to guide the selection of locations for electron microprobe analysis. This is because variations in mineral composition, and thus average atomic number, manifest as differences in contrast within the BSE images. By carefully examining these variations, scientists can identify specific mineral zones of interest within the sample.

For instance, if a sample contains regions with minerals rich in elements like iron (Fe) or titanium (Ti) – which have higher atomic numbers – these areas would appear brighter in the BSE images compared to regions with minerals containing lighter elements like silicon (Si) or oxygen (O). This contrast allows researchers to pinpoint areas of interest for further analysis using techniques such as electron microprobe analysis.

SERPENTINE: The major element composition of serpentine species reveals distinct differences, particularly between lizardite and chrysotile compositions (**Table 4.1.3.**). (**Figure. 4.2.1.**) illustrates that the dominant serpentine species are primarily lizardite and chrysotile. Chemical variation in serpentine minerals and serpentized rocks" is one study of this type that was published in the journal *Geology of Ore Deposits* in 2018 by Evgenii Alexandrovich Kiselev and colleagues. The authors of this study talk on the chemical makeup of serpentine minerals, such as chrysotile, lizardite, and antigorite.

As the most prevalent serpentine mineral, antigorite has a structurally well-studied composition and has the chemical formula $(\text{Mg,Fe})_3\text{Si}_2\text{O}_5(\text{OH})_4$, with a larger magnesium concentration than iron. Antigorite Mg# levels have been observed to range from around 0.90 to 0.95 or higher in certain investigations. These Figures, however, may differ based on elements like the parent rock's composition and the metamorphic circumstances.

With the formula $(\text{Mg,Fe})_3\text{Si}_2\text{O}_5(\text{OH})_4$, serpentine can also take the form of lizardite. When compared to antigorite, it usually contains more iron. Hydrothermal veins and low-grade metamorphic rocks are common places to find lizardite. The literature's reported values of Lizardite Mg# might be as low as 0.90 or as high as 0.80. Once more, a number of variables, including the metamorphic conditions and geological context, can affect these numbers (Bish & Von Dreele, 1989).

Another serpentine polymorph is chrysotile, or white asbestos; its chemical formula is $(\text{Mg,Fe})_3\text{Si}_2\text{O}_5(\text{OH})_4$. Generally speaking, it has a larger iron concentration than antigorite and lizardite. Fibrous chrysotile has been widely employed in a variety of industrial applications. Its high iron and other cation concentration frequently causes its magnesium level to decrease. Chrysotile Mg# levels can be as low as 0.85 or as high as around 0.70 in the literature (Post et al., 2003).

Now, based on the average values we have got by studying the Mg# ratios it is prominent to say that the samples are belonging to the Antigorite as the values are ranging from 84.30514- 95.9434 with an average value of 93.3351, for the EPMA data.

The studied mineral chemistry (**Figure 4.2.1.**) indicates that the majority of the samples have a lizardite composition, with only one sample falling into the chrysotile group. The coexistence of chrysotile and lizardite on the plot may indicate processes

related to serpentinization. In ultramafic rocks, a frequent alteration process known as serpentinization occurs when water interacts with minerals, transforming them from olivine to serpentine minerals. These minerals belong to the serpentine group, and under certain geological circumstances, the alteration of ultramafic rocks which are rich in iron and magnesium influences their composition. Compared to other minerals like feldspar or quartz, serpentine minerals, such as chrysotile and lizardite, have comparatively lower aluminium and silicon contents. One of the minerals in the serpentine group, lizardite is formed when ultramafic rocks, usually olivine-rich rocks like peridotite, undergo alteration. Specifically, serpentine minerals like lizardite are important in the metamorphic process called serpentinization. The low-temperature polymorph of serpentine minerals in the serpentine group is called lizardite. Unlike other serpentine minerals like antigorite and chrysotile, which originate at greater temperatures, it is stable in comparatively colder environments. A rock or mineral assemblage's lizardite content suggests that the serpentinization process took place at a lower temperature. Lizardite is frequently found in serpentinized rocks and settings, such as ophiolite complexes, mantle peridotites, and regions with strong tectonic activity, such mid-ocean ridges. During the lizardite/chrysotile to antigorite transition, commonly noted phenomena include Al_2O_3 depletion and SiO_2 enrichment (e.g., Dungan, 1979; Fryer, 2002; Lafay et al., 2013; **Figure.4.2.1.**)

Analysis of the serpentine phases across all examined rocks indicates chemical signatures consistent with serpentines derived from olivine and orthopyroxene, suggesting a harzburgitic protolith (**Figure: 4.2.2.**) Based on the olivine and orthopyroxene concentration in the rock, by virtue of which it was known that, each mineral has a distinctive chemical composition, and the process of serpentinization involves the addition of water to the original minerals, resulting in the formation of

serpentine minerals. The chemical signatures mentioned likely refer to the elemental composition of the analyzed serpentine phases, indicating that the composition aligns with the expected characteristics of serpentines derived from olivine and orthopyroxene. the original rock from which another rock or mineral has formed. In this context, the statement suggests that the serpentine phases in the studied rocks have chemical characteristics indicative of a harzburgitic protolith. Harzburgite is a type of ultramafic rock that typically consists of olivine and orthopyroxene. Thus, the initial rock that was mostly made of olivine and orthopyroxene prior to serpentinization is referred to as a harzburgitic protolith. According to the information given, the rocks under study appear to have undergone a serpentinization process, and the ensuing serpentine phases show chemical characteristics that are compatible with the alteration of orthopyroxene and olivine. And further clue to the original composition of the rocks before to modification is provided by the discovery of a harzburgitic protolith.

SPINEL and MAGNETITE: Hellebrand et al. (2001) used spinel as a quantitative melting indicator of mantle residues. The chromium number of spinel (Cr#) is an important geochemical parameter for the estimation of the degree of partial melting (Lee, 1999; Dick and Bullen, 1984). The equation $[F=10\ln(\text{Cr\#})+24]$ has been widely used to describe the extent of melting (F) as a function of spinel Cr#, which is applicable when spinel Cr# values is between 0.10 and 0.60 (Hellebrand et al., 2001). In this study, the fresh core of spinel can be used to estimate melting degree of dredge abyssal peridotite (**Table 4.1.1 and 4.1.2.**). The average extent of melting (F) calculated by Cr# is about 16.22%.

The composition of Cr-spinel displays considerable variability, as indicated in (**Table 4.1.1 and 4.1.2.**). The Cr# (defined as $[\text{Cr}/(\text{Cr} + \text{Al})]$) and Mg# (defined as $[\text{Mg}/(\text{Mg} + \text{Fe}^{2+})]$) ratios within the Cr-spinel cores range from 0.454 to 0.463 and 0.61 to 0.68, respectively. Notably, the cores exhibit high Fe^{3+} content, reaching up to 0.027 in terms of the $[100 \text{ Fe}^{3+}/(\text{Fe}^{3+} + \text{Cr} + \text{Al})]$ atomic ratio, for the studied samples from the Central Indian Ridge (CIR). Magnetite is predominantly found within the groundmass and in the form of veins in the samples under investigation. (**Table 4.1.1.**) provides the analyzed compositions of magnetite within these samples.

In **Figure (4.2.4).**, a triangle diagram is utilized to categorize trivalent cations in spinel-group minerals from serpentinite-hosted peridotites (SSPs). This diagram serves to illustrate compositional variations based on three trivalent cations: Cr^{3+} , Fe^{3+} , and Al^{3+} . Plots within the diagram represent different compositions of spinel-group minerals, and their distribution provides insights into the concentration of trivalent cations. Each vertex of the triangle corresponds to 100% of the respective trivalent cation.

The positioning of plots within the triangle diagram indicates enrichment in Fe within specific fields. This enrichment suggests that the spinel-group minerals in these areas contain a higher proportion of Fe^{3+} compared to other trivalent cations. The presence of plots within the Fe-enriched field indicates that magnetite exhibits particularly high Fe^{3+} compositions in this specific geological context. Analyzing plot placements within the Fe-enriched field offers valuable geochemical information regarding the composition of spinel-group minerals in SSPs, especially highlighting the significant Fe^{3+} enrichment in magnetite found within serpentinite-hosted peridotites.

The categorization diagram aids in understanding the petrogenetic processes responsible for the formation of these spinel-group minerals, particularly emphasizing Fe enrichment as indicative of specific geological conditions such as metamorphic degree or mineral assemblages, especially in the case of magnetite.

Additionally, the field of chromiferous spinel, denoting spinel minerals containing chromium in their chemical composition, is delineated within the diagram. Chromiferous spinels, characterized by the general formula AB_2O_4 where A and B represent distinct metal ions, owe their coloration to chromium within their crystal structure. Chromium, a transition metal, can substitute other elements in the spinel crystal lattice, resulting in red-colored spinels. The term "chromiferous" underscores the chromium content of these spinels, commonly found in various geological settings including kimberlites, basalts, metamorphic rocks, igneous rocks, and certain mineral deposits.

The composition of chromiferous spinel, including its chromium and trace element content, plays a crucial role in determining its unique colors and properties. The identification and examination of chromiferous spinel contribute significantly to understanding rock formation and alterations in geological investigations.

In Figure 4.2.5., a triangle plot is utilized to depict the compositional variations of spinel-group minerals based on the trivalent cations Cr^{3+} , Fe^{3+} , and Al^{3+} . Each corner of the triangle represents one of these cations, allowing for a visual representation of how the compositions of spinel-group minerals change depending on the relative amounts of Cr, Fe, and Al.

The positioning of spinel plots within the triangle plot indicates that their compositions lie between Cr and Al. This geochemical representation illustrates the fluctuation in

Cr, Fe, and Al compositions of spinel-group minerals found in peridotites hosted by serpentinite. This variability suggests a foundation for understanding the equilibrium relationships between olivine and spinel-group minerals in these geological settings.

The observed field of spinel plots falling between Cr and Al implies that the compositions of spinel-group minerals in serpentinite-hosted peridotites are intermediate between those dominated by Al and Cr compositions. This finding provides insights into the geological history and petrogenetic processes of peridotites within serpentinite environments, showcasing the compositional diversity and the relative proportions of Cr, Fe, and Al in spinel-group minerals.

The Cr# vs. Mg# (**Figure.12a**), Fe# vs. Mg# plots (**Figure.4.2.6 and 4.2.7.**) depict the compositional characteristics of spinel-group minerals in peridotites hosted by serpentinite. The Cr# ratio represents the percentage of trivalent (Cr^{3+}) chromium relative to total chromium, indicating the degree of chromium oxidation. Similarly, the Fe# ratio signifies the proportion of trivalent iron (Fe^{3+}) relative to total trivalent iron, aluminum, and chromium, providing insights into the degree of iron oxidation. Both ratios also show the percentage of magnesium in the divalent (Mg^{2+}) state relative to the total amount of magnesium and iron, offering information on the magnesium abundance in relation to iron.

These plots enable the characterization of spinel-group minerals based on their magnesium and chromium content, as well as their oxidation states. The distribution of data points reveals patterns related to oxidation states and the relative enrichment of magnesium in spinel-group minerals.

The enrichment observed in spinel for magnesium suggests that areas with higher magnesium content may have higher concentrations of spinel-group minerals or

exhibit increased magnesium enrichment. Conversely, magnetite shows enrichment for iron and chromium, indicating a connection with locations having higher iron and chromium concentrations.

The present study focuses on understanding the distribution of rock types and their associated mineralogical compositions, with a particular emphasis on spinel ratios. Spinel Cr# (Cr number) to spinel Fe# (Fe number) ratios serve as vital geochemical markers, offering insights into the formation, development, and petrological processes that have influenced these rocks.

The plots presented, notably **(Figure 4.2.8.)**, are instrumental in visualizing the relationships between the rock compositions and spinel mineral values. These plots span the overlapping fields of back-arc peridotites, abyssal peridotites, and forearc peridotites, providing a comprehensive view of the geological contexts under investigation.

The Cr# ratio, derived from the molar concentration of chromium to the total chromium and aluminum in spinel, signifies the refractoriness of the source material. Higher Cr# levels suggest a purer mantle source with limited involvement in melt extraction or crystallization. On the other hand, the Fe# ratio, calculated from the molar iron concentration to the total iron and magnesium content in spinel, reflects the primitive or developed nature of the composition. Lower Fe# readings indicate a more developed or depleted mantle

Electron microprobe analysis of magnetite from Ridge segment Rocks						
Sample No.	SK 195/1	SK 195/1	SK 195/1	SK 195/1	SK 195/7	SK 195/7
DataSet/Point	D4	E3	F3	F4	C1	E5
SiO ₂	5.22	3.85	2.18	3.89	0.14	0.12
TiO ₂	0.03	0.05	0.01	0.04	0.21	0.05
Al ₂ O ₃	0.66	0.04	-0.01	-0.01	0.12	0.03
Cr ₂ O ₃	0.1	0.01	0	0.01	1.58	-0.01
Fe ₂ O ₃	0	0	0	0	0	0
FeO	82.51	86	88.88	87.51	91.64	94.19
MnO	0.1	0.11	0.19	0.18	0.01	0.16
MgO	4.24	4.21	2.17	3.5	0.56	0.32
Na ₂ O	0.18	0.01	0.03	-0.01	-0.03	0.04
P ₂ O ₅	0	0	0.01	0.05	-0.02	-0.02
K ₂ O	0.02	-0.01	0	-0.01	-0.02	-0.03
CaO	0.03	0.06	0.01	0.01	0.08	0.01
SO ₂	0.05	0.02	-0.01	0.01	0.03	0
NiO	0.09	0.1	-0.07	0.15	0.12	0.02
Total	93.22	94.43	93.41	95.32	94.42	94.87
Cr#	0.092265	0.143623	0	-2.03805	0.898299	-0.28802
Mg#	0.195529	0.201123	0.112873	0.166925	0.031291	0.017971
Fe#	0.980459	0.99883	1.000241	1.000082	0.973351	0.999479

Table: 4.1.1. Representative EPMA data of Magnetite.

Electron microprobe analysis of spinel from Ridge segment Rocks					
Sample No.	SK 195/1	SK 195/1	SK 195/1	SK 195/1	SK 195/1
Point	A6	B1	B2	C5	C6
SiO ₂	-0.01	0.03	0.05	0.09	0.02
TiO ₂	0.05	0.07	0.06	0.06	0.07
Al ₂ O ₃	28.96	30.59	30.28	30.66	29.71
Cr ₂ O ₃	37.2	38.44	38.37	38.02	38.25
Fe ₂ O ₃	0	0	0	0	0
FeO	18.33	15.6	15.65	15.95	16.37
MnO	0.18	0.13	0.12	0.1	0.1
MgO	13.68	15.66	15.61	15.26	14.76
Na ₂ O	-0.02	0.01	0	0.01	-0.01
P ₂ O ₅	-0.01	-0.01	0	0.02	-0.02
K ₂ O	0.01	0.03	-0.01	0	-0.01
CaO	0.1	0.06	-0.05	0.05	0.05
SO ₂	0.01	0.01	0	0	0.02
NiO	0	0.16	0.08	0.05	0.02
Total	98.49	100.77	100.17	100.26	99.33
Cr#	0.462861	0.457404	0.45948	0.454112	0.463425
Mg#	0.617544	0.680317	0.680701	0.664828	0.653109
Fe#	0.027914	0.020598	0.021675	0.018632	0.020241

Table:4.1.2. Representative EPMA data of spinel.

Electron microprobe analysis of Serpentine from Ridge segment Rocks					
Sample No.	SK 195/1				
DataSet/Point	A2	A3	B5	B6	C4
Na ₂ O	0.05	0.07	0.08	0.06	0.02
MgO	38.11	39.28	36.72	40.54	40.26
SiO ₂	38.82	41.81	38.46	39.94	41.22
Al ₂ O ₃	2.44	0.37	2.46	0.29	0.33
P ₂ O ₅	0.04	0	0.01	0	0.02
K ₂ O	0.02	0.02	0.01	0	0
CaO	0.04	0.03	0.06	0.03	0.02
TiO ₂	0.04	0	0.01	0.01	0.01
MnO	0.01	0.03	0.03	0.02	0.02
FeO	3.93	2.14	4.12	1.88	1.88
SiO ₂	0.06	0.04	0.08	0.03	0.03
Cr ₂ O ₃	1.11	-0.01	1.04	0.05	0.02
NiO	0.14	0	0.12	0.18	0.09
Total	84.82	83.78	83.22	83.02	83.92

Table: 4.1.3. Representative EPMA data of serpentine mineral.

Electron microprobe analysis of Serpentine from Ridge segment Rocks						
Sample No.	SK 195/1					
DataSet/Point	C7	D1	D2	D3	D5	D6
Na ₂ O	-0.01	-0.02	0.06	0.04	0.08	0.01
MgO	41.46	39.62	39.91	39.99	36.62	39.16
SiO ₂	41.02	40.83	40.69	41.51	39.39	41.36
Al ₂ O ₃	0.22	0.58	0.45	0.18	2.73	0.78
P ₂ O ₅	0.01	0	0	0.01	0.01	-0.01
K ₂ O	-0.02	0	-0.01	0	-0.01	0
CaO	0.01	0.03	0.03	0.02	0.07	0.02
TiO ₂	0.04	0	0.03	0.03	0.03	0
MnO	0.07	0.01	0.02	0.03	0.07	-0.01
FeO	2.12	1.97	2.21	2.61	3.92	1.67
SiO ₂	0.04	0.05	0.01	0.04	0.06	0.06
Cr ₂ O ₃	0.02	-0.01	0.05	0.01	0.87	0.03
NiO	0.09	0.06	0.04	0.15	0.03	0.25
Total	85.05	83.11	83.49	84.61	83.86	83.34

Table:4.1.3. (Contd.)

Electron microprobe analysis of serpentine from Ridge segment Rocks										
Sample No.	SK 195/7									
DataSet/Point	A2	A5	B2	B3	C2	C5	D2	D4	E2	E2
Na2O	0.09	-0.02	0.03	0	0.02	0.05	0.08	0.01	0.02	0.02
MgO	38.22	40.68	39.46	40.55	36.58	40.19	37.53	40.31	38.41	40.54
SiO2	39.87	41.43	40.48	39.8	40.02	40.99	39.26	41.33	38.73	41.29
Al2O3	1.95	0.23	0.44	0.62	0.64	0.22	1.7	0.21	2.22	0.24
P2O5	0	-0.01	0.01	0.02	-0.01	0.01	-0.01	0.02	0.03	-0.04
K2O	0.02	0	0	0	0.02	0.01	0	-0.01	0.02	0.02
CaO	0.07	0.04	0.01	0.01	0.05	0.03	0.06	0.02	0.07	0.02
TiO2	-0.01	0.04	-0.01	0.01	-0.01	0	0.06	0.01	0.03	0.01
MnO	0.03	0.03	0.03	0.01	0.28	0.05	0.03	0.04	0.04	0.04
FeO	3.35	1.72	1.61	1.81	6.81	2.19	3.13	1.74	4	1.81
SO2	0.09	0.07	0.05	0.03	-0.01	0.04	0.09	0.05	0.09	0.03
Cr2O3	1.2	0.03	0.05	0.05	0.08	0.06	1.21	-0.02	1.04	-0.02
NiO	0.16	0.28	0.12	0	0	0.27	0.2	-0.04	0.05	0.16
Total	85.04	84.52	82.29	82.9	84.47	84.1	83.34	83.67	84.75	84.13

Table:4.1.3. (Contd.)

Electron microprobe analysis of serpentine from Ridge segment Rocks										
Sample No.	SK 195/7									
DataSet/Point	A2	A5	B2	B3	C2	C5	D2	D4	E2	E2
Na2O	0.09	-0.02	0.03	0	0.02	0.05	0.08	0.01	0.02	0.02
MgO	38.22	40.68	39.46	40.55	36.58	40.19	37.53	40.31	38.41	40.54
SiO2	39.87	41.43	40.48	39.8	40.02	40.99	39.26	41.33	38.73	41.29
Al2O3	1.95	0.23	0.44	0.62	0.64	0.22	1.7	0.21	2.22	0.24
P2O5	0	-0.01	0.01	0.02	-0.01	0.01	-0.01	0.02	0.03	-0.04
K2O	0.02	0	0	0	0.02	0.01	0	-0.01	0.02	0.02
CaO	0.07	0.04	0.01	0.01	0.05	0.03	0.06	0.02	0.07	0.02
TiO2	-0.01	0.04	-0.01	0.01	-0.01	0	0.06	0.01	0.03	0.01
MnO	0.03	0.03	0.03	0.01	0.28	0.05	0.03	0.04	0.04	0.04
FeO	3.35	1.72	1.61	1.81	6.81	2.19	3.13	1.74	4	1.81
SO2	0.09	0.07	0.05	0.03	-0.01	0.04	0.09	0.05	0.09	0.03
Cr2O3	1.2	0.03	0.05	0.05	0.08	0.06	1.21	-0.02	1.04	-0.02
NiO	0.16	0.28	0.12	0	0	0.27	0.2	-0.04	0.05	0.16
Total	85.04	84.52	82.29	82.9	84.47	84.1	83.34	83.67	84.75	84.13

Table:4.1.3. (Contd.)

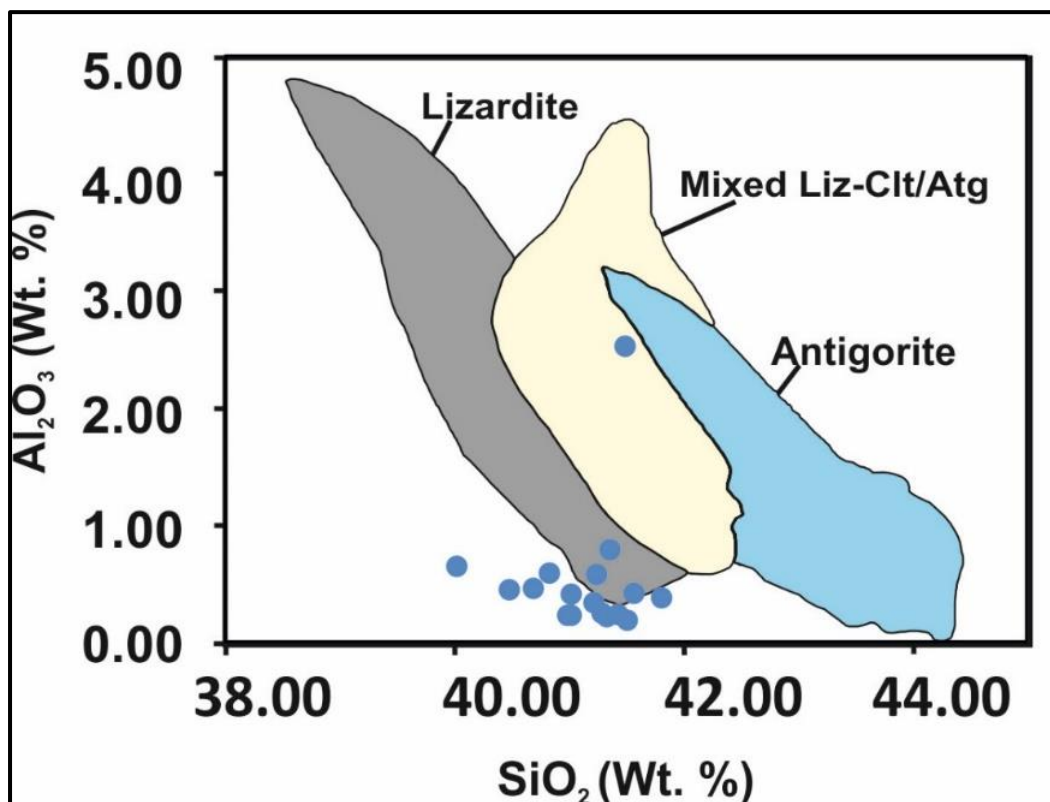


Figure:4.2.1. Al_2O_3 vs. SiO_2 (wt%). Fields of different serpentine minerals after Schwartz et al. (2013).

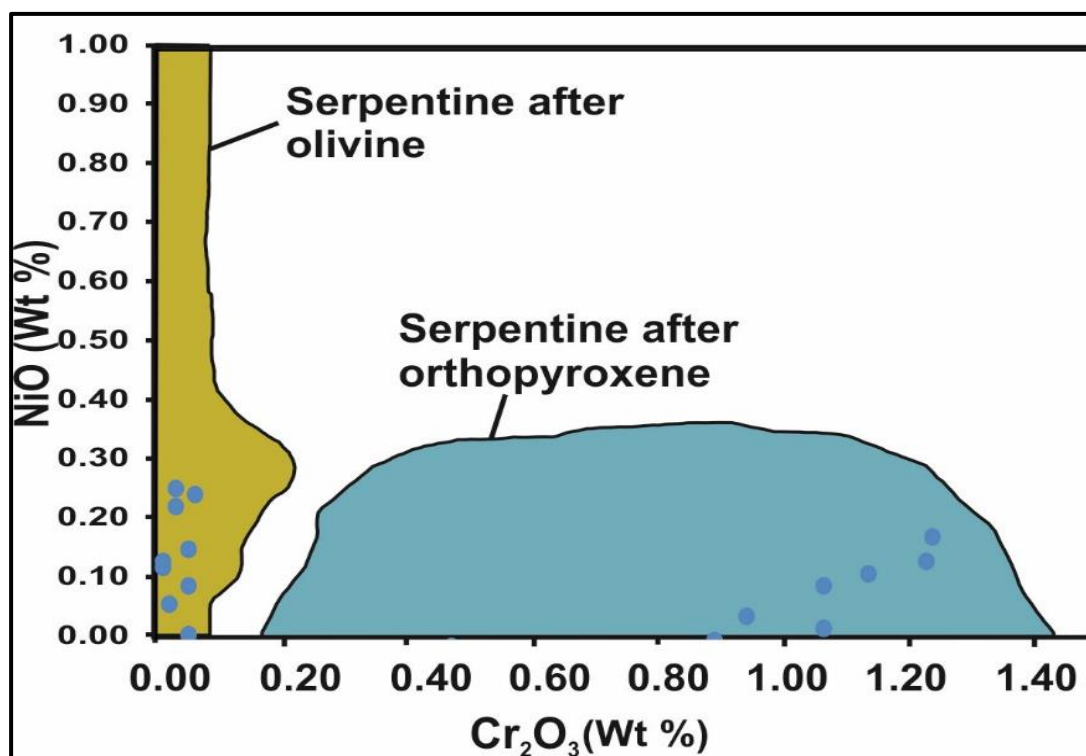


Figure:4.2.2. NiO vs. Cr_2O_3 (wt%). Fields for olivine and orthopyroxene after Kodolányi et al. (2012).

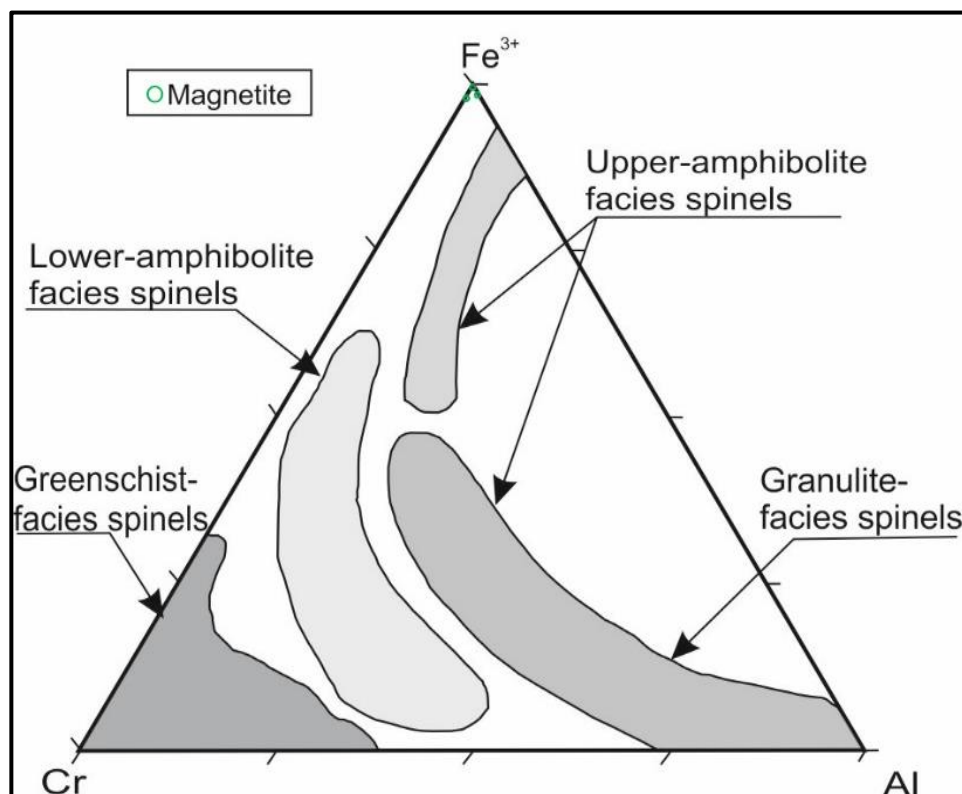


Figure:4.2.3. Triangular diagram showing chemical compositions of magnetite which plotted onto the Fe axis Fields of different metamorphic facies for altered spinel phases were concluded by Hamdy and Lebda (2011).

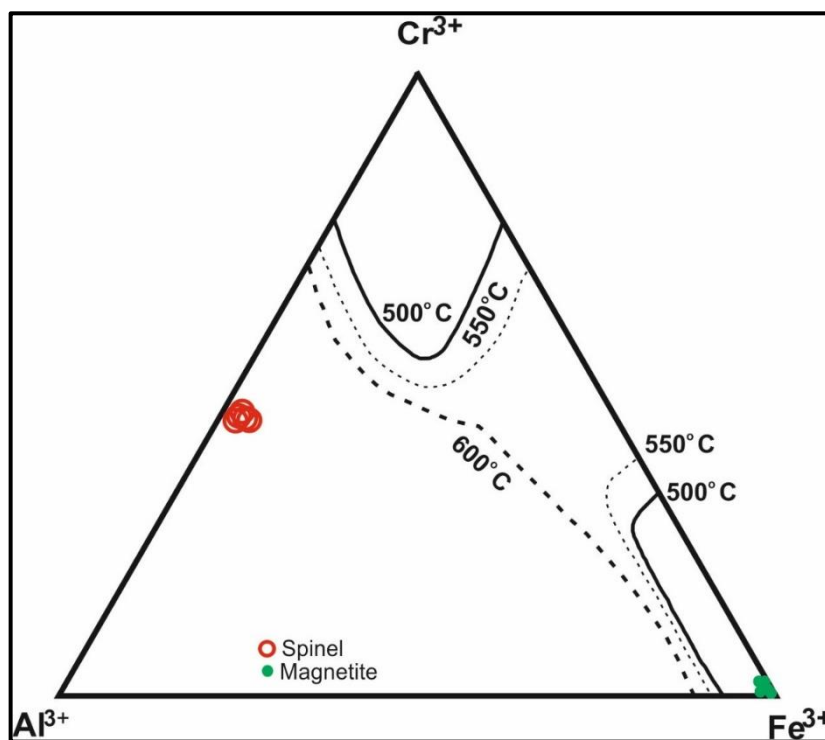


Figure:4.2.4. A trivalent cation classification triangular diagram, in the context of spinel-group minerals from serpentinite-hosted peridotites (SSPs), is used to illustrate the compositional variations based on three trivalent cations: Cr^{3+} , Fe^{3+} , and Al^{3+} .

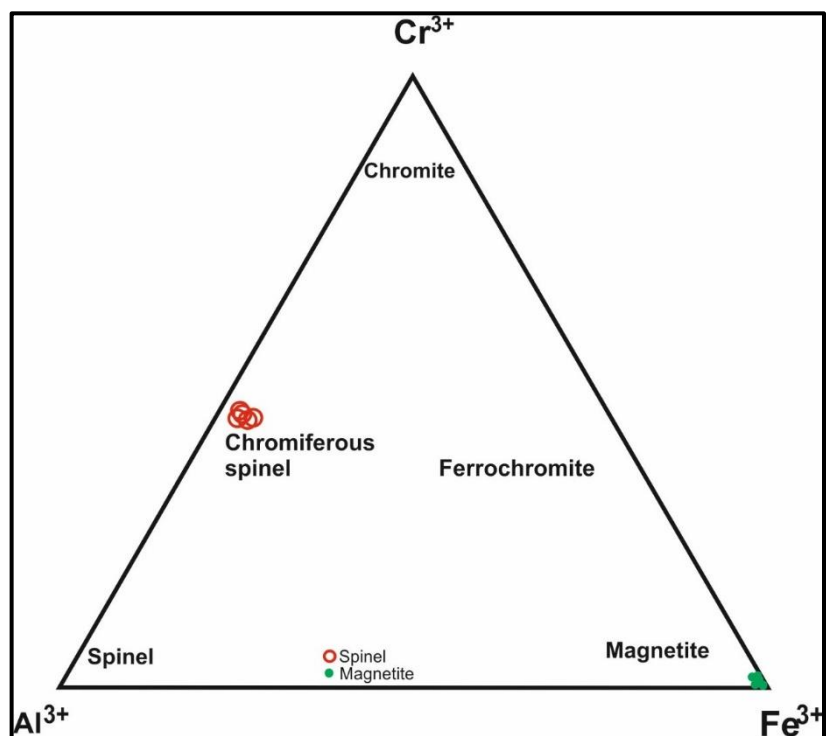


Figure:4.2.5. Compositional variability in spinel-group minerals from SSPs in a triangular Cr^{3+} - Fe^{3+} - Al^{3+} plot.

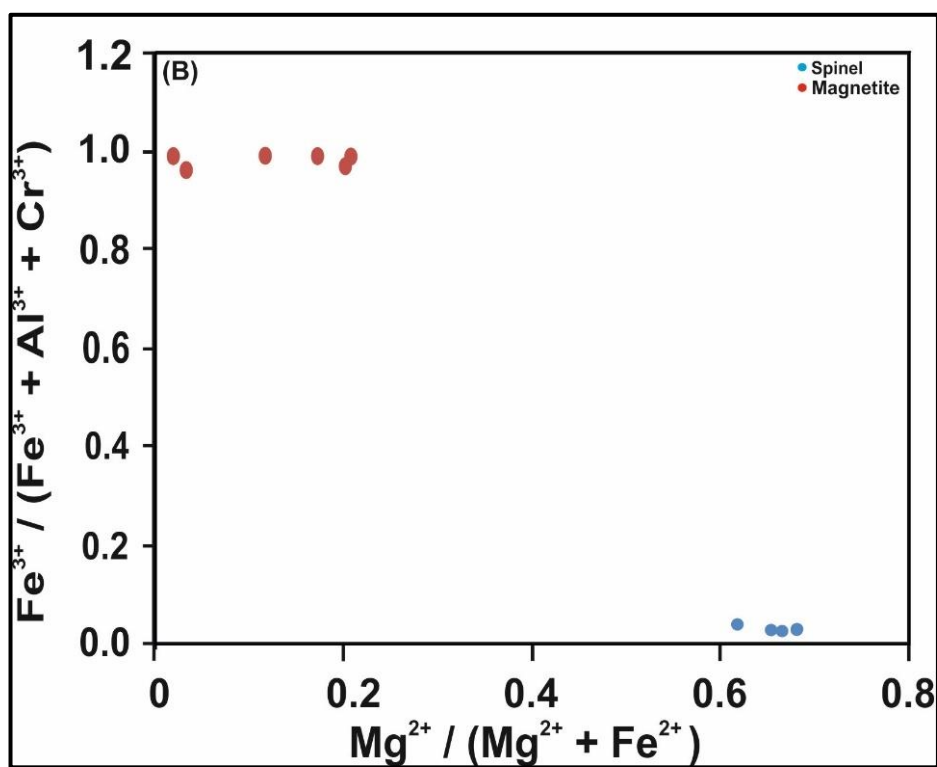
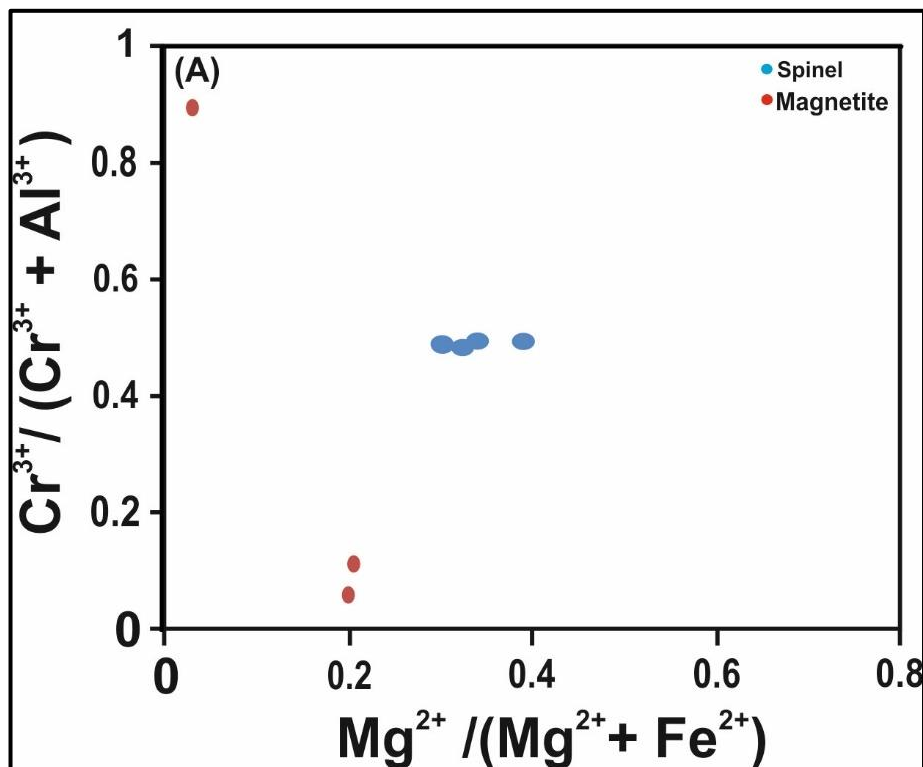


Figure:4.2.6. Spinel-group mineral compositions from SSPs plotted in (a) $\text{Cr}^{3+}/(\text{Cr}^{3+} + \text{Fe}^{3+})$ against $\text{Mg}^{2+}/(\text{Mg}^{2+} + \text{Fe}^{2+})$

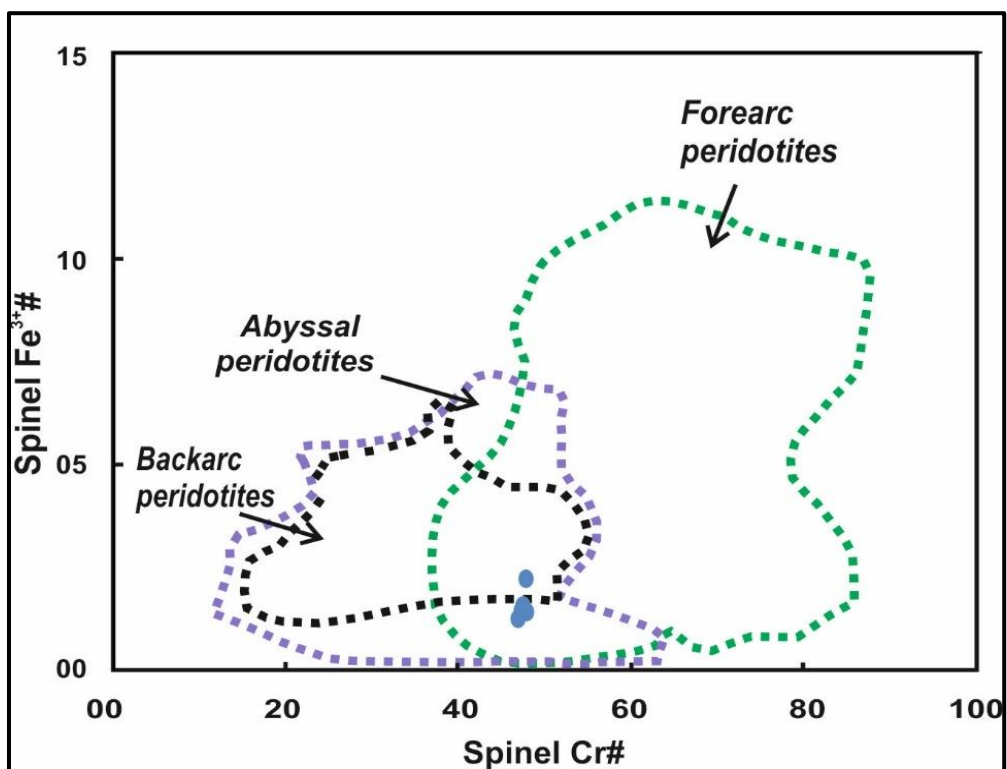


Figure: 4.2.7. Spinel Fe³⁺ # versus Cr#. Fields of forearc, backarc and abyssal peridotites are from Lian et al. (2019)

4.3 Trace and REE

The Rock/chondrite vs REE plot (**Figure 4.3.1.**) reveals a distinct trend in the elements, particularly showcasing a positive peak for Europium (Eu) across numerous samples, suggesting the absence of plagioclase feldspar within the rock. This trend also highlights an enrichment in both Light Rare Earth Elements (LREE) and Heavy Rare Earth Elements (HREE) when compared to Medium Rare Earth Elements (MREE). Notably, there is a noticeable U-shaped pattern in the Rare Earth Elements (REE) from LREE to MREE, indicating potential processes such as fractional crystallization.

Fractional crystallization, a process where LREE are preferentially incorporated into early-formed minerals, resulting in a melt richer in HREE, is mirrored in this U-shaped trend. The positive Eu anomaly signifies the selective incorporation of Eu into minerals like plagioclase.

Magmatic differentiation, akin to fractional crystallization, delineates how magma separates into distinct chemical compositions during its cooling and solidification phases. The mineral fractionation that occurs during this process contributes to the U-shaped REE trend and the presence of the Eu anomaly.

The distribution of REEs within rocks can also be influenced by the composition of the initial magma source. Therefore, the observed REE patterns may stem from variances in mantle sources or varying degrees of mantle melting, further contributing to the overall trends noted in the REE patterns.

REE and trace element data (**Figure 4.3.2.**) were plotted, revealing various trends and anomalies. Among these, a positive U anomaly was noted, with approximately seven samples exhibiting a negative anomaly for Nb and positive peaks for Hf, Zr, and Eu.

Additionally, Y displayed a small positive peak, while Ho showed a slight negative anomaly.

A positive U anomaly typically indicates decreasing conditions during the rock's formation. This suggests that under such circumstances, uranium was preferentially mobilized and concentrated. It could imply an origin in an environment with restricted oxygen supply, like a decreasing marine or lacustrine setting (lake environment).

The negative Nb anomaly may indicate preferential removal of Nb during specific geological processes or Nb depletion compared to other elements in the rock. For example, Nb extraction from magmas or its incorporation into minerals like rutile often leads to depletion in subduction zones.

The positive peaks for Hf and Zr suggest higher abundance in the rock compared to average crustal levels. These elements are commonly associated with heavy minerals such as zircon, indicating processes like crustal melting and magmatic differentiation. The positive Eu anomaly indicates selective incorporation into minerals like plagioclase during crystallization.

There is some yttrium enrichment in the rock, indicated by a small positive signal for Y. Yttrium is often linked with heavy rare earth elements, suggesting shared magmatic processes with Hf and Zr.

The slight negative Ho anomaly suggests relative holmium depletion in the rock, possibly due to removal during rock formation or incompatibility with minerals under specific conditions.

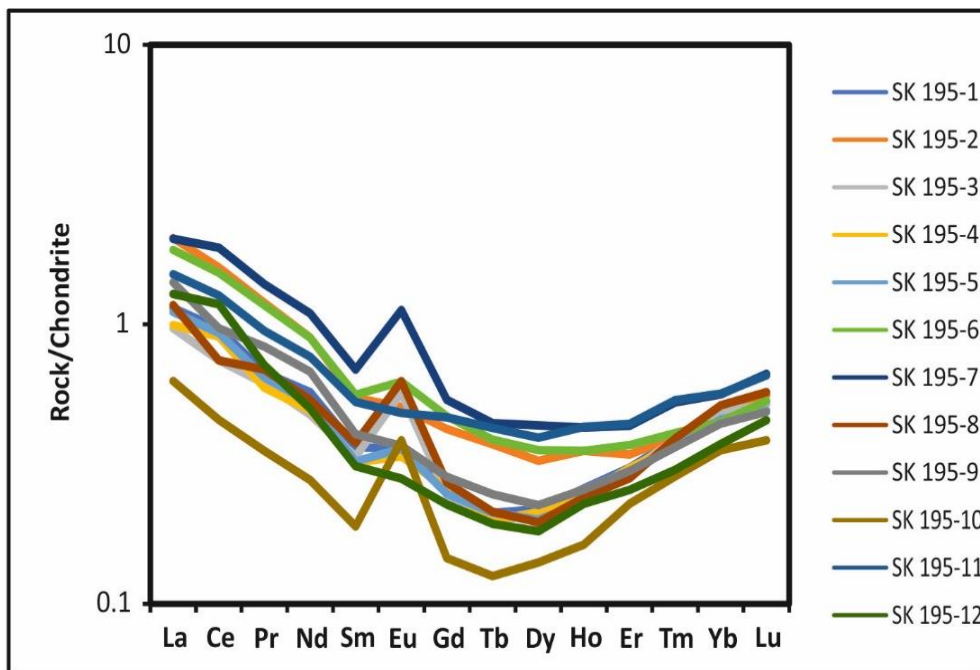


Figure:4.3.1 Chondrite normalised V/S REE plot showing U shape trend and positive Eu anomaly for serpentinised peridotite. Normalising factors are from Sun and Mc Donough (1989).

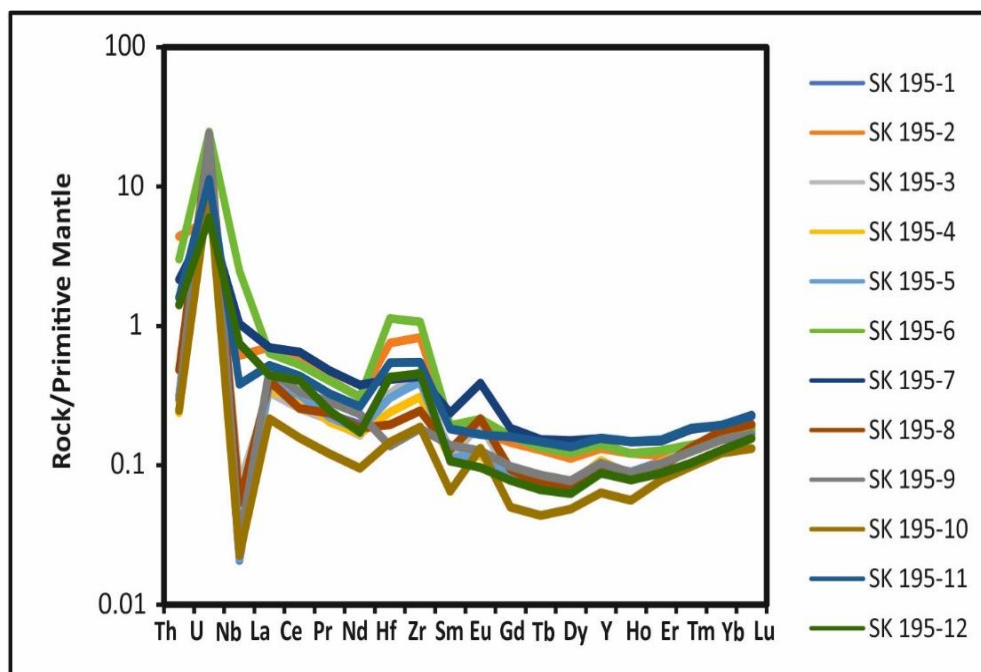


Figure:4.3.2. Primitive Mantle normalised V/S REE plot showing U shape trend and positive Eu anomaly for serpentinised peridotite. Normalising factors are from Sun and Mc Donough (1989).

CHAPTER V: DISCUSSION

5.1 Effects of serpentinization

The investigation of abyssal peridotites has traditionally been hindered by their extensive serpentinization, which is known to obscure magmatic signatures within their compositions (Dick & Fisher, 1984; Dick et al., 1984; Michael & Bonatti, 1985; Dick, 1989; Johnson et al., 1990; Johnson & Dick, 1992; Niu & Hekinian, 1997b). Consequently, major element analyses of bulk-rock abyssal peridotites were not deemed valuable for elucidating pre-serpentinization processes. In an effort to overcome this challenge and to characterize melting processes from residual materials, Niu et al. (1997) employed mineral chemical data and estimated primary mineral modes to reconstruct the bulk-rock compositions of abyssal peridotites prior to serpentinization, following previous work by Dick (1989). Subsequent quantitative analysis of this reconstructed data by Niu (1997) revealed several noteworthy phenomena pertaining to mantle melting and melt extraction processes, sparking debates among researchers (Asimow, 1999; Baker & Beckett, 1999; Niu, 1999, 2003; Walter, 1999; Lundstrom, 2000).

In the MgO/SiO_2 vs. $\text{Al}_2\text{O}_3/\text{SiO}_2$ diagram (**Figure. 5.1.1.**), the 'terrestrial array' represents the progressive magmatic depletion of a primitive mantle, with highly depleted compositions characterized by low $\text{Al}_2\text{O}_3/\text{SiO}_2$ values (Jagoutz et al., 1979; Hart and Zindler, 1986). Upon comparison with the global dataset of abyssal peridotite compiled by Niu (2004), it is evident that these samples exhibit a similar trend, albeit systematically offset towards lower MgO/SiO_2 values due to MgO loss during seafloor weathering (Snow and Dick, 1995; Niu, 2004). The observed increase in $\text{Al}_2\text{O}_3/\text{SiO}_2$ with decreasing MgO/SiO_2 in this dataset can be attributed, at least partially, to melt impregnation processes within the thermal boundary layer (Niu, 2004). A trend

analogous to the terrestrial array, as reported by Jagoutz et al. (1979), is observed in a global collection of abyssal peridotites provided by Niu (2004), indicating a larger tendency consistent with worldwide trends despite heterogeneity in samples from the Central Indian Ridge region. Plots for $\text{Al}_2\text{O}_3/\text{SiO}_2$ and MgO/SiO_2 fall within typical ranges observed in abyssal peridotites, with values between 0.1 and 0.3 for $\text{Al}_2\text{O}_3/\text{SiO}_2$ and between 1 and 1.2 for MgO/SiO_2 , with a maximum of 1.4 for this axis, suggesting that the samples conform to the expected geochemical characteristics of abyssal peridotites. The absence of Si-Mg mass transfer effects suggests that natural geological processes such as hydrothermal alteration and modal mineralogical composition likely contribute to the observed geochemical variations. Overall, the variation observed in the studied abyssal peridotite samples indicates the impact of regional geological processes and environments, while the overall trend aligns with global patterns observed in abyssal peridotites.

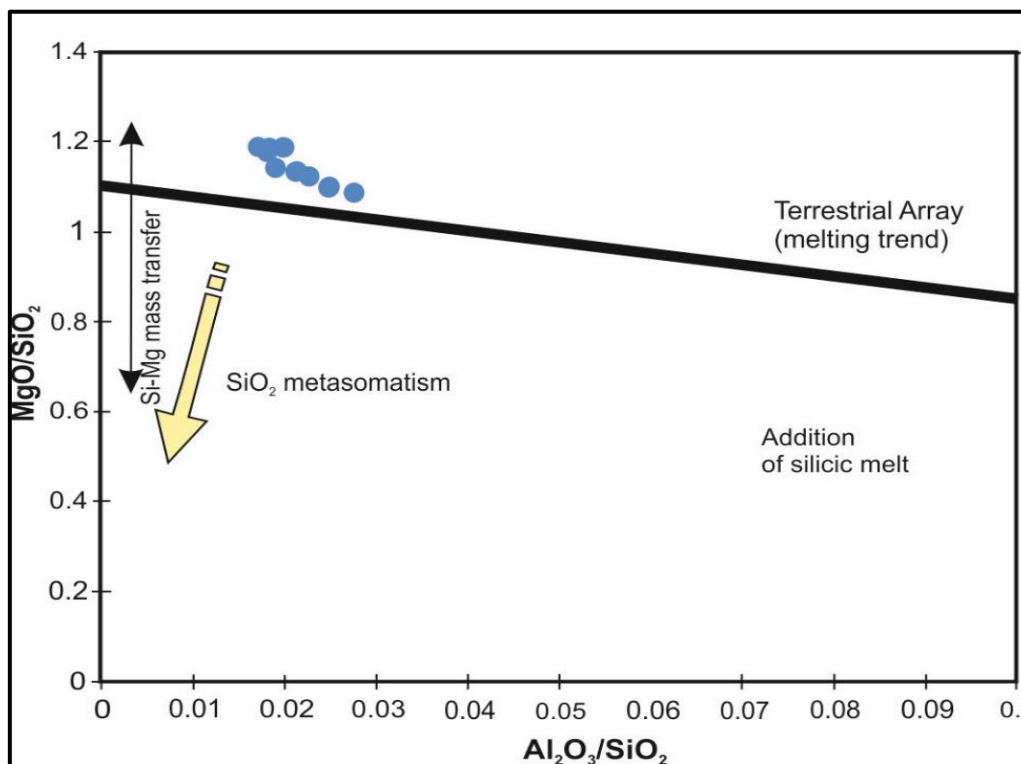


Figure:5.1.1. In MgO/SiO_2 , vs. $\text{Al}_2\text{O}_3/\text{SiO}_2$, space the data of the abyssal peridotite from the CIR area show a considerable variability whereas analyses of a global set of abyssal Peridotite presented by Niu (2004) define a trend parallel to the terrestrial array (Jagoutz et al., 1979).

5.2 Degree of mantle melting

Lherzolites and harzburgites are two common types of peridotites, distinguished by their mineralogical compositions and Mg# ratios. Lherzolites typically contain significant amounts of magnesium-rich olivine and orthopyroxene, resulting in moderate to high Mg# values. Conversely, harzburgites are characterized by their refractory nature, minimal to absent clinopyroxene content, and predominant presence of olivine and orthopyroxene. Due to the absence of clinopyroxene in harzburgites, they often exhibit higher Cr# values compared to lherzolites in Cr# vs. Mg# plots. This discrepancy arises because clinopyroxene tends to lower the Cr# ratio, and its absence in harzburgites allows for higher Cr# values. Consequently, harzburgites typically fall within a field of greater Cr# values, while lherzolites occupy a field with lower Cr# values.

The studied samples in this research encompass a range of lherzolite, harzburgite, and abyssal peridotite compositions, as observed from overlapping fields in the Cr# vs. Mg# plot (**Figure. 5.2.1**). The Cr# values of spinel within abyssal peridotites are commonly constrained by an upper limit of 0.6. Additionally, abyssal peridotites from fast-spreading ridges typically exhibit Cr# values ranging from 0.3 to 0.6, while those from slow-spreading ridges range from 0.1 to 0.3 (Lee, 1999). The primary spinels in abyssal peridotites generally display low Cr# values, typically ranging from 0.13 to 0.18, with those at the lower end of the abyssal range often associated with lherzolites (Hellebrand et al., 2001).

In the present study, the analyzed samples exhibit Cr# values ranging from 0.45 to 0.46, placing them within the central to upper range of abyssal peridotites when

plotted. This observation aligns with the composition of spinel in harzburgite from ocean ridges (Hamdy and Lebda, 2011; Lee, 1999).

The Cr# value of spinel found in mantle-derived harzburgite and lherzolite serves as an indicator of the degree of magma extraction (Hellebrand et al., 2001) during partial melting processes. For instance, the average extent of melting calculated for the studied abyssal harzburgite using Cr# is approximately 16.22%. This finding aligns with previous studies indicating that the extent of mantle melting ranges around 10% at the end of a slow-spreading rate and about 22% at the end of a fast-spreading rate across the entire spreading rate variation range (Niu and Hékinian, 1997). Hellebrand et al. (2001) further demonstrated that the range of melting for abyssal peridotites extends from approximately 2% to 18%. This variation in melting extent highlights the influence of spreading rates on the degree of mantle melting and underscores the utility of Cr# values in assessing magma extraction processes in mantle-derived rocks. The rock being Abyssal harzburgite was also confirmed by the plots of FeO, Al₂O₃, CaO, SiO₂ V/S. MgO % plots. **(Figure 5.2.2, 5.2.3)**

Submerged peridotites are considered remnants of the Earth's mantle and are typically associated with the oceanic lithosphere. The degree of contact with the Earth's crust can be inferred from the Mg# levels, with higher Mg# values suggesting minimal crustal interaction. Cr# values, on the other hand, provide insights into the extent of partial melting during mantle processes, where higher Cr# values indicate a wider range of melting. In our study, the samples examined fell within the field of Abyssal Peridotites on a partial melting trend of 15%, indicative of the proportion of chromium in relation to the overall amount of chromium and aluminium. This ratio is commonly used to assess the extent of partial melting.

Serpentinization, a process in which olivine and pyroxene in peridotite are transformed into serpentine minerals due to hydration, can significantly alter the composition of peridotites. The preferential retention of magnesium in serpentine minerals often leads to an increase in Mg# concentrations. Conversely, Cr# values may decrease due to the loss of chromium to fluid phases during alteration. Thus, higher Mg# concentrations in serpentinized peridotites may indicate a more advanced stage of serpentinization. Changes in Cr# values can provide insights into the degree of chemical modification and depletion during serpentinization.

Abyssal peridotites, commonly associated with oceanic spreading centers, may represent partially melted mantle rocks. The extent of partial melting can be inferred from the weight % of titanium dioxide (TiO₂), with higher TiO₂ concentrations suggesting greater melting. The TiO₂ vs. Cr# plot (**Figure: 5.2.4.**) can reveal differences in the composition of abyssal peridotites compared to other peridotites, indicating varying degrees of melting or different mantle sources.

The Cr# ratio, representing the concentration of chromium relative to the total of aluminium and chromium, is frequently used as a geochemical indicator in peridotites. Higher Cr# readings suggest a more refractory mantle source with a lower melting point, as partial melting reduces the likelihood of chromium mobilization. The 15% melting trend observed in our study signifies the anticipated geochemical trace of a rock that has experienced 15% melting of its initial composition. Points along or near this trend indicate rocks or samples that have undergone a comparable level of partial melting, while deviations from this pattern may suggest other source materials or differences in the melting process.

Abyssal peridotites encompass a spectrum of compositions, ranging from simple residues of mantle melting to those influenced by complex processes such as melt impregnation and fluid alteration prior to their exposure on the seafloor (Johnson et al., 1990). These diverse processes can introduce variations in the geochemical signatures of peridotites compared to pristine melting residues. However, it is noteworthy that despite these alterations, the primary magmatic signals remain discernible, enabling the estimation of the degree of mantle melting through various analytical methods.

Serpentinization and seafloor weathering are known to cause magnesium (Mg) loss in peridotites (Snow and Dick, 1995; Niu, 2004). Nevertheless, the inherent magmatic characteristics are retained, as evidenced by robust correlations observed between MgO and Al₂O₃ (**Figure 5.2.3**), and CaO. These correlations can be ascribed to the preferential depletion of the basaltic component during mantle melting processes (Dick and Bullen, 1984). Additionally, the parallel relationship observed between peridotites and the terrestrial array in the MgO/SiO₂ versus Al₂O₃/SiO₂ diagram (**Figure 5.2.3d**) supports the notion of continuous magmatic depletion originating from specific mantle sources. Consequently, major composition indicators such as Al₂O₃, CaO, MgO/SiO₂, and Al₂O₃/SiO₂ serve as valuable tools for constraining the extent of mantle peridotite depletion.

Major elements of peridotite have long served as essential proxies for estimating the extent of mantle melting across diverse tectonic regimes, including mid-ocean ridges and subduction zones (Niu, 1997; Takazawa et al., 2000, 2003; Barth et al., 2008). In **Figure 3** of our study, we juxtapose the peridotites from our investigation area with a model representing near-fractional mantle melting of major elements, as computed by Niu (1997), utilizing a primitive mantle (PM) source and a pressure range spanning

2.5–0.4 GPa. Despite the loss of MgO, which is a common consequence of alteration processes such as serpentinization, the correlations among the major oxides and the degree of mantle melting remain well-preserved.

Specifically, the Al_2O_3 content within our peridotite samples falls within the range of 0–1%, which corresponds to a model melting range of 25–30% (**Figure 5.2.6**). Traditionally, one would expect an inverse relationship between the concentrations of MgO and Al_2O_3 in peridotites. This anticipation stems from the fact that aluminium is preferentially incorporated into secondary minerals during differentiation processes, leading to an increase in Al_2O_3 content as MgO content decreases. Hence, higher MgO concentrations are typically associated with lower Al_2O_3 concentrations, indicating a negative correlation trend, which is apparent from the data points observed in our study.

The CaO content of the examined peridotites indicates a partial melting extent exceeding 25%, likely influenced by the combined effects of MgO depletion and CaO reduction due to clinopyroxene (cpx) alteration (Ulrich et al., 2010). A decrease in CaO concentration is associated with the data points clustering around 44–48 weight percent for MgO and 0–1% weight percent for CaO. This pattern reflects a decline in CaO content concurrent with increasing MgO content, a phenomenon consistent with mineral fractionation processes observed in peridotites. Notably, the data points are expected to exhibit a negative correlation trend, wherein lower CaO values correspond to higher MgO values.

The model suggests a degree of mantle melting ranging approximately from 6–8% when considering Na_2O concentrations between 0.5–0.7% (**Figure 5.2.6.c**). This

notably low degree of melting may be attributed to Na_2O 's heightened susceptibility to mantle heterogeneity and melt refertilization due to its scarcity in the primitive mantle (PM) composition (Workman and Hart, 2005) and its high incompatibility during mantle melting processes. Furthermore, Na_2O is susceptible to enhanced melt refertilization, potentially making it more fertile than the primitive mantle.

In contrast, CaO and Al_2O_3 represent major constituents of mantle mineral phases and exhibit a consistent rate of decrease prior to clinopyroxene (cpx) melting out (> 25% melt fraction). Consequently, they serve as more reliable indicators for estimating the degree of mantle melting. It is worth noting that while rough estimates of mantle melting can be derived by accounting for alteration effects, these indicators may not precisely represent the exact degree of melting.

In **(Figures 5.2.7.a and 5.2.7.b)**, the relationship between uranium (U) vs. thorium (Th) and zirconium (Zr) vs. thorium (Th) concentrations is investigated. **(Figure 4a)** displays notable variability in Th concentrations across the samples, indicating distinct geochemical signatures possibly influenced by diverse geological processes or sources. U and Th are commonly utilized as tracers for geochemical processes like melt-rock interactions and fluid-rock interactions due to their differential behaviour and mobility.

In contrast, **(Figure 5.2.7.b)** reveals an interesting trend where Zr concentrations show enrichment while Th concentrations exhibit depletion among the samples. This trend suggests a specific geochemical pattern characterized by Th depletion and Zr enrichment, possibly associated with geological system processes such as differentiation or fractionation.

The observed Th variability in the U vs. Th plot suggests the influence of multiple factors or processes altering the geochemistry of the samples, leading to varying Th concentrations. Meanwhile, the enrichment in Zr concentrations coupled with Th depletion in the Zr vs. Th plot indicates complex geochemical processes at play, potentially including melt-rock interactions and other variables impacting the geochemistry of the studied samples.

It is suggested that the observed enrichment in Zr concentrations and depletion in Th concentrations may be linked to interactions between serpentinites rich in immobile trace elements and melts. During such interactions, immobile trace elements like Zr are less prone to mobilization compared to more mobile components like Th, contributing to the enrichment-depletion pattern observed.

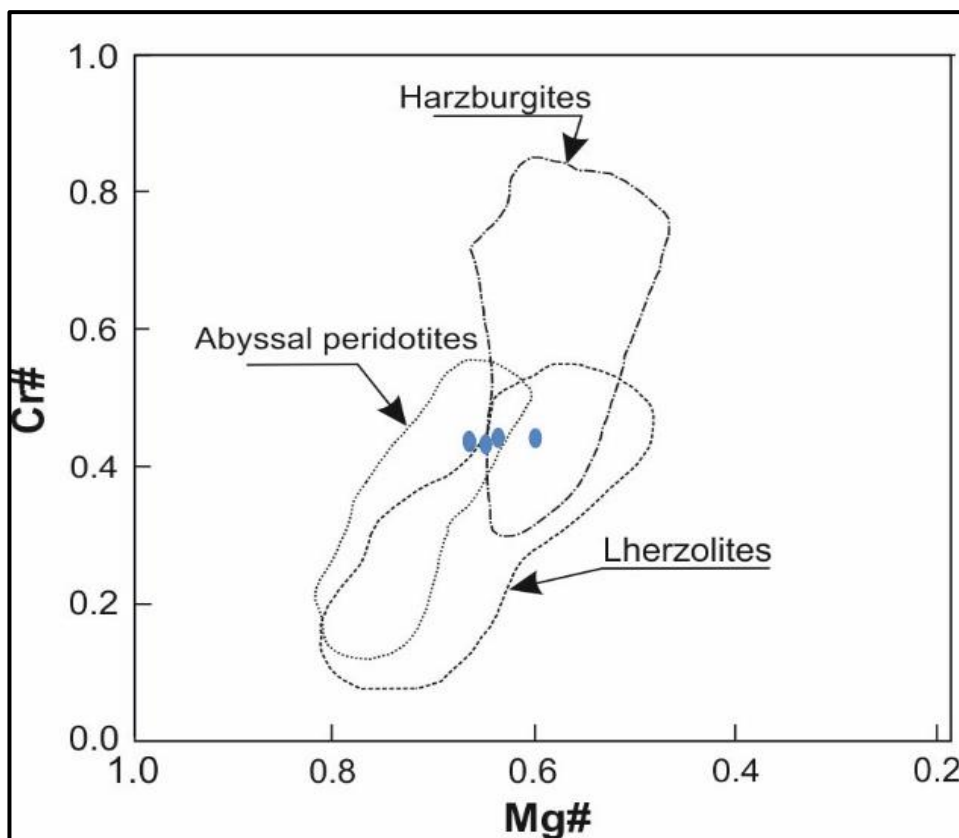


Figure: 5.2.1 Diagram showing the chemical composition of spinels (blue dots) which are plotted in lherzolite, Harzburgites and abyssal peridotite fields. The range of spinel from different rocks was concluded by Dick and Bullen (1984)

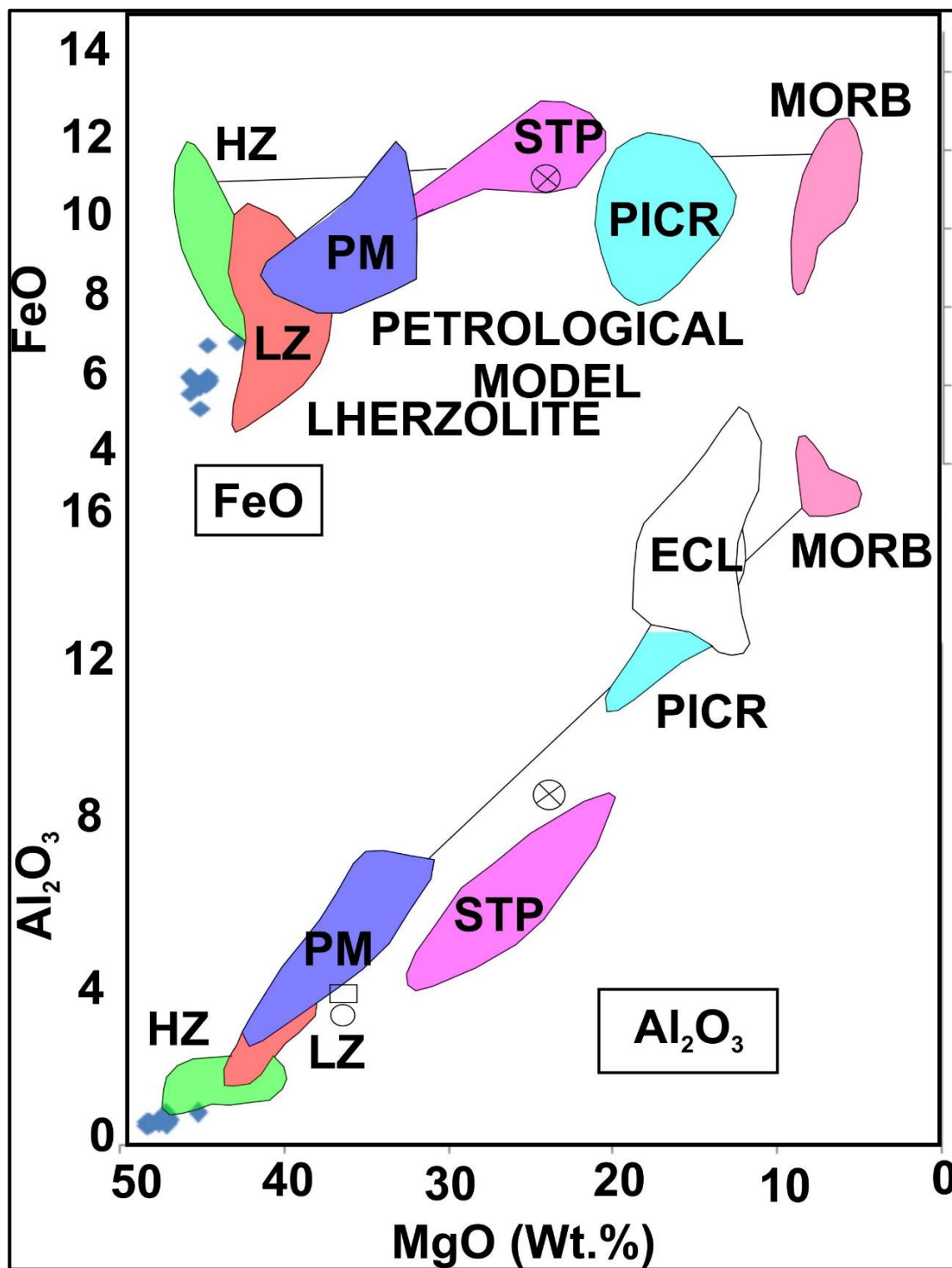


Figure: 5.2.2. Plot Of FeO vs. MgO, Al₂O₃ vs. MgO, SiO₂ vs. MgO, CaO vs. MgO, indicative of the type of abyssal peridotite.

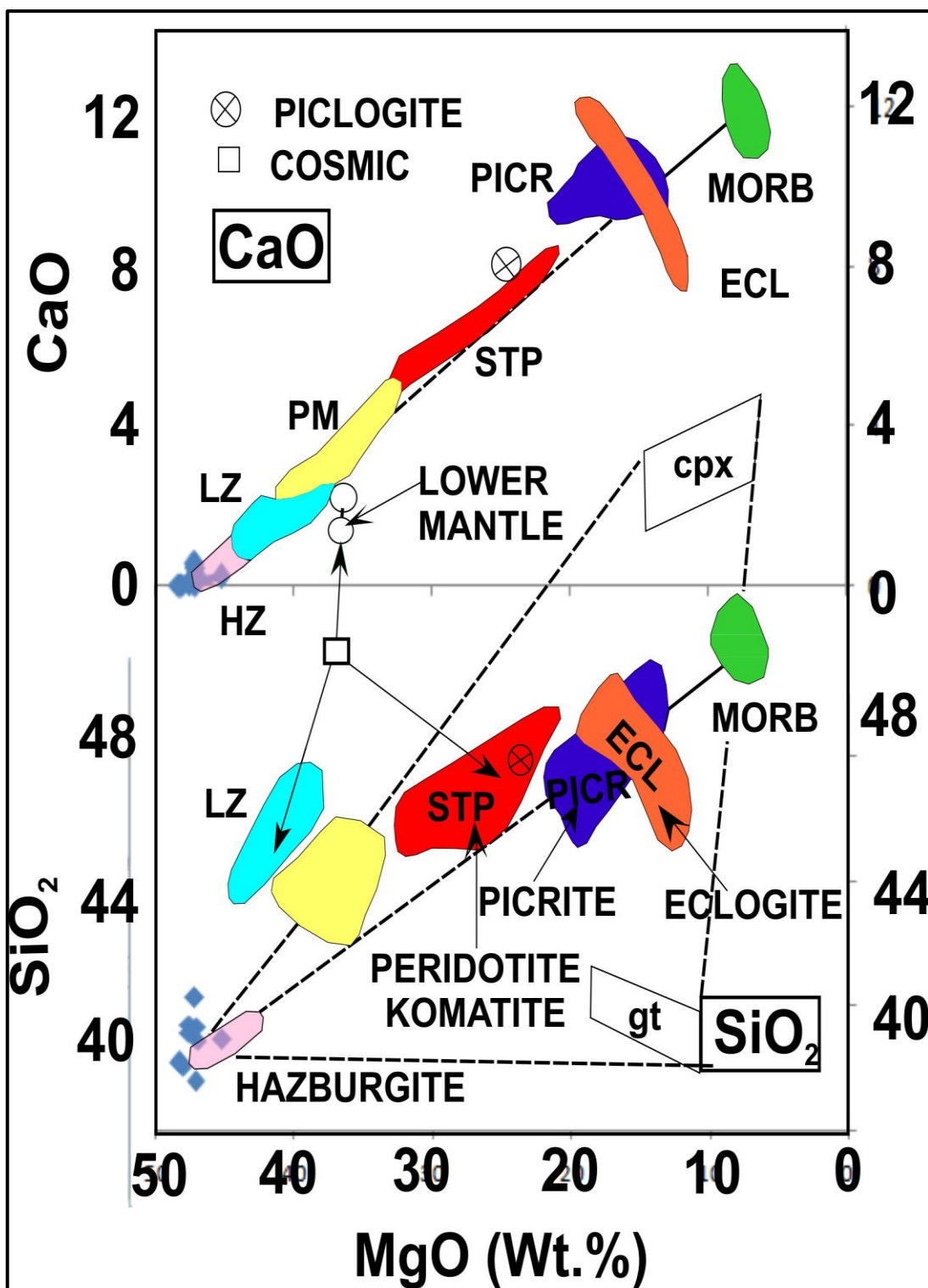


Figure: 5.2.2. (Contd.)

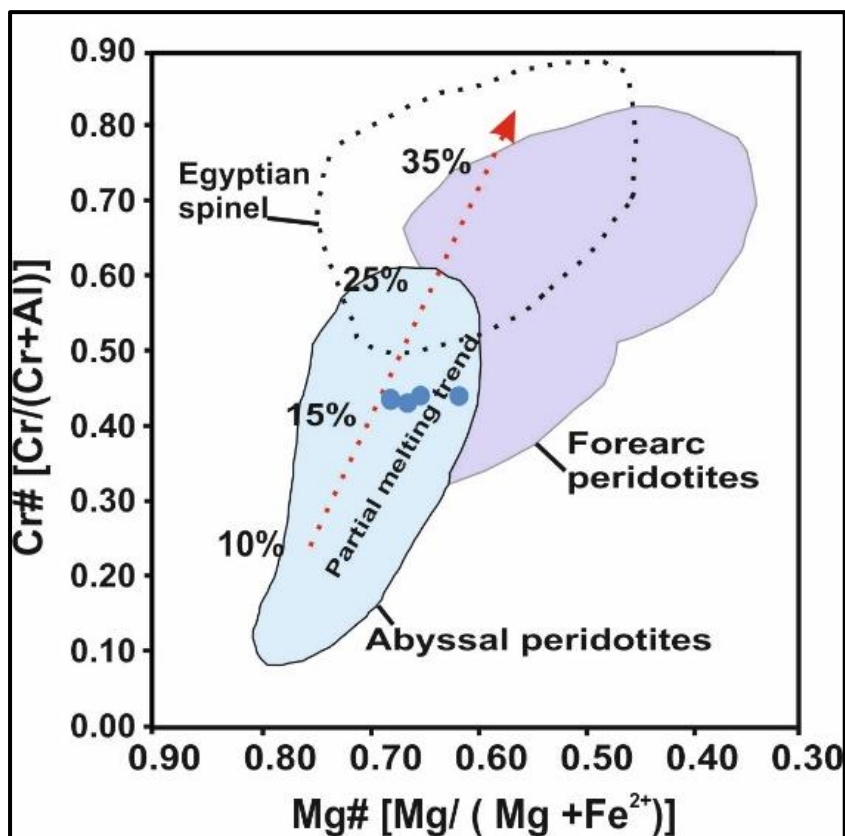


Figure:5.2.3. Spinel compositions of the studied serpentinite samples plotted on Mg# [Mg/ (Mg + Fe²⁺)] vs. Cr# [Cr/(Cr + Al)] diagram. Partial melting trend (red arrow) is from Dick and Bullen (1984) and Arai (1992)

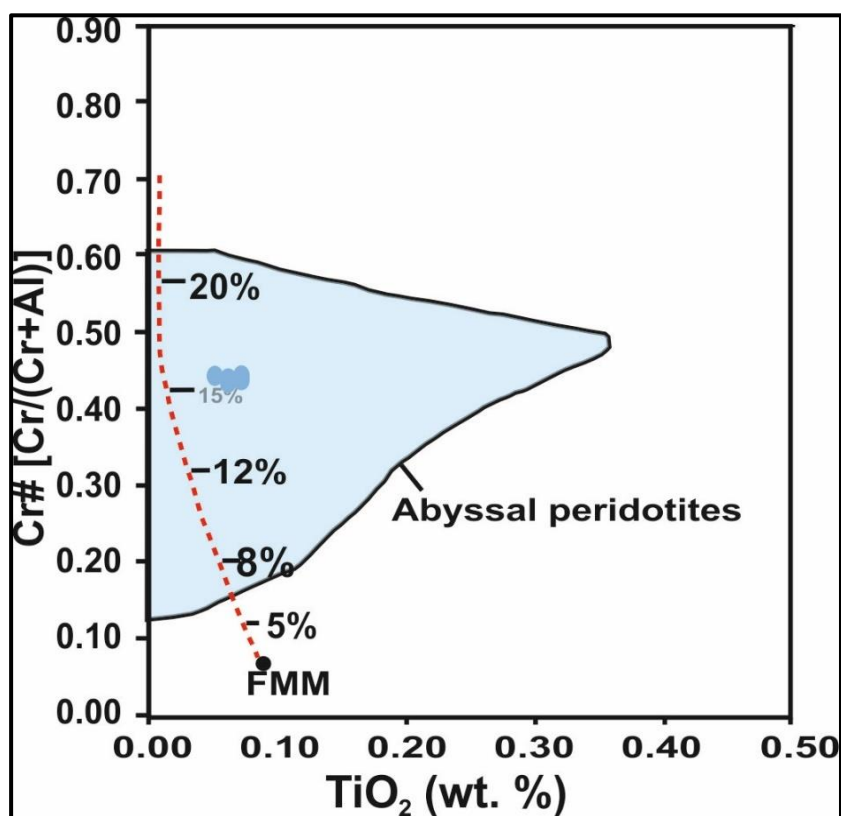


Figure:5.2.4. Cr# [Cr / (Cr + Al)] vs. TiO₂ (wt. %). The degrees of melt extractions are from Hellebrand et al. (2001) and Uysal et al. (2012).

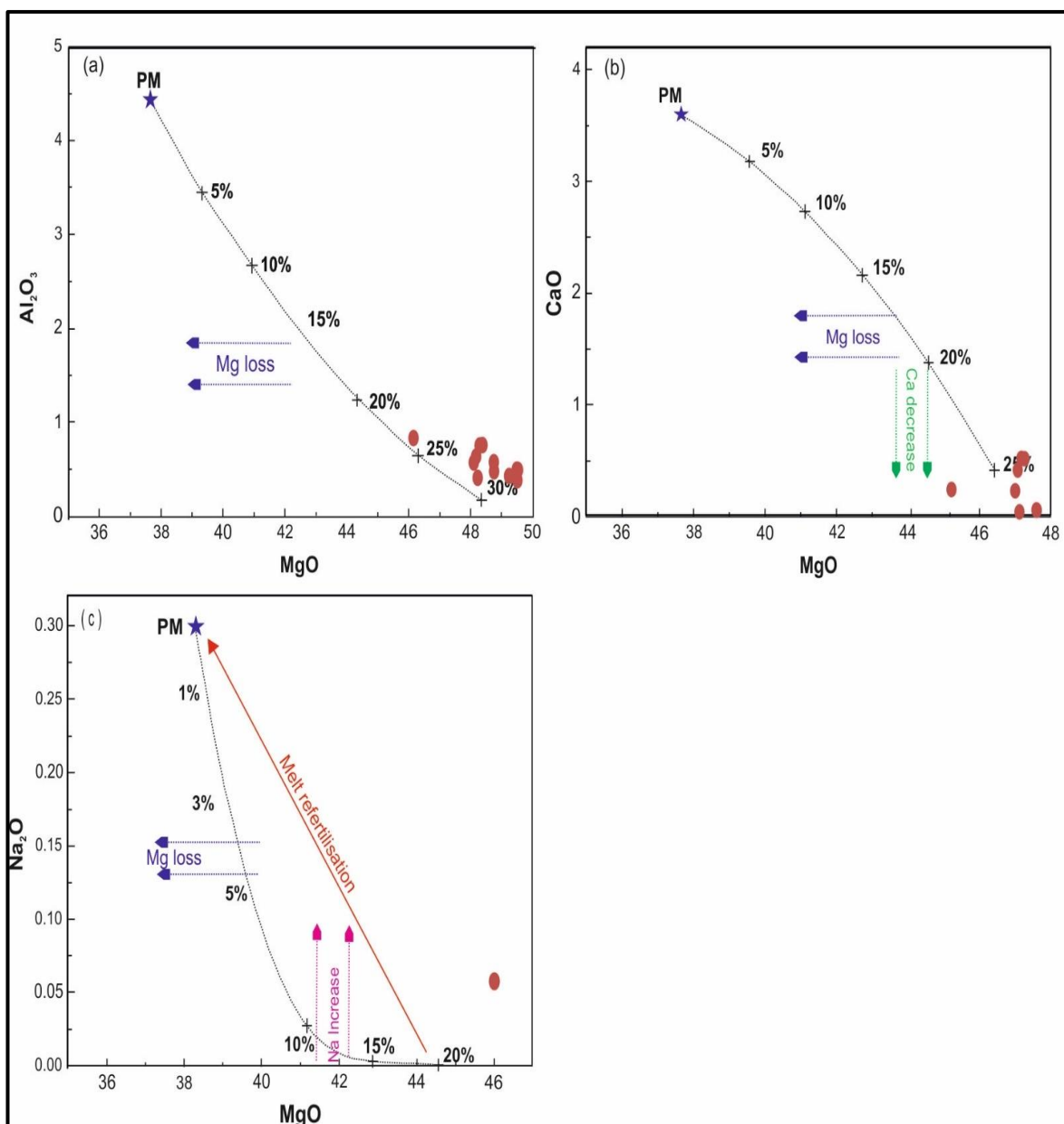


Figure: 5.2.5. Plots of whole-rock MgO contents against Al₂O₃ (a), CaO (b), and Na₂O (c) (all in wt.%). Element concentrations have been recalculated to 100% on an LOI-free basis. The calculated melting trend for residual serpentinised peridotites using the model of Niu (1997) is shown, which assumes anhydrous polybaric near-fractional melting of a PM source from 2.5 GPa to 0.4 GPa. Numbers along the line indicate percentage melting.

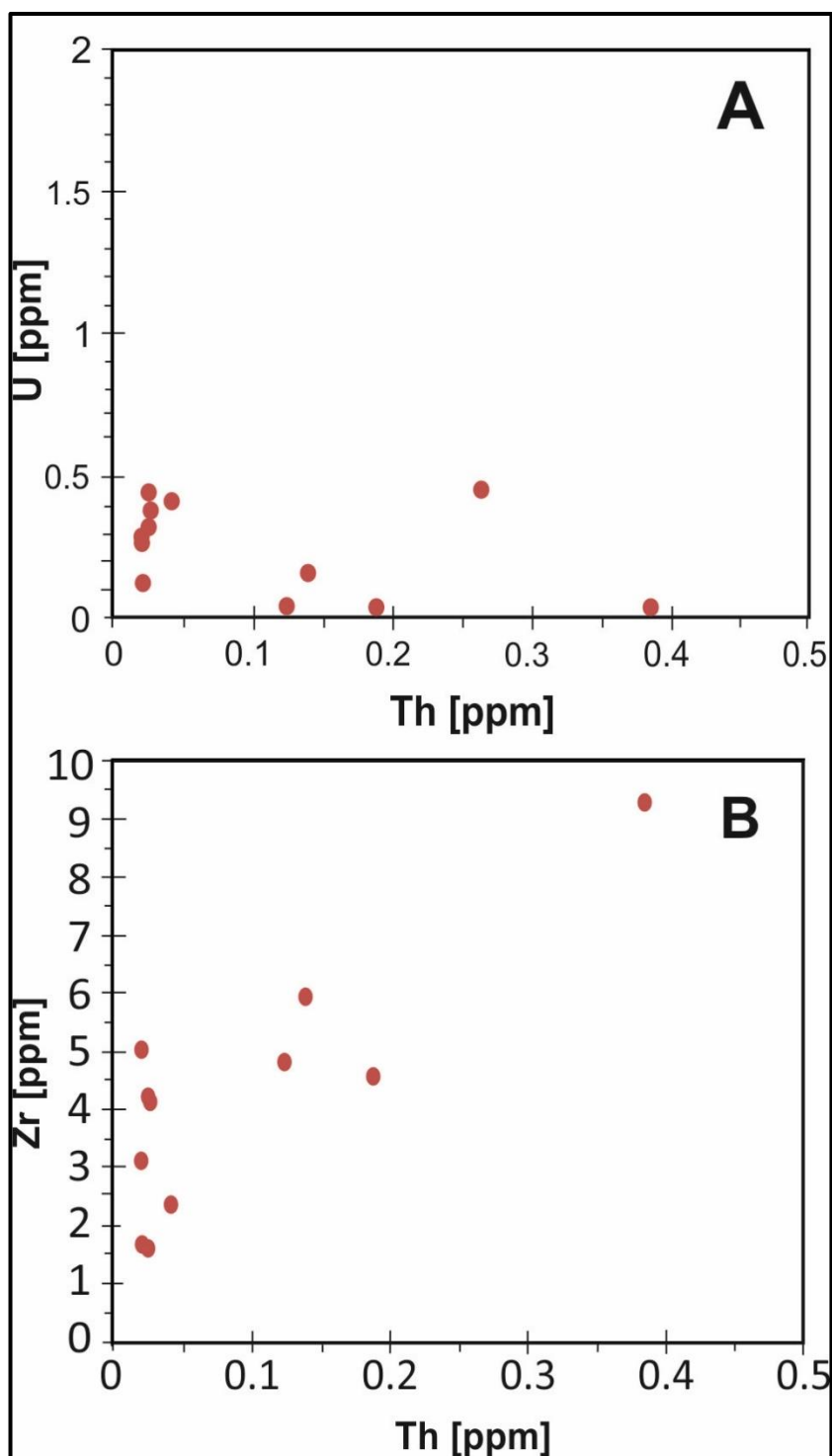


Figure:5.2.6. Serpentinites from the given study show relatively high immobile trace element concentration indicative for melt-rock interaction processes. Symbols as in Figure. 3. (A). U vs. Th (B). Zr vs.Th).

5.3 Melt rock interaction and hydrothermal interaction

The peridotites examined from CIR exhibit significant compositional differences, with evident variations in rare earth elements (REE) due to both melt–rock interaction (as shown in **Figure 5.3. A, B**) and hydrothermal alteration (as illustrated in **Figure 5.3 C, D**). To better understand the impact of these processes across different sites, it's crucial to analyse the behaviour of highly incompatible elements (HFSE) and REE. In aqueous solutions, light REE (LREE) are more easily transported compared to heavy REE (HREE) and HFSE. Conversely, during melt–rock interaction, both LREE and HFSE are added to the rock in approximately equal proportions (Niu, 2004).

Figure (5.3.) displays positive trends in Nb vs. La and Th vs. Ce space, suggesting that melt–rock interaction plays a predominant role in driving compositional variations. This observation aligns with petrographic evidence indicating melt impregnation, as the samples in question conform to the overall trend observed in the global dataset, where melt–rock interaction stands out as the dominant process influencing compositional changes.

In (**Figures 5.3A, 5.3B, 5.3C, and 5.3D**), it's evident that the samples are situated in both the melt/rock interaction and fluid/rock interaction fields. This indicates that both processes have impacted the geochemistry of these samples. Notably, Nb and La are commonly used as tracers for these interactions due to their distinct behavior during these processes.

The majority of the studied samples are clustered in the melt/rock interaction field (**Figure 5.3A**), suggesting that interactions with silicic melts have predominantly influenced the geochemical makeup of these samples, in contrast to interactions with fluids.

However, an unexpected distribution is observed in the Nd vs. GdN/LuN plot, diverging from the anticipated trend for melt/rock contact and hydrothermal alteration. This deviation implies the presence of additional factors influencing the behavior of these components beyond straightforward melt/rock or fluid/rock interactions.

Similarly, in the Th vs. GdN/LuN plot, the samples display disparate patterns for hydrothermal alteration and melt/rock interaction. This discrepancy suggests the involvement of mechanisms other than typical melt/rock or fluid/rock interactions in influencing the behavior of Th and GdN/LuN.

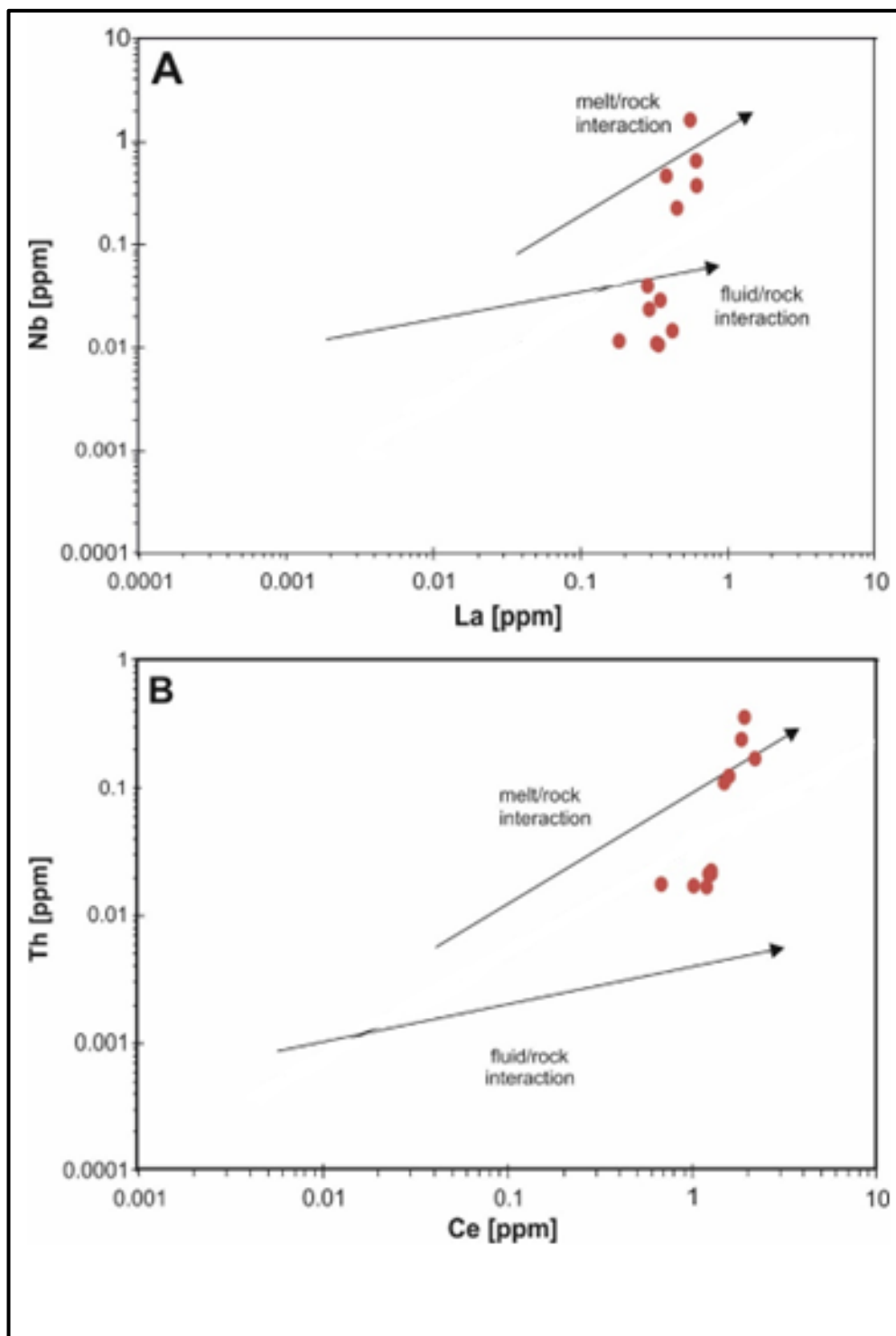


Figure:5.3. Deviating trends for melt-rock interaction and hydrothermal alteration are defined in LREE vs. HFSE space. This is due to the higher solubility of LREE in aqueous solutions compared to HFSE. In contrast, LEE and HFSE are equally soluble in silicic melts. (A). Nb vs. La (B). Th vs. Ce (C). Nd vs. Gd /LuN (D). Th vs. Gd /LuN.

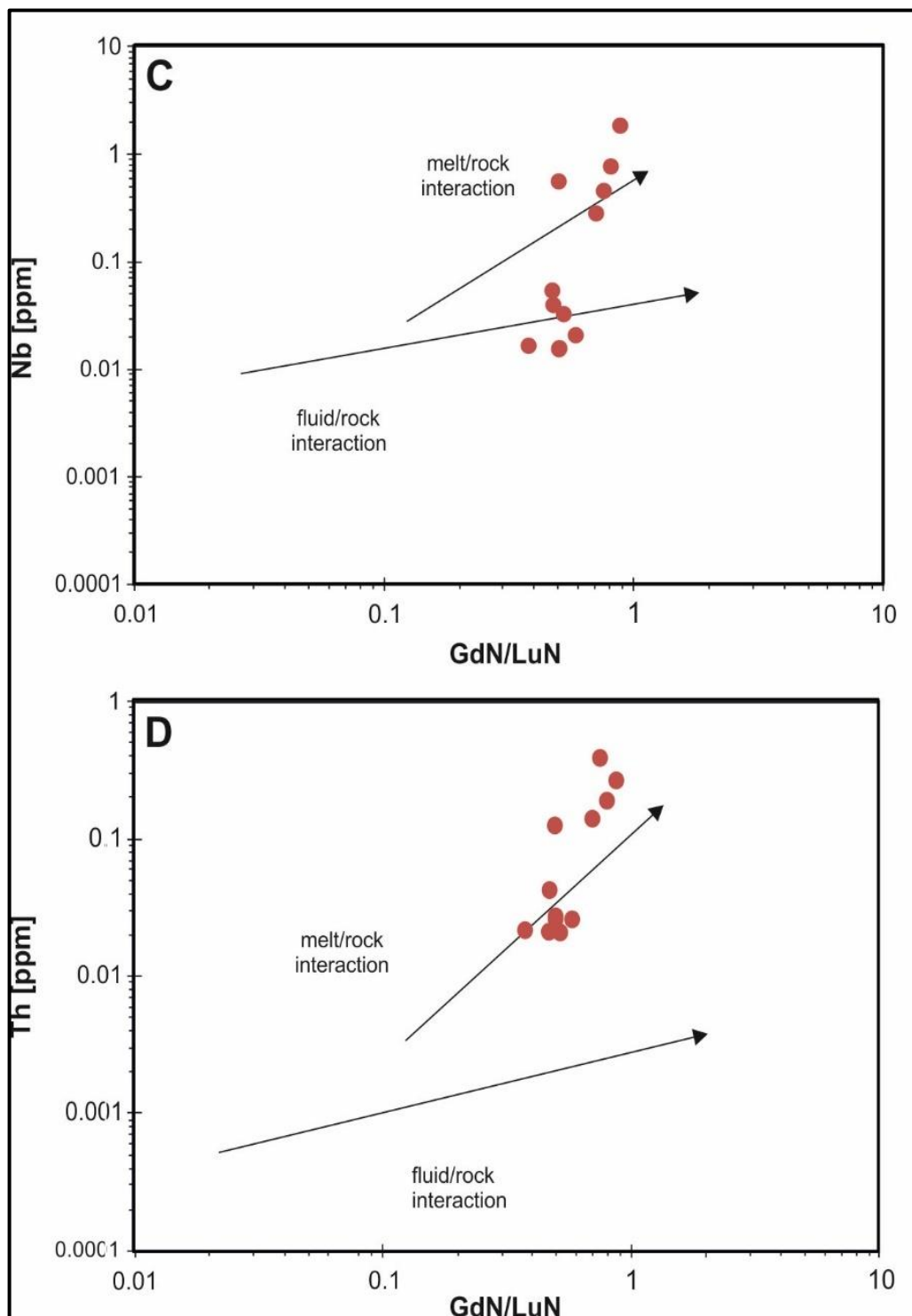


Figure:5.3. (Contd.)

5.4 Tectonic setting

The investigated samples exhibit overlapping characteristics of supra-subduction zone and abyssal peridotites (**Figure. 5.4.1.**), indicating a heterogeneous origin likely influenced by multiple tectonic episodes. This complexity suggests that the rocks have retained signatures reflecting the nature of the environments they originated from. A geochemical Figure depicting the concentrations of titanium dioxide (TiO_2) and aluminium oxide (Al_2O_3) in Cr-spinels was utilized for this analysis. Such plots are commonly employed to characterize and classify rocks based on their mineral compositions. The geochemical plot may be used to link the compositions of Cr-spinels to certain geological contexts, based on the comparison to contemporary tectonic conditions. Al_2O_3 and TiO_2 concentration may show different patterns in peridotites from different tectonic environments, such as supra-subduction zone peridotites and abyssal peridotites. According to the statement, all of the data points on the plot are entirely located in the field related to supra-subduction zone and abyssal peridotites. This suggests that the Cr-spinel composition in the examined samples is in line with the distinctive geochemical characteristics of these two distinct tectonic environments. The geological setting of the rocks containing Cr-spinels may be inferred from the particular field in which the data points are located. Whereas supra-subduction zone peridotites are connected to subduction zones, abyssal peridotites are related with oceanic spreading centres. As a result, the map assists in differentiating and classifying the samples according to how well they fit into various tectonic contexts. The petrogenetic processes, mineralogical compositions, and tectonic histories of the rocks bearing Cr-spinels may all be understood from the Al_2O_3 vs. TiO_2 binary plot. The plot's unique location in the supra-subduction zone and abyssal

peridotite fields suggests a useful resource for comprehending the samples' geological setting.

Figure (5.4.2). was used to determine the formation environment of the studied rock samples, revealing characteristics indicative of alpine peridotites based on their placement in the trivalent cations triangle diagram (Al^{3+} , $\text{Fe}^{3+} + 2\text{Ti}^{4+}$, and Cr^{3+}). This diagram, likely derived from a ternary diagram, is commonly employed to assess Cr-spinels in peridotites hosted by serpentinite, known as the Serpentinite-Spinel Phase (SSP) diagram. Plots inside the alpine peridotite field indicate a particular geochemical signature linked to this environment. Three trivalent cations are included in the triangle plot: Cr^{3+} , $\text{Fe}^{3+} + 2\text{Ti}^{4+}$, and Al^{3+} . Ternary diagrams are frequently used in mineralogy and geochemistry to show the relative amounts of three components. The selection of trivalent cations (Cr^{3+} , $\text{Fe}^{3+} + 2\text{Ti}^{4+}$, Al^{3+}) is probably due to their importance in comprehending the compositional changes of Cr-spinels in peridotites hosted by serpentinite. The foundation for deciphering the compositional connections between Al, Fe, Ti, and Cr in the examined Cr-spinels is probably established by their study. The triangle diagram's data points/plots lie inside the field linked to alpine peridotite, which is an important finding. This indicates that the Cr-spinel compositions in the peridotites hosted by serpentinite are in line with the geochemical signature that is characteristic of alpine peridotites. Based on the composition of their trivalent cations, Cr-spinels may be categorised and characterised using the triangular trivalent cation plot. The focus on the alpine peridotite field suggests that these peridotites housed by serpentinite have a geochemical signature consistent with alpine peridotite properties. Alpine peridotites can provide insights into their mantle source, extent of melting, and interactions with other crustal materials during ascent through geochemical investigations. The minerals that make up the geochemical signature include spinel,

pyroxene, and olivine. Alpine peridotites can occasionally be discovered as components of ophiolite complexes, which are made up of pieces of oceanic lithosphere that plate boundaries push upon as a result of tectonic activity. Peridotites are among the ultramafic and mafic rocks that may be found in ophiolites. Alpine peridotites frequently have a complicated metamorphic past, with high temperatures and pressures being involved in their development during the orogeny. The mineral assemblages and textures found in these rocks show evidence of this past. Alpine peridotites may also include amphibole and spinel in addition to olivine and pyroxene. The circumstances of mantle melting and the ensuing ascension to the Earth's crust are revealed by the mineralogical composition. These peridotites are connected to subduction and continental convergence processes, as well as continental collision zones. Mountain ranges were raised as a result of the Alpine orogeny, which took place during the Cenozoic era and featured the collision and convergence of tectonic plates.

Figure (5.4.3.) also confirms the rock type is belonging to the abyssal peridotite settings, In petrology, a ternary plot of Fe-Cr-Al is frequently used to show how the composition of minerals or rocks varies according to the three main elements: iron (Fe), chromium (Cr), and aluminium (Al). The ternary plot's zones that correspond to the geochemical compositions of certain peridotite types in various geological contexts are probably the nidar peridotites, abyssal peridotites, and Mariana forearc peridotites that were specifically highlighted. Plotting of spinel samples in the ternary plot's field of abyssal peridotites indicates that their geochemical makeup is comparable to that of abyssal peridotites. These similarities might point to a shared geological mechanism or origin for both the abyssal peridotites and the spinel samples. The spinel samples could have originated in abyssal plains or oceanic spreading centres, two geological environments that are comparable to those of abyssal peridotites. The spinel samples

and abyssal peridotites may have a shared source material or mantle reservoir, as suggested by the geochemical similarities. Given their site within the abyssal peridotite field, it is possible that similar tectonic and magmatic processes affected both the spinel samples and the abyssal peridotites. The samples' placement in the abyssal peridotite region may indicate a comparable degree of partial melting or magma differentiation if they are connected to igneous events.

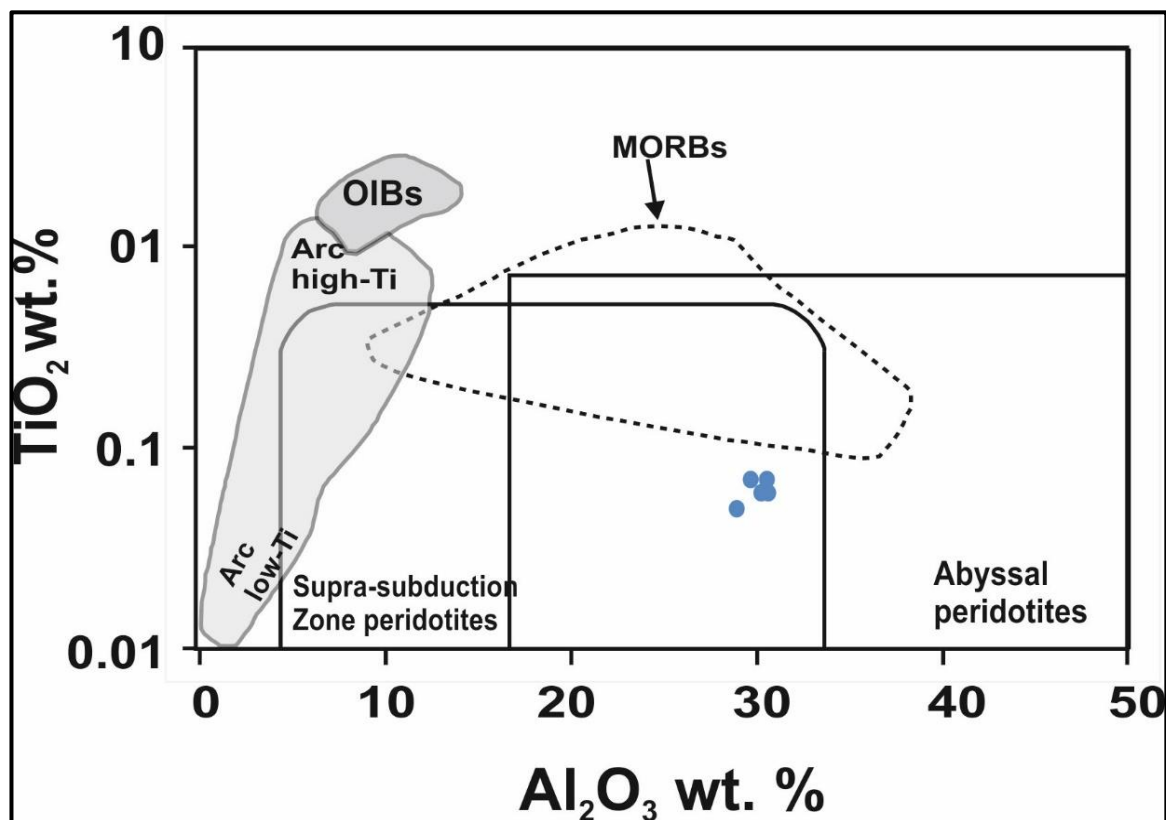


Figure: 5.4.1. Al_2O_3 vs. TiO_2 binary plot (after Kamenetsky et al., 2001) of Cr-spinels in comparison to modern-day tectonic settings.

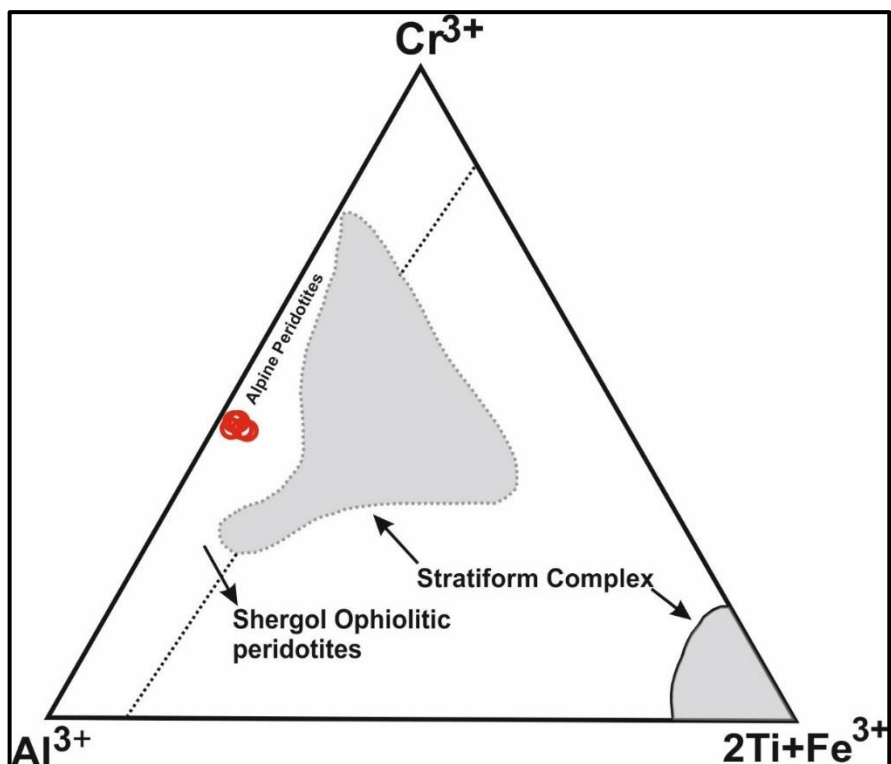


Figure: 5.4.2. Triangular trivalent cation plot of $Al^{3+} - (Fe^{3+} + 2Ti^{4+}) - Cr^{3+}$ (after Jan and Windley, 1990) for Cr-spinels from SSPs.

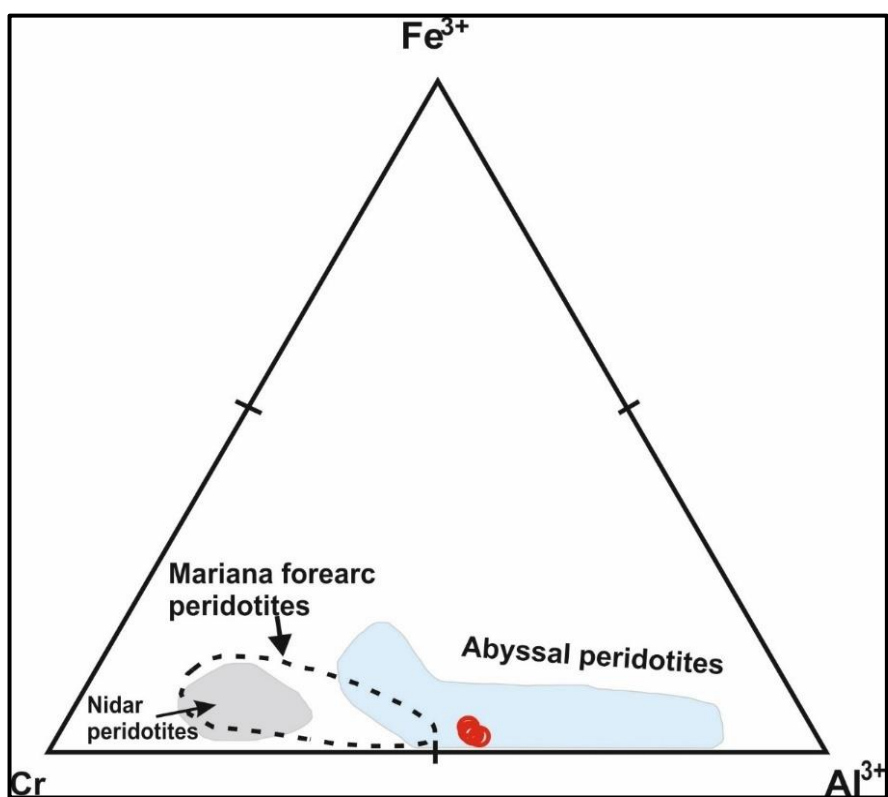


Figure: 5.4.3. Ternary plot of Fe-Cr-Al showing fields such as nidar peridotites mariana forearc peridotites abyssal peridotites where in the spinel samples are plotting in the field of abyssal peridotites.

CHAPTER VI: CONCLUSION

The petrographic examination of serpentinized peridotite aimed to elucidate mineralogical compositions, including olivine, pyroxene, spinel, magnetite, serpentine, and others. The presence of inclusions, alteration veins, mesh textures, and brucite textures were identified, indicative of high levels of serpentinization, confirmed by the presence of antigorite and serpentine polymorphs. Major oxide analysis revealed a negative trend in magnesium loss, contrary to sea floor weathering patterns, possibly due to differentiation processes evident in mineral transformations from olivine to serpentine.

Trace and rare earth element analyses shed light on the influence of these elements on serpentinization. Positive anomalies of Hf and Zr suggested crystal melting and magma differentiation, while negative Nb anomalies indicated magma extraction and incorporation into minerals at subduction zones. The mantle-rock and hydrothermal interactions were assessed using Cr# vs TiO₂ and Mg# plots, indicating an abyssal harzburgite rock type located at ocean ridges, with partial melting values confirming the mantle source and degree of melting.

The tectonic settings of these rocks were inferred from mineral classifications, with traces of supra-subduction zones and alpine peridotite settings observed. However, the predominant setting identified was abyssal peridotite, supported by the presence and characteristics of Cr-spinel, suggesting a common geological mechanism and origin for the serpentinized peridotite in the abyssal peridotite setting.

REFERENCES

- Agarwal, D. K., Roy, P., Prakash, L. S., & Kurian, P. J. (2020). Hydrothermal signatures in sediments from eastern Southwest Indian Ridge 63 E to 68 E. *Marine Chemistry*, 218, 103732. <https://doi.org/10.1016/j.marchem.2019.103732>.
- Asimow, P. D. (1999). A model that reconciles major-and trace-element data from abyssal peridotites. *Earth and Planetary Science Letters*, 169(3-4), 303-319.
- Baker, M. B., & Beckett, J. R. (1999). The origin of abyssal peridotites: a reinterpretation of constraints based on primary bulk compositions. *Earth and Planetary Science Letters*, 171(1), 49-61.
- Banerjee, R., Ray, D., & Ishii, T. (2015). Mineral chemistry and alteration characteristics of spinel in serpentinised peridotites from the Northern Central Indian Ridge. *Journal of the Geological Society of India*, 86, 41-51. <https://doi.org/10.1007/s12594-015-0279-3>.
- Banerjee, R., Ray, D., & Ishii, T. (2015). Mineral chemistry and alteration characteristics of spinel in serpentinised peridotites from the Northern Central Indian Ridge. *Journal of the Geological Society of India*, 86, 41-51.
- Bassias, Y., & Triboulet, C. (1992). Petrology and PTt evolution of the South West Indian Ridge peridotites. A case study: east of the Merlville Fracture zone at 62° E. *Lithos*, 28(1), 1-19. [https://doi.org/10.1016/0024-4937\(92\)90020-Y](https://doi.org/10.1016/0024-4937(92)90020-Y).
- Bhat, I., Ahmad, T., & Rao, D. (2017). Compositional variability of spinel-group minerals from the shergol serpentinized peridotites along indus suture zone, ladakh himalaya (India): constraints on tectonomagmatic history.

Chemie Der Erde-geochemistry, 77, 587-595.

<https://doi.org/10.1016/J.CHEMER.2017.10.003>.

- Bish, D. L., & Von Dreele, R. B. (1989). Rietveld refinement of carbonate-fluorapatite solid solutions. *American Mineralogist*, 74(7-8), 840-847.
- Blatter, D. L., & Carmichael, I. S. E. (1998). Hornblende peridotite xenoliths from the Big Pine volcanic field, California: evidence for metasomatism by hydrous alkali-basalt. *Contributions to Mineralogy and Petrology*, 133(2), 176–191. <https://doi.org/10.1007/s004100050446>
- Bodinier, J.-L., & Godard, M. (2004). Orogenic, Ophiolitic, and Abyssal Peridotites. In R. H. D. R. H. D. Holland & K. K. K. K. Turekian (Eds.), *Treatise on Geochemistry* (Vol. 3, pp. 195-226). Elsevier.
- Cannat, M., Bideau, D., & Bougault, H. (1992). Serpentinized peridotites and gabbros in the Mid-Atlantic Ridge axial valley at 15°37'N and 16°52'N. *Earth and Planetary Science Letters*, 109, 87-106. [https://doi.org/10.1016/0012-821X\(92\)90076-8](https://doi.org/10.1016/0012-821X(92)90076-8).
- Cannat, M., Bideau, D., & Bougault, H. (1992). Serpentinized peridotites and gabbros in the Mid-Atlantic Ridge axial valley at 15 37' N and 16 52' N. *Earth and Planetary Science Letters*, 109(1-2), 87-106.
- Chen, L., Chu, F., Zhu, J., Dong, Y., Yu, X., Li, Z., & Tang, L. (2015). Major and trace elements of abyssal peridotites: evidence for melt refertilization beneath the ultraslow-spreading Southwest Indian Ridge (53° E segment). *International Geology Review*, 57, 1715 - 1734. <https://doi.org/10.1080/00206814.2015.1029014>.

- Chen, T., Jin, Z., Shen, A. H., & Li, W. (2016). Altered spinel as a petrotextonic indicator in abyssal peridotite from the easternmost part of Southwest Indian Ridge. *Journal of Earth Science*, 27, 611-622.
- Chen, T., Jin, Z., Shen, A., & Li, W. (2016). Altered spinel as a petrotextonic indicator in abyssal peridotite from the easternmost part of Southwest Indian Ridge. *Journal of Earth Science*, 27, 611-622. <https://doi.org/10.1007/s12583-016-0707-3>.
- Cullen, H. M. (1981). Late Quaternary paleo-oceanography of the Gulf of Aden: ODP Leg 63. *Initial Reports of the Deep Sea Drilling Project*, 63, 795–799. <https://doi.org/10.2973/dsdp.proc.63.135.1981>
- Debret, B., Andréani, M., Godard, M., Nicollet, C., Schwartz, S., & Lafay, R. (2012). Trace element behavior during serpentinization/de-serpentinization of an eclogitized oceanic lithosphere: A LA-ICPMS study of the Lanzo ultramafic massif (Western Alps). *Chemical Geology*, 357, 117-133. <https://doi.org/10.1016/J.CHEMGEO.2013.08.025>.
- DeMott, P. J., Hill, T. C. J., McCluskey, C. S., Prather, K. A., Collins, D. B., Sullivan, R. C., ... & Kreidenweis, S. M. (2015). Sea spray aerosol as a unique source of ice nucleating particles. *Proceedings of the National Academy of Sciences*, 113(21), 5797-5803.
- Desbruyères, D. G., Purkey, S. G., McDonagh, E. L., Johnson, G. C., & King, B. A. (2017). Deep and abyssal ocean warming from 35 years of repeat hydrography. *Geophysical Research Letters*, 44(11), 5668-5676.
- Dessimoulie, L., Delacour, A., Guillaume, D., Chevet, J., & Cottin, J. (2020). Major and trace elements exchanges during fluid-rock interaction at ultraslow-

spreading oceanic lithosphere: Example of the South West Indian Ridge (SWIR). *Lithos*, 105233. <https://doi.org/10.1016/j.lithos.2019.105233>.

- Dessimoulie, L., Delacour, A., Guillaume, D., Chevet, J., & Cottin, J. Y. (2020). Major and trace elements exchanges during fluid-rock interaction at ultraslow-spreading oceanic lithosphere: Example of the South West Indian Ridge (SWIR). *Lithos*, 352, 105233.
- Dick, H. J. B. (1989). Abyssal peridotites, very slow spreading ridges and ocean ridge magmatism. *Geological Society, London, Special Publications*, 42(1), 71-105.
- Dick, H. J. B., & Fisher, R. L. (1984). Mineralogic studies of the residues of mantle melting: abyssal and alpine-type peridotites. In *Developments in Petrology* (Vol. 11, No. 2, pp. 295-308). Elsevier.
- Dick, H. J., & Bullen, T. (1984). Chromian spinel as a petrogenetic indicator in abyssal and alpine-type peridotites and spatially associated lavas. *Contributions to mineralogy and petrology*, 86, 54-76.
- Dick, H. J., & Bullen, T. (1984). Chromian spinel as a petrogenetic indicator in abyssal and alpine-type peridotites and spatially associated lavas. *Contributions to mineralogy and petrology*, 86, 54-76.
- Dick, H. J., Fisher, R. L., & Bryan, W. B. (1984). Mineralogic variability of the uppermost mantle along mid-ocean ridges. *Earth and Planetary Science Letters*, 69(1), 88-106.
- Duplessy, J.-C. (1982). Glacial to interglacial contrasts in the northern Indian Ocean. *Nature*, 295(5845), 494–496. <https://doi.org/10.1038/295494a0>
- Eakins, B. W., & Sharman, G. F. (2010). Volumes of the World's Oceans from ETOPO1. NOAA National Geophysical Data Center.

- Escartin, J., Hirth, G., & Evans, B. (2001). Strength of slightly serpentinized peridotites: Implications for the tectonics of oceanic lithosphere. *Geology*, 29(11), 1023-1026.
- Escartín, J., Hirth, G., & Evans, B. (2001). Strength of slightly serpentinized peridotites: Implications for the tectonics of oceanic lithosphere. *Geology*, 29, 1023-1026. [https://doi.org/10.1130/0091-7613\(2001\)029<1023:SOSSPI>2.0.CO;2](https://doi.org/10.1130/0091-7613(2001)029<1023:SOSSPI>2.0.CO;2).
- Evans, B., Hattori, K., & Baronnet, A. (2013). Serpentinite: What, Why, Where?. *Elements*, 9, 99-106. <https://doi.org/10.2113/GSELEMENTS.9.2.99>.
- Fontugne, M. R., & Duplessy, J. C. (1986). Changes in surface productivity and bottom water ventilation in the northern Indian Ocean during the past 200,000 years: Evidence from carbon isotopes. *Paleoceanography*, 1(2), 171–183. <https://doi.org/10.1029/PA001i002p00171>
- Frisby, C., Bizimis, M., & Mallick, S. (2016). Hf–Nd isotope decoupling in bulk abyssal peridotites due to serpentinization. *Chemical Geology*, 440, 60-72.
- Frisby, C., Bizimis, M., & Mallick, S. (2016). Seawater-derived rare earth element addition to abyssal peridotites during serpentinization. *Lithos*, 248, 432-454. <https://doi.org/10.1016/J.LITHOS.2016.01.025>.
- Hamdy, M. M., & Lebda, E. M. (2011). Al-compositional variation in ophiolitic chromitites from the south Eastern Desert of Egypt: petrogenetic implications. *Journal of Geology and Mining Research*, 3(9), 232-250.
- Hart, S. R., & Zindler, A. (1986). In search of a bulk-Earth composition. *Chemical Geology*, 57(3-4), 247-267.

- Hattori, K., & Guillot, S. (2007). Geochemical character of serpentinites associated with high- to ultrahigh-pressure metamorphic rocks in the Alps, Cuba, and the Himalayas: Recycling of elements in subduction zones. *Geochemistry*, 8. <https://doi.org/10.1029/2007GC001594>.
- Hazra, A., Ghosh, S., & Pattanaik, D. R. (2017). Monsoon prediction: progress and challenges. *Current Science*, 113(9), 1686-1696.
- Hellebrand, E., Snow, J. E., & Mühe, R. (2002). Mantle melting beneath Gakkel Ridge (Arctic Ocean): abyssal peridotite spinel compositions. *Chemical Geology*, 182(2-4), 227-235.
- Hellebrand, E., Snow, J. E., & Mühe, R. (2002). Mantle melting beneath Gakkel Ridge (Arctic Ocean): abyssal peridotite spinel compositions. *Chemical Geology*, 182(2-4), 227-235.
- Hellebrand, E., Snow, J. E., Dick, H. J., & Hofmann, A. W. (2001). Coupled major and trace elements as indicators of the extent of melting in mid-ocean-ridge peridotites. *Nature*, 410(6829), 677-681.
- Hernández-Guerra, A., & Talley, L. D. (2016). *The oceans and climate*. John Wiley & Sons.
- Herzberg, C. (2004). Petrology and thermal structure of the Hawaiian plume from Mauna Kea volcano. In J. A. Wolff, & D. M. A. D. M. A. Clague (Eds.), *The Mauna Kea Volcano, Hawaii: Composition, Structure, and Evolution* (pp. 195-231). American Geophysical Union. <https://doi.org/10.1029/GM157>
- Jackson, J. A. (Ed.). (1997). *Glossary of Geology* (4th ed.). American Geological Institute.
- Janecky, D., & Seyfried, W. (1986). Hydrothermal serpentinization of peridotite within the oceanic crust: Experimental investigations of mineralogy

- and major element chemistry. *Geochimica et Cosmochimica Acta*, 50, 1357-1378. [https://doi.org/10.1016/0016-7037\(86\)90311-X](https://doi.org/10.1016/0016-7037(86)90311-X).
- Johnson, K. T., Dick, H. J., & Shimizu, N. (1990). Melting in the oceanic upper mantle: an ion microprobe study of diopsides in abyssal peridotites. *Journal of Geophysical Research: Solid Earth*, 95(B3), 2661-2678.
 - Klein, F., Bach, W., Jöns, N., McCollom, T., Moskowitz, B., & Berquó, T. (2009). Iron partitioning and hydrogen generation during serpentinization of abyssal peridotites from 15°N on the Mid-Atlantic Ridge. *Geochimica et Cosmochimica Acta*, 73, 6868-6893. <https://doi.org/10.1016/J.GCA.2009.08.021>.
 - Li, X., Feng, M., & Lee, T. (2017). Climate variability and change in the South China Sea: A review. In *The South China Sea* (pp. 333-351). Springer, Cham.
 - Lim, D., Kim, J., Kim, W., Kim, J., Kim, D., Zhang, L., Kwack, K., & Xu, Z. (2022). Characterization of Geochemistry in Hydrothermal Sediments From the Newly Discovered Onnuri Vent Field in the Middle Region of the Central Indian Ridge. , 9. <https://doi.org/10.3389/fmars.2022.810949.1111111>
 - Lumpkin, R., & Speer, K. (2007). Global ocean meridional overturning. *Journal of Physical Oceanography*, 37(10), 2550-2562.
 - Macdonald, A., & Fyfe, W. (1985). Rate of serpentinization in seafloor environments. *Tectonophysics*, 116, 123-135. [https://doi.org/10.1016/0040-1951\(85\)90225-2](https://doi.org/10.1016/0040-1951(85)90225-2).
 - Malvoisin, B., Brunet, F., Carlut, J., Rouméjon, S., & Cannat, M. (2012). Serpentinization of oceanic peridotites: 2. Kinetics and processes of San Carlos olivine hydrothermal alteration. *Journal of Geophysical Research: Solid Earth*, 117(B4). <https://doi.org/10.1029/2011JB008842>.

- Marcaillou, C., Munoz, M., Vidal, O., Parra, T., & Harfouche, M. (2011). Mineralogical evidence for H₂ degassing during serpentinization at 300 C/300 bar. *Earth and Planetary Science Letters*, 303(3-4), 281-290. <https://doi.org/10.1016/J.EPSL.2011.01.006>.
- Matusiak-Małek, M., Kryza, R., & Mazur, S. (2017). Carbonate–silicate metasomatism in the mantle xenoliths from Wilcza Góra, Lower Silesia, SW Poland: implications for mantle beneath the Bohemian Massif. *Mineralogy and Petrology*, 111(4), 565–582. <https://doi.org/10.1007/s00710-017-0524-0>
- McDonagh, E. L., Bryden, H. L., King, B. A., Sanders, R., Cunningham, S. A., & Marsh, R. (2008). Decadal changes in the South Indian Ocean thermocline. *Journal of Climate*, 21(18), 4750-4766.
- Mével, C. (2003). Serpentinization of abyssal peridotites at mid-ocean ridges. *Comptes Rendus Geoscience*, 335, 825-852. <https://doi.org/10.1016/J.CRTE.2003.08.006>.
- Mével, C. (2003). Serpentinization of abyssal peridotites at mid-ocean ridges. *Comptes Rendus Geoscience*, 335(10-11), 825-852.
- Moll, M., Paulick, H., Suhr, G., & Bach, W. (2007). Data Report: Microprobe analyses of primary phases (olivine, pyroxene, and spinel) and alteration products (serpentine, iowaite, talc, magnetite, and sulfides) in Holes 1268A, 1272A, and 1274A. <https://doi.org/10.2973/ODP.PROC.SR.209.003.2007.1111111111>
- Morishita, T., Hara, K., Nakamura, K., Sawaguchi, T., Tamura, A., Arai, S., Okino, K., Takai, K., & Kumagai, H. (2009). Igneous, Alteration and Exhumation Processes Recorded in Abyssal Peridotites and Related Fault

Rocks from an Oceanic Core Complex along the Central Indian Ridge. *Journal of Petrology*, 50, 1299-1325. <https://doi.org/10.1093/PETROLOGY/EGP025>.

- Morishita, T., Nakamura, K., Sawaguchi, T., Hara, K., Arai, S., & Kumagai, H. (2008). Elemental Mobilizations during Hydrothermal Alteration of Oceanic Lithosphere. *Chigaku Zasshi (journal of Geography)*, 117, 220-252. <https://doi.org/10.5026/JGEOGRAPHY.117.220>.
- Morishita, T., Nakamura, K., Shibuya, T., Kumagai, H., Sato, T., Okino, K., Sato, H., Nauchi, R., Hara, K., & Takamaru, R. (2015). Petrology of Peridotites and Related Gabbroic Rocks Around the Kairei Hydrothermal Field in the Central Indian Ridge. , 177-193. https://doi.org/10.1007/978-4-431-54865-2_14.
- Morishita, T., Nakamura, K., Shibuya, T., Kumagai, H., Sato, T., Okino, K., ... & Takamaru, R. (2015). Petrology of peridotites and related gabbroic rocks around the Kairei hydrothermal field in the Central Indian Ridge. *Subseafloor Biosphere Linked to Hydrothermal Systems: TAIGA Concept*, 177-193.
- Murton, J. B., Peterson, R., Brachfeld, S., & Grant, J. (2005). Evidence from the South Georgia microcontinent for a decrease in the extent of the Weddell Sea prior to Gondwana break-up. *Earth and Planetary Science Letters*, 237(3-4), 451-470.
- Murtugudde, R., McCreary, J. P., & Busalacchi, A. J. (2000). Oceanic processes associated with anomalous events in the Indian Ocean with relevance to 1997–1998. *Journal of Geophysical Research: Oceans*, 105(C2), 3295–3306. <https://doi.org/10.1029/1999JC900294>

- Niu, Y. (1997). Mantle melting and melt extraction processes beneath ocean ridges: evidence from abyssal peridotites. *Journal of Petrology*, 38(8), 1047-1074.
- Niu, Y. (2003, December). Excess Olivine and Positive FeO-MgO Trend in Bulk-rock Abyssal Peridotites as a Consequence of Porous Melt Migration Beneath Ocean Ridges. In *AGU Fall Meeting* Jagoutz, E., Palme, H., Baddenhausen, H., Blum, K., Cendales, M., Dreibus, G., ... & Wänke, H. (1979). The abundances of major, minor and trace elements in the earth's mantle as derived from primitive ultramafic nodules. In *In: Lunar and Planetary Science Conference, 10th, Houston, Tex., March 19-23, 1979, Proceedings. Volume 2.(A80-23617 08-91) New York, Pergamon Press, Inc., 1979, p. 2031-2050. Research supported by the Deutsche Forschungsgemeinschaft.* (Vol. 10, pp. 2031-2050). *Abstracts* (Vol. 2003, pp. V22H-05).
- Niu, Y. (2004). Bulk-rock Major and Trace Element Compositions of Abyssal Peridotites: Implications for Mantle Melting, Melt Extraction and Post-melting Processes Beneath Mid-Ocean Ridges. *Journal of Petrology*, 45, 2423-2458. <https://doi.org/10.1093/PETROLOGY/EGH068>.
- Niu, Y. (2004). Bulk-rock major and trace element compositions of abyssal peridotites: implications for mantle melting, melt extraction and post-melting processes beneath mid-ocean ridges. *Journal of Petrology*, 45(12), 2423-2458.
- Niu, Y., & Hekinian, R. (1997). Spreading-rate dependence of the extent of mantle melting beneath ocean ridges. *Nature*, 385(6614), 326-329.
- Niu, Y., & Hekinian, R. (1997). Spreading-rate dependence of the extent of mantle melting beneath ocean ridges. *Nature*, 385(6614), 326-329.

- Oliver, E. C. J., Donat, M. G., Burrows, M. T., Moore, P. J., Smale, D. A., Alexander, L. V., ... & Sen Gupta, A. (2018). Longer and more frequent marine heatwaves over the past century. *Nature Communications*, 9(1), 1-12.
- Paulick, H., Bach, W., Godard, M., Hoog, J., Suhr, G., & Harvey, J. (2006). Geochemistry of abyssal peridotites (Mid-Atlantic Ridge, 15°20'N, ODP Leg 209): Implications for fluid/rock interaction in slow spreading environments. *Chemical Geology*, 234, 179-210. <https://doi.org/10.1016/J.CHEMGEO.2006.04.011>.
- Post, J. E., Heaney, P. J., & Hanson, S. L. (2003). Synchrotron powder X-ray diffraction study of chrysotile at high pressure: Implications for serpentinization reactions. *American Mineralogist*, 88(12), 2030-2035.
- Prell, W. L., Kutzbach, J. E., & Imbrie, J. (1980). Variability in the circulation patterns of the northern Indian Ocean during the past 15,000 years. *Paleoceanography*, 4(6), 685–696. <https://doi.org/10.1029/PA004i006p00685>
- Prichard, H. (1979). A petrographic study of the process of serpentinisation in ophiolites and the ocean crust. *Contributions to Mineralogy and Petrology*, 68, 231-241. <https://doi.org/10.1007/BF00371544>.
- Prichard, H. M. (1979). A petrographic study of the process of serpentinisation in ophiolites and the ocean crust. *Contributions to Mineralogy and Petrology*, 68(3), 231-241.
- Rhodes, J. M., Dungan, M. A., Blanchard, D. P., & Long, P. E. (1979). Magma mixing at mid-ocean ridges: evidence from basalts drilled near 22 N on the Mid-Atlantic Ridge. *Tectonophysics*, 55(1-2), 35-61.
- Roumejon, S., Cannat, M., Agrinier, P., Godard, M., & Andreani, M. (2015). Serpentinization and fluid pathways in tectonically exhumed peridotites from

the Southwest Indian Ridge (62–65 E). *Journal of Petrology*, 56(4), 703-734.
<https://doi.org/10.1093/PETROLOGY/EGV014>.

- Roxy, M. K., Ritika, K., Terray, P., & Murtugudde, R. (2014). The curious case of Indian Ocean warming. *Journal of Climate*, 27(22), 8501-8509.
- Saji, N. H., Goswami, B. N., Vinayachandran, P. N., & Yamagata, T. (1999). A dipole mode in the tropical Indian Ocean. *Nature*, 401(6751), 360–363.
<https://doi.org/10.1038/43854>
- Scambelluri, M., Rampone, E., & Piccardo, G. (2001). Fluid and Element Cycling in Subducted Serpentinite: a Trace-Element Study of the Erro–Tobbio High-Pressure Ultramafites (Western Alps, NW Italy). *Journal of Petrology*, 42, 55-67. <https://doi.org/10.1093/PETROLOGY/42.1.55>.
- Scambelluri, M., Rampone, E., & Piccardo, G. B. (2001). Fluid and element cycling in subducted serpentinite: a trace-element study of the Erro–Tobbio high-pressure ultramafites (Western Alps, NW Italy). *Journal of Petrology*, 42(1), 55-67.
- Schmitz Jr, W. J. (1995). On the World Ocean Circulation: Volume I: Some Global Features/North Atlantic Circulation. Woods Hole Oceanographic Institution.
- Schroeder, T., John, B., & Frost, B. (2002). Geologic implications of seawater circulation through peridotite exposed at slow-spreading mid-ocean ridges. *Geology*, 30, 367-370. [https://doi.org/10.1130/0091-7613\(2002\)030<0367:GIOSCT>2.0.CO;2](https://doi.org/10.1130/0091-7613(2002)030<0367:GIOSCT>2.0.CO;2). 111111
- Schulte, J., Schäfer, P., Ittekkot, V., & Fischer, G. (1999). Seasonal and interannual variability of particle fluxes to the deep Arabian Sea. *Deep Sea*

Research Part II: Topical Studies in Oceanography, 46(8-9), 1859–1902.
[https://doi.org/10.1016/S0967-0645\(99\)00051-5](https://doi.org/10.1016/S0967-0645(99)00051-5)

- Schwartz, S., Guillot, S., Reynard, B., Lafay, R., Debret, B., Nicollet, C., ... & Auzende, A. L. (2013). Pressure–temperature estimates of the lizardite/antigorite transition in high pressure serpentinites. *Lithos*, 178, 197–210.
- Shaji, C., & Ruma, A. (2020). Physical oceanographic properties and their relation with the satellite-derived primary productivity during the transition phases of Indian Ocean Dipole (IOD) events in the central equatorial Indian Ocean. *Oceanologia*, 62(2), 153–169.
<https://doi.org/10.1016/j.oceano.2019.11.006>
- Shibata, T., & Thompson, G. (1986). Peridotites from the Mid-Atlantic Ridge at 43° N and their petrogenetic relation to abyssal tholeiites. *Contributions to Mineralogy and Petrology*, 93, 144–159. <https://doi.org/10.1007/BF00371316>.
- Snow, J. E., & Dick, H. J. (1995). Pervasive magnesium loss by marine weathering of peridotite. *Geochimica et Cosmochimica Acta*, 59(20), 4219–4235.
- Strutton, P. G., & Chavez, F. P. (2015). Biological impacts of the 1997–1998 El Niño in the equatorial Pacific region. *IGBP Newsletter*, 59, 26–27. Retrieved from
http://www.igbp.net/download/18.316f18321323470177580001401/IGBP_News59.pdf
- Takazawa, E., Okayasu, T., & Satoh, K. (2003). Geochemistry and origin of the basal lherzolites from the northern Oman ophiolite (northern Fizh block). *Geochemistry, Geophysics, Geosystems*, 4(2).

- Talley, L. D. (2013). Closure of the global overturning circulation through the Indian, Pacific, and Southern Oceans: Schematics and transports. *Oceanography*, 26(1), 80-97.
- Thompson, G., & Melson, W. (1970). Boron contents of serpentinites and metabasalts in the oceanic crust: Implications for the boron cycle in the oceans. *Earth and Planetary Science Letters*, 8, 61-65. [https://doi.org/10.1016/0012-821X\(70\)90100-7](https://doi.org/10.1016/0012-821X(70)90100-7).
- Uysal, I., Ersoy, E. Y., Dilek, Y., Kapsiotis, A., & Sarıfakıoğlu, E. (2016). Multiple episodes of partial melting, depletion, metasomatism and enrichment processes recorded in the heterogeneous upper mantle sequence of the Neotethyan Eldivan ophiolite, Turkey. *Lithos*, 246, 228-245.
- Verencar, A., Saha, A., Ganguly, S., & Manikyamba, C. (2021). Tectono-magmatic evolution of Tethyan oceanic lithosphere in supra subduction zone fore arc regime: Geochemical fingerprints from crust-mantle sections of Naga Hills Ophiolite. *Geoscience Frontiers*, 12(3), 101096.
- Webster, P. J., Moore, A. M., Loschnigg, J. P., & Leben, R. R. (1999). Coupled ocean-atmosphere dynamics in the Indian Ocean during 1997-98. *Nature*, 401(6751), 356-360. <https://doi.org/10.1038/43848>
- White, W. M. (2013). *Geochemistry*. Wiley-Blackwell. <https://doi.org/10.1002/gj.2762>
- Workman, R. K., & Hart, S. R. (2005). Major and trace element composition of the depleted MORB mantle (DMM). *Earth and Planetary Science Letters*, 231(1-2), 53-72.
- Wu, T., Tian, L., Gao, J., & Dong, Y. (2019). Petrology and geochemistry of serpentinitized peridotites from Hahajima Seamount in Izu-Bonin forearc

region. *Acta Oceanologica Sinica*, 38, 110 - 99.
<https://doi.org/10.1007/s13131-019-1469-x>.

- Wu, T., Tian, L., Gao, J., & Dong, Y. (2019). Petrology and geochemistry of serpentinitized peridotites from Hahajima Seamount in Izu-Bonin forearc region. *Acta Oceanologica Sinica*, 38, 99-110.
- Xiao-hu, L. (2011). Advances in research of abyssal peridotite serpentinitization. *Journal of Marine Sciences*.
- Yang, J., Dick, H. J. B., & Natland, J. (1998). An experimental study of the reaction between lherzolite and basaltic melt: implications for the genesis of ocean island basalts. *Contributions to Mineralogy and Petrology*, 131(1), 75–86. <https://doi.org/10.1007/s004100050380>
- Zhang, L., Zhang, Q., & Cai, W. (2018). Contributions of the Indian Ocean and local atmospheric variability to Indian Ocean Dipole events. *Journal of Climate*, 31(1), 335-354.